

# **Dissertation**

---

**Intracellular and extracellular death regulation:  
identification of molecules for apoptosis and  
necroptosis regulation in malignant melanoma**

---

submitted to the  
Combined Faculties for the Natural Sciences and for Mathematics  
of the Ruperto-Carola University of Heidelberg, Germany  
for the degree of  
Doctor of Natural Sciences

presented by

**Jing Wang**

# **Dissertation**

## **Intracellular and extracellular death regulation: identification of molecules for apoptosis and necroptosis regulation in malignant melanoma**

submitted to the  
Combined Faculties for the Natural Sciences and for Mathematics  
of the Ruperto-Carola University of Heidelberg, Germany  
for the degree of  
Doctor of Natural Sciences

presented by

**Jing Wang, diploma in Pharmaceutical Chemistry**

Born in Tianshui, China

Date of examination: 13.September.2016

**Intracellular and extracellular death regulation:  
identification of molecules for apoptosis and  
necroptosis regulation in malignant melanoma**

Referees: Prof. Dr. Viktor Umansky

Prof. Dr. Jochen Utikal

Declarations according to § 8 (3) b) and c) of the doctoral degree regulations:  
b) I hereby declare that I have written the submitted dissertation myself and in this process have used no other sources or materials than those expressly indicated,  
c) I hereby declare that I have not applied to be examined at any other institution, nor have I used the dissertation in this or any other form at any other institution as an examination paper, nor submitted it to any other faculty as a dissertation.

Mannheim, 01.June.2016

Jing Wang

**Table of content**

<b>List of Figures .....</b>	<b>IV</b>
<b>List of Tables.....</b>	<b>V</b>
<b>Abstract (English).....</b>	<b>VI</b>
<b>Abstract (German) .....</b>	<b>VII</b>
<b>1. Introduction .....</b>	<b>1</b>
1.1 Human skin structure and function .....	1
1.2 Human malignant melanoma .....	1
1.2.1 Malignant melanoma cells characteristics .....	2
1.2.2 Risk factors for melanoma.....	3
1.2.3 Therapy option for malignant melanoma.....	4
1.3 Programmed cell death .....	5
1.3.1 Apoptosis.....	5
1.3.2 Necroptosis.....	9
1.3.3 Regulatory effect of IAPs on programmed cell death.....	12
1.4 Suppression of gene expression and cell death via DNA methylation.....	13
1.5 Regulation of programmed cell death by NF- $\kappa$ B signalling pathway .....	14
1.5.1 NF- $\kappa$ B signalling pathway.....	14
1.5.2 Regulatory effect of NF- $\kappa$ B on programmed cell death.....	15
<b>2. Materials and Methods .....</b>	<b>16</b>
2.1 Chemicals and Buffers.....	16
2.2 Methods .....	19
2.2.1 Cell culture .....	19
2.2.2 Cell death assay .....	20
2.2.3 Plasmid transformation and isolation.....	22
2.2.4 Ca-phosphate mediated transfection of lentiviral or retroviral DNA and virus production.....	22
2.2.5 Retroviral and lentiviral transduction .....	23
2.2.6 CD95 Receptor staining.....	23

2.2.7 Western blot analysis.....	23
2.2.8 Caspase-8 Co-immunoprecipitation.....	25
2.2.9 RNA isolation and reverse transcription.....	26
2.2.10 Quantitative real time polymerase chain reaction (qPCR).....	26
2.2.11 Genomic DNA isolation .....	27
2.2.12 Bisulfite conversion of DNA and Methylation specific PCR (MSP).....	27
<b>3. Aim of the thesis .....</b>	<b>29</b>
<b>4. Results .....</b>	<b>30</b>
4.1 Identification of regulatory proteins for programmed cell death in melanomas .....	30
4.1.1 Loss of IAPs sensitizes human melanoma cells to CD95L-induced cell death.....	30
4.1.2 Necroptosis is limited by absence of RIPK3 expression in melanoma cells.....	32
4.1.3 Reconstitution of RIPK3 promotes MLKL phosphorylation and allows for CD95L-induced necroptosis in malignant melanomas.....	34
4.1.4 RIPK3 promotes CD95L-induced necroptosis without altering CD95 expression.....	37
4.1.5 CD95L-mediated apoptosis and necroptosis in RIPK3 overexpressing A375 cells are independent of IAP antagonist-mediated autocrine TNF activation.....	38
4.1.6 Death ligands promote MLKL phosphorylation during the process of necroptosis in RIPK3-reconstituted melanoma cells.....	40
4.1.7 RIPK1 and RIPK3 kinase activity are determinant for MLKL phosphorylation in CD95L induced necroptosis.....	41
4.1.8 Inhibition of RIPK3 kinase activity promotes TNF-complex II formation.....	43
4.1.9 DNA-Demethylation by DAC reconstituted RIPK3 expression in both human and murine melanoma cells .....	45
4.1.10 Demethylation-mediated RIPK3 restoration is not competent for necroptosis execution .....	47
4.1.11 Dabrafenib blocks necroptotic cell death through inhibition of RIPK3 kinase activity.....	48
4.2 Identification of NF- $\kappa$ B regulatory effect on melanoma cell death .....	51
4.2.1 IKK2 activation leads to constitutive activation of both canonical and non-canonical NF- $\kappa$ B pathway .....	52

---

4.2.2	Constitutive activation of NF- $\kappa$ B renders melanoma cells resistance to TNF-mediated apoptosis.....	54
4.2.3	Spontaneous apoptosis of IKK2 EE cells in absence of IAPs was independent from IAP antagonist-mediated autocrine TNF activation .....	57
4.2.4	Loss of cIAP1 promotes formation of RIPK1-dependent Ripoptosome to induce apoptosis by constitutive NF- $\kappa$ B activation .....	58
<b>5.</b>	<b>Discussion .....</b>	<b>63</b>
5.1	IAPs inhibits CD95L-mediated cell death in melanoma.....	63
5.2	RIPK3 is lost during the development of melanoma because of promoter methylation .....	64
5.3	RIPK3 kinase and partial RIPK1 activity is critical for MLKL phosphorylation and necroptosis initiation .....	66
5.4	Constitutively active IKK2 EE renders cell resistance to TNF stimulation via expression of anti-apoptotic proteins in melanoma cells .....	68
5.5	Constitutive activation of IKK2 promotes melanoma cell death in absence of cIAP1 independent from IAP antagonist-mediated autocrine TNF activation .....	70
5.6	Loss of cIAP1 promotes RIPK1-dependent Ripoptosome formation in IKK2 active melanoma cells.....	71
	<b>References .....</b>	<b>74</b>
	<b>Publications.....</b>	<b>91</b>
	<b>Acknowledgements .....</b>	<b>92</b>
	<b>Abbreviations.....</b>	<b>93</b>

## List of Figures

<b>Figure 1</b> Scheme of human skin. ....	2
<b>Figure 2</b> Transformation of normal to malignant cells during uncontrolled cell division. ....	3
<b>Figure 3</b> Molecular mechanisms of the crosstalk between intrinsic and extrinsic signalling pathways in apoptosis. ....	8
<b>Figure 4</b> The role of molecular signalling platforms for transmission of apoptotic and necroptotic cell death. ....	11
<b>Figure 5</b> Chemical structure of Compound A .....	12
<b>Figure 6</b> Loss of IAPs sensitizes melanoma cell lines to CD95L-mediated apoptotic cell death.....	31
<b>Figure 7</b> Melanoma cell lines are lack of RIPK3 expression in both mRNA and protein level. ....	33
<b>Figure 8</b> Overexpression of RIPK3 promotes spontaneous phosphorylation of MLKL and CD95L-induced necroptotic cell death.....	35
<b>Figure 9</b> RIPK3 overexpression promotes CD95L-mediated necroptosis in melanoma cells. ....	36
<b>Figure 10</b> RIPK3 reconstitution does not alter CD95 surface expression.....	37
<b>Figure 11</b> CD95L-induced apoptosis and necroptosis in A375-RIPK3 cells are independent from Compound A-mediated TNF signalling. ....	39
<b>Figure 12</b> MLKL is phosphorylated during the death ligand-mediated necroptosis in RIPK3 overexpressing A375 cell.....	40
<b>Figure 13</b> RIPK3 and partially RIPK1 is required for MLKL phosphorylation mediated necroptosis. ....	42
<b>Figure 14</b> RIPK3 inhibitor increased assembly of TNF-complex II formation. ....	44
<b>Figure 15</b> DNA demethylation by 5-aza-2'-deoxytidine (DAC) was able to restore RIPK3 expression in melanomas.. ....	45
<b>Figure 16</b> RIPK3 promoter is methylated in human melanoma cell lines.. ....	46
<b>Figure 17</b> Reconstitution of RIPK3 by demethylation is not sufficient to induce CD95L-mediated necroptosis.....	48
<b>Figure 18</b> BRAF inhibitor Dabrafenib but not Vemurafenib prevent A375 RIPK3 overexpressing cells from death ligand-mediated necroptosis.....	49
<b>Figure 19</b> Dabrafenib negatively regulated necroptosis via inhibition of RIPK3 mediated spontaneous and CD95L-mediated MLKL phosphorylation. ....	50
<b>Figure 20</b> IKK2 EE overexpression promotes target genes expression and activation of non-canonical NF- $\kappa$ B activation.....	53
<b>Figure 21</b> Overexpression of IKK2 EE increase cell resistance to TNF and increased cell sensitivity to IAP antagonist. ....	54
<b>Figure 22</b> IAP antagonist decreases cIAP1 and slightly cIAP2 and promotes caspase 8 cleavage to induce apoptosis. ....	56
<b>Figure 23</b> IAP antagonist-induced apoptosis is independent from IAP antagonist-mediated autocrine TNF activation in IKK2 EE IGR cells.. ....	57
<b>Figure 24</b> Loss of cIAP1 promotes Ripoptosome formation in IKK2 EE cells. ....	59
<b>Figure 25</b> IAP antagonist-mediated Ripoptosome assembly and apoptosis in IKK2 EE overexpressing cells is RIPK1 dependent. ....	61
<b>Figure 26</b> Identification of RIPK3 and NF- $\kappa$ B for melanoma cell death regulation.....	73

---

## List of Tables

<b>Table 1</b> Chemicals for buffer solution.....	16
<b>Table 2</b> Buffer composition.....	17
<b>Table 3</b> Reagents and Kits.....	18
<b>Table 4</b> Cell culture medium and related reagents .....	19
<b>Table 5</b> Cytokines and inhibitors .....	20
<b>Table 6</b> Plasmids .....	22
<b>Table 7</b> Primary and secondary antibodies.....	24
<b>Table 8</b> qPCR primers.....	26
<b>Table 9</b> Reaction components for PCR .....	26
<b>Table 10</b> Thermal cycling profile for qPCR.....	27
<b>Table 11</b> <i>RIPK3</i> primers for MSP .....	28
<b>Table 12</b> Reaction components for PCR .....	28
<b>Table 13</b> Thermal cycling profile for MSP .....	28

## Abstract (English)

Over the last decades, novel therapies against melanoma have allowed for a prolonged survival rate of malignant melanoma while not allowing for a cure because of its aggressiveness and death resistance. Therefore, adaptation of existing and development of innovative therapeutic interventions for melanoma are required. One promising option could be discovery of drugs that are able to induce programmed cell death in melanoma. Another strategy is to inhibit molecules and cell signalling that are relevant for cell death resistance of melanoma to therapies. Thus, the detailed understanding of cell death regulation and potential resistance mechanisms of melanoma are indispensable.

IAPs exert their inhibitory effect on cell death through impairing caspase activities and ubiquitination targeted proteins. In our study, the negative regulatory role of IAPs in CD95L-mediated cell death was confirmed by using IAP antagonist in a panel of human melanoma cell lines *in vitro*. Furthermore, we found that CD95L-induced cell death in absence of IAPs in melanoma cells was dominantly mediated by caspase-dependent apoptosis but not necroptosis, which suggested the resistance of melanoma to the necroptotic signalling. When we analysed expression of necroptosis-related proteins, we found that the protein expression of RIPK3 was low or absent in melanoma cell lines compared with cultured keratinocytes, primary melanocytes and nevus cells, which resulted from absence of *RIPK3* mRNA expression. Ectopical expression of RIPK3 in melanoma uncovered the CD95L-mediated necroptosis which was correlated with MLKL phosphorylation. The indispensability of RIPK3 in necroptosis was further confirmed by mutation of RIPK3 kinase domain and RIPK3 specific inhibitors. Hypermethylation of *RIPK3* DNA promoter was identified as the reason for RIPK3 absence in melanoma cell lines. Restoration of RIPK3 expression was successful via demethylation reagent. Unexpectedly, demethylation-mediated RIPK3 reconstitution failed to induce necroptosis in treated melanoma cells.

NF- $\kappa$ B activation mainly as a pro-survival signalling initiates a variety of genes induction in melanomas. In our study, NF- $\kappa$ B activation led to expression or upregulation of cIAPs and cFLIP which rendered cell death resistance to melanoma. Cell death assay results confirmed the negative regulatory role of NF- $\kappa$ B in TNF-mediated cell death. Unusually, NF- $\kappa$ B activation resulted in spontaneous cell sensitivity to IAP antagonist via promotion of RIPK1-dependent complex formation in IKK2 constitutively activated melanomas.

Our data verified the negatively regulatory effect of IAPs and NF- $\kappa$ B activation on cell death in melanoma cells. RIPK3 was also identified as essential link for necroptotic cell death in melanomas. Therefore, overcoming cell death resistance by antagonizing IAP activity is a promising strategy for melanoma treatment. In addition, reconstitution of RIPK3 to induce necroptosis in melanoma is as an alternative option for melanoma therapy.

## Abstract (German)

Das maligne Melanom ist eine der aggressivsten Tumorentitäten und gehört zu den gefährlichsten Hautkrebsformen. In den letzten Jahrzehnten wurden neue chemo- und immuntherapeutische Behandlungen etabliert, die zwar die Überlebensrate von Melanompatienten verlängert aber bisher keine Heilung ermöglicht. Daher ist die Anpassung bestehender und die Entwicklung neuer innovativer therapeutischer Interventionen zur Bekämpfung des Melanoms wichtig und erforderlich. Eine vielversprechende Möglichkeit bieten Therapeutika die in der Lage sind, apoptotische, nekroptotische und autophagische Zelltodprozesse zu induzieren. Eine andere Strategie beschäftigt sich mit der Inhibition von Zelltod-blockierenden Proteinen oder von Signalwegen, die bedeutend sind für Zelltodresistenzen. Durch Inhibition dieser Signalwege und Moleküle könnte die Sensitivität gegenüber entsprechender Zelltod-induzierenden Therapeutika im Melanom begünstigt werden. Die Identifizierung dieser Zelltod-regulierenden Prozesse einschließlich der potentiellen Resistenzmechanismen ist für die Entwicklung neuer therapeutischer Interventionen unabkömmlich.

IAPs vermitteln Zelltodresistenzen durch Inhibition von Caspase-Aktivitäten oder durch Ubiquitinierungen von entsprechenden Zielproteinen. In dieser Studie wurde die funktionelle Relevanz der IAPs (Inhibitor of apoptosis proteins) bei der Todesrezeptor-vermittelten Zelltodregulation in einem Panel von menschlichen Melanomzelllinien *in vitro* untersucht. Des Weiteren fanden wir, dass der CD95L-vermittelte Zelltod in Abwesenheit der IAPs in Melanomzellen dominant durch Caspase-abhängige Apoptose und nicht durch Nekroptose vermittelt wird, wodurch eine Resistenz der Melanomzellen gegenüber nekroptotischer Signalgebung identifiziert wurde. Durch Untersuchungen der endogenen Expressionen von Proteinen der Nekroptose-Signalkaskade wurde eine substantiell niedriges oder abwesendes RIPK3-Expressionniveau auf Protein- und mRNA-Ebene in humanen und murinen Melanomzelllinien gefunden, während RIPK3 in kultivierten Keratinozyten, primären Melanozyten und Nävuszellen präsent ist. Die artifizielle, ektopische Expression von RIPK3 in Melanomzellen demaskierte die CD95L-vermittelte Nekroptose, welches mit MLKL-Phosphorylierungen einhergeht. Die unabkömmliche Rolle von RIPK3 für die Nekroptose in Melanomzellen wurde durch die Überexpression einer Kinase-inaktiven RIPK3-Mutante als auch durch chemische RIPK3-spezifische Inhibitoren gezeigt, welche insbesondere die MLKL-Phosphorylierung blockiert. Hypermethylierung im RIPK3-Promotor wurden als Ursache für die Abwesenheit der RIPK3-mRNA und damit des RIPK3 Proteins identifiziert. Die Rekonstitution der RIPK3 Expression in Melanomzellen konnte erfolgreich durch demethylierende Reagenzien erzielt werden. Obwohl dadurch die Reexpression von RIPK3 erreicht wurde, konnte keine CD95L-vermittelte Nekroptose in den behandelten Melanomzellen beobachtet werden.

Ein weiterer wichtiger Untersuchungsschwerpunkt in dieser Arbeit war die

Identifizierung der Rolle von NF- $\kappa$ B für die Regulation von Proteinen, die in der Zelltodregulation im Melanom eine Rolle spielt. Die Aktivierung von NF- $\kappa$ B dient als Überlebenssignal und vermittelt Zelltodresistenzen durch verstärkte Expression von einer Vielzahl von Proteinen, insbesondere von cIAPs und cFLIP-Proteinen, wie wir es in dieser Studie im Melanom zeigen konnten. Die negative Rolle von NF- $\kappa$ B im TNF-vermitteltem Zelltod konnte durch Zelltodanalysen bestätigt werden. Interessanter Weise und ungewöhnlich werden Melanomzellen mit konstitutiver NF- $\kappa$ B-Aktivierung sensitiv gegenüber IAP-Antagonist-vermitteltem Zelltod und fördern die Formierung von RIPK1-abhängige Proteinsignalkomplexe.

Unsere Daten konnten den negative-regulierenden Effekt von IAPs und von NF- $\kappa$ B für Zelltodprozesse in Melanomzellen verifizieren. RIPK3 wurde als essentiellen Link für den nekroptotischen Zelltod in Melanomzellen identifiziert. Die Überwindung von Zelltodresistenzen durch Inhibition von IAP-Aktivitäten stellt somit eine vielversprechende Strategie zur Behandlung von Melanomerkrankungen dar. Zusätzlich kann die Rekonstitution von RIPK3 in Melanomen zur Induktion von nekroptotischen Zelltodprozessen beitragen, welche eine weitere und alternative Option für Therapien bei Melanomerkrankungen darstellen kann.

## 1. Introduction

### 1.1 Human skin structure and function

Skin is the largest organ serving as a natural barrier to protect human body from exterior injury. According to the location and structural components (Figure 1), human skin can be characterized into epidermis (outer), dermis (interior) and subcutaneous fat layer (basal, also called fat layer).

The outer layer of the skin is named as epidermis which is relatively thin and tough (Figure 1). Epidermis is further segmented into five stratum, including stratum corneum, stratum lucidum, stratum granulosum, stratum spinosum, and stratum basale [1]. The epidermis is mainly composed of keratinocytes (95%), melanocytes, Langerhans cells and Merkel cells [2,3]. Keratinocytes (Figure 1), distributed in stratum basale act as a barricade to protect the skin from exterior injury and also to prevent underlying tissues from dehydration [4]. Melanocytes (Figure 1), also scattered in the stratum basale of epidermis, is responsible for melanin production to filtrate UV radiation from sunlight, which can result in DNA damages and further skin carcinomas, mainly melanoma [5]. In addition, Langerhans cells in epidermis are parts of the skin immune system to detect and defend against foreign substances [6]. Dermis (Figure 1), lying in the middle tier of skin, can be dissected into the thin upper layer adjoining to the epidermis (papillary region) and the thick bottom layer extending to the fat layer (reticular region) [2]. 70% percent of the dermis is made up of collagen fibres, elastin and proteoglycans to render skin strength, firmness, elasticity, and flexibility. Embedded within the fibrous tissue of the dermis is the dermal vasculature, including blood vessels, lymphatic vessels, sensory nervous endings, sebaceous glands, sweat glands and hair follicles, which are involved in supplying nutrients and oxygen for skin, providing protection from injury, sensing and reacting to pain, touch, pressure and temperature, and keeping skin moist and soft [7,8]. The innermost layer of skin is the subcutaneous fat layer (Figure 1), which is essentially composed of adipocytes for accumulating and storing fats. The fat stocking in the adipocytes can be transformed into energy biochemically and served as pressure cushion to prevent body from outside injury physically [2]. The fat layer also offers inner body with thermal insulation to decelerate the heat loss [9].

### 1.2 Human malignant melanoma

There are three most common types of human skin cancers: basal cell carcinoma (BCC), squamous cell carcinoma (SCC) and malignant melanoma. In all of skin cancers, malignant melanoma is the most aggressive and fatal form. With the low overall 5-year survival rate, incidence of malignant melanoma continues to increase worldwide. Melanoma ranks the 19th among the most common human cancer, with approximately 232,000 new cases diagnosed in 2012 accounting for 2% the total number of cancers [10]. Therefore, better understanding human skin and

carcinogenesis of melanoma will help the discovery effective therapies against malignant melanoma.

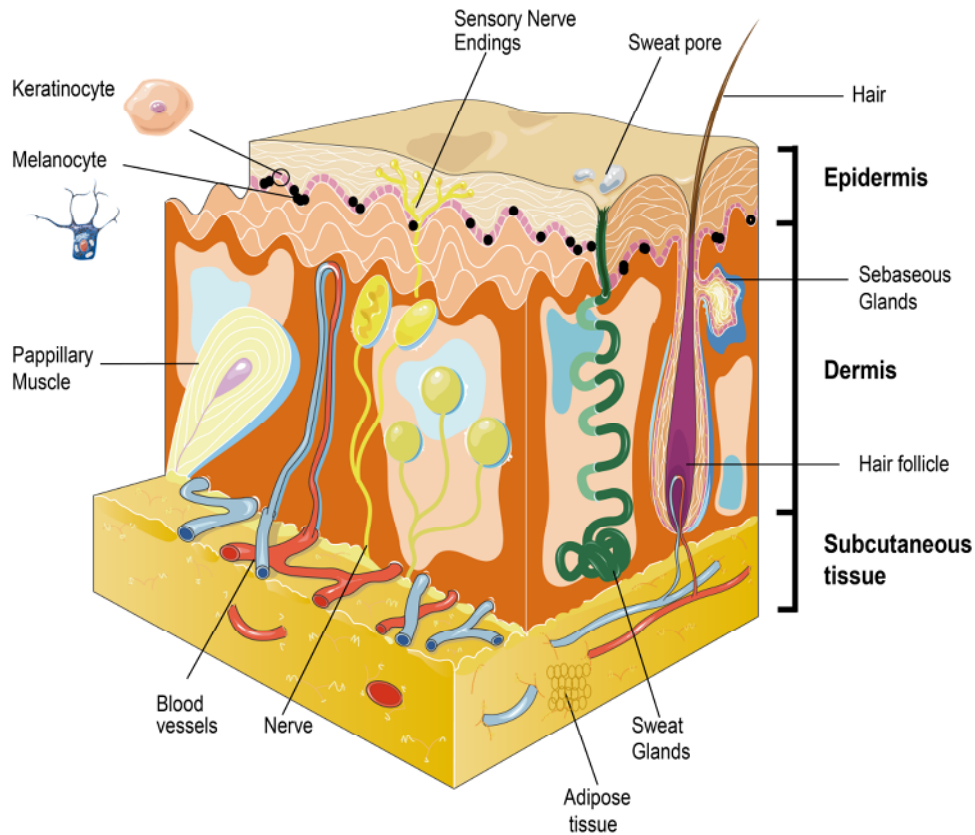


**Figure 1 Scheme of human skin.** The structure of human skin can be parted into epidermis, dermis and subcutaneous fat layer based on their positions and components.

### 1.2.1 Malignant melanoma cells characteristics

Cells are the basic unit that arrange tissues and organs in the human body. Normal cells divide and develop in a well-regulated manner in order to ensure the organism to function properly. While alterations (genetic or epigenetic mutations) in normal cells potentially result in uncontrolled and dysregulated growth and carcinogenesis as a result (Figure 2). Escape from cell death is one hallmark of cancer cells that is critical for malignant transformation and tumour maintenance.

In terms of malignant melanoma, it usually originates from the abnormal pigment melanocytes scattered in the basal layer of the epidermis [11]. Under the normal condition, melanocytes produce melanin which is then transferred to neighbouring keratinocytes to protect skin from ultraviolet radiation (UV)-caused damage. Abnormal melanocytes resulted from mutations initially develop into pigmented lesions and further transform into dysplastic nevi [12]. Uncontrollably melanocytes of dysplastic nevi lead to an *in situ* melanoma that is mostly confined to the

epidermis, which is referred as radial growth phase (RGP) of melanoma. If the RGR melanoma is not found and treated immediately, it acquires the metastatic potential during the vertical growth phase (VGP) to invade to dermis and further lung, bone or brain [13,14]. Rapid division and impaired ability to undergo programmed cell death in response to a wide range of external stimuli allow melanomas a selective advantage for progression and metastasis as well as their notorious resistance to therapy. Typical features of normal and tumour cells offer us with extensive comprehension of melanoma and improvements for melanoma treatments and therapies without injuring normal cells.

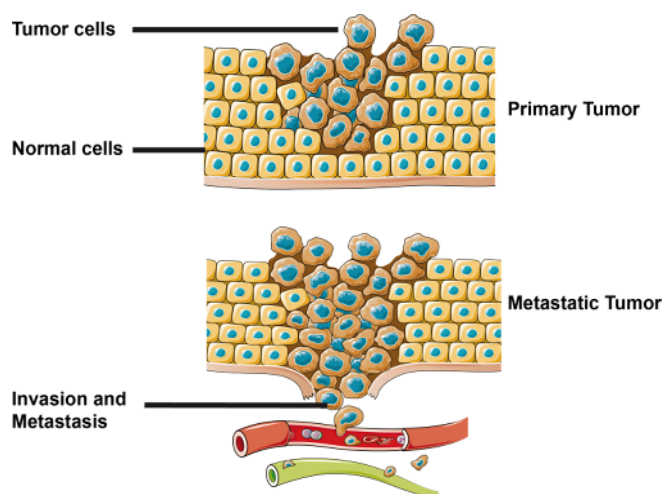


**Figure 2 Transformation of normal to malignant cells during uncontrolled cell division.** When normal cells divided and proliferated in a dysregulated manner, they develop into a tumour and metastasize to other organs when tumour cells moved with the blood stream.

### 1.2.2 Risk factors for melanoma

**Environmental factors** Sun exposure, as the main source of UV rays, is the major environmental risk factor for melanoma. UVB (280-320 nm) is proposed to be the most carcinogenic waveband, which can be absorbed by nucleic acids and proteins respectively. UVB radiation mainly leads to C-T or CC-TT transitions and minor C-A and G-T transversions as genetic mutations. In addition, DNA strand breaks resulted from UV radiation are also considered to be involved in the development of melanoma [15,16]. In addition to UV rays exposure, contact with environmental carcinogenetic chemicals, including polycyclic aromatic hydrocarbons, benzene, polychlorinated biphenyls and chromium, is able to induce melanoma. Production of reactive oxygen species (ROS), endocrine disruption and immune suppression are also regarded as the potential inducer for melanoma [17-19].

**Host factors** refer to pigmentation characteristics of nevi, eyes, skin, hair colours and also the ability to tan and propensity to burn on individual basis. An analysis of 10 cases controlled studies supported that both fair skin and degree of freckling were

associated with increased risk of developing melanoma [20,21]. In brief, incidences of melanoma are reversely correlated with extent of skin pigmentation.

**Germline genetic factors** Familial history of melanoma is an alternative useful predictor for melanoma incidence. Sharing the certain germline genetic alterations is the main reason for the occurrence of melanoma in a family setting. Familial genetic linkage studies have identified *CDKN2A* and *CDK4* as high-penetrance susceptibility genes for melanoma. Germline mutations of these genes render an increasing risk of melanoma occurrences [22-25]. With the development of gene screening techniques, the discovery germline genetic mutations of melanoma will help the early prediction and effective treatment for melanoma.

### 1.2.3 Therapy option for malignant melanoma

**Surgery** As the primary treatment for melanoma, wide excision is applied to remove melanoma lesions. In addition, if the result of lymph node biopsy is positive, lymph node dissection is executed in some cases.

**Radiation therapy** refers as application of rays of high energy, including X-rays, gamma-rays and charged particles to kill melanoma cells via DNA damage mediated cell death. Radiation therapy is often used as an adjuvant treatment for melanoma post-surgery to get rid of the remaining tumour cells [26,27].

**Chemotherapy** The main clinical chemotherapy reagents for melanoma can be characterized into mitosis inhibitors (paclitaxel), alkylating-like agents (cisplatin, carboplatin) and alkylating agents (dacarbazine, temozolomide). Chemotherapeutic agents exert anti-tumour function through inducing DNA damage, interfering with cell cycle and inducing cell death as consequences [28].

**Immunotherapy** The primary objective of immunotherapy is to increase activity of immune system to destroy tumour cells by cytokines (Interleukin-2 and Interferon- $\alpha$ ) [29,30]. With the discovery of cancer-related antigens and their inhibitory effect on T-lymphocytes to render melanoma cells ability to escape from adaptive immune surveillance [31,32], monoclonal antibodies (PD-1 and CTLA-4) are designed to attach to specific proteins of cancer cells allow the immune system itself to destroy the cancer cells. Immunotherapy because of its highly specificity, is a promising strategy to boost immune system response against melanoma cells [33].

**Targeted Therapy** Increasing understanding of molecules driving melanoma has allowed considerably novel therapeutic options. Approximate 50% melanoma patients possess *BRAF* mutation (mainly V600E and V600K) which leads to constitutive activation of MAPK signalling pathway [34,35]. Selective BRAF inhibitors (Vemurafenib and Dabrafenib) have been shown to adjourn melanoma progression in patients identified *BRAF*<sup>V600</sup> mutation [36,37]. Encouragingly, increasing evidences have demonstrated that concomitant administration of BRAF and MEK inhibitors (Trametinib and Selumetinib) prolong progression-free survival,

and consequently increase the overall survival rate of melanoma patients [38]. Discovery of targeted inhibitors represents an alternative promising strategy for melanoma treatment. Also the activation of extrinsic or intrinsic cell death signalling pathways by e.g. death ligands or Bcl-2 antagonists can be a strategy for melanoma treatment.

### 1.3 Programmed cell death

The conception of programmed cell death was firstly proposed in 1965 to describe the death process as a biological planned program in muscles cells of large American silkmoths [39]. Multicellular organisms have evolved a self-demise machinery to eliminate the damaged, infected, and unwanted cells to assure the whole body can better survive. Continuous studies of programmed cell death (PCD) along with the development of model organisms and technologies have allowed a better understanding of the fundamental process related with mammalian development and various diseases.

#### 1.3.1 Apoptosis

Apoptosis is a well-regulated cell suicide program that comes in force from early embryonic development and continues in the adult life. Apoptosis is thus essential to maintain normal body homeostasis, defence against pathogen infection and genotoxic stress. Disruption of this native regulatory mechanism of cells leads to uncontrolled growth and a wide variety of human diseases including acquired immune deficiency disease (AIDS), neurodegenerative disorders, autoimmune diseases, stroke, and cancers. Furthermore, understanding of programmed cell death has reinforced the development of new therapeutic strategies against human diseases [40-43].

Apoptosis manifests with cell shrinkage, chromatin condensation, plasma membrane blebbing, and finally breakdown of cells into small membrane-bound vesicles named as apoptotic bodies. The apoptotic bodies are quickly removed through phagocytosis by macrophages, parenchymal cells or neighbouring cells [44]. Apoptosis also characterizes with biochemical features including caspases cascade activation, DNA breakdown, phosphatidylserine externalization and protein cleavage [45]. The dissemination of apoptosis is tightly regulated by two well-understood signal transduction pathways, the intrinsic pathway (also known as the mitochondrial mediated pathway) and the extrinsic pathway (also known as the death receptor mediated pathway). These two pathways converge at the point of caspases activation.

##### 1.3.1.1 Caspases

As the core for apoptosis initiation, caspases (cysteine aspartate-specific proteases),

a group of intracellular cysteine proteases, utilize a catalytic cysteine to cleave their peptide substrates after aspartate specific residues. Human caspases are functionally categorized into apoptotic caspases (caspase 2, 3, 6, 7, 8, 9, 10) and inflammatory caspases (caspase 1, 4, 5, 12). And the apoptotic caspases can be further classified into initiator caspases (caspase 2, 8, 9, 10) and effector caspases (caspase 3, 6, 7) according to their entry points into the apoptotic cascade [46,47].

Similar with most proteolytic enzymes, caspases initially reside as inactive zymogens known as procaspases, which are triggered into mature active form upon stimulation. During the process of apoptosis, the procaspase is cleaved into a small subunit and a large subunit through proteolysis. These two cleaved subunits further pattern into a heterotetramer as the active form of caspase.

The inactive initiator caspases are composed of an N-terminal prodomain and a catalytic domain (a large and a small subunit linked by a inter subunit). The prodomain, serving as an adaptor domain for protein interaction, can be characterised into a caspase activation and recruitment domain (CARD, caspase-1, 2, 4, 5, and 9) and a death effector domain (DED, caspase-8, 10). During the maturation, the prodomain is removed and the inter subunit loop forms an active heterotetramer. The active initiator caspases cleave inactive effector caspases into the large and small subunits resulting in two active sites of the executioner caspase dimer. Functional mature effector caspase subsequently coordinate their activities to demolish key structural proteins and activate other enzymes to induce apoptosis [48-50].

The synthetic caspase inhibitors are as well useful tools for analysis of caspase activity in cell death process. Active-site inhibitors as one kind of caspase inhibitors (such as zVAD-fmk, Q-VD (OMe)-OPh, VX-765) are designed based upon the binding and cleaving sites of caspase substrates [51].

### 1.3.1.2 The extrinsic apoptosis pathway

The extrinsic pathway is often described as receptor mediated pathway in which extracellular ligands bind to specific transmembrane death receptors and subsequently induce cell death [21, 22]. Death receptors belong to the tumour necrosis factor receptor superfamily (TNFRSF) with a broad range of biological activities in regulating cell death and immune response. All members in the TNF receptor super family are characterized with the extracellular cysteine rich domains (CRDs) which are responsible for recognition of ligands with specificity. Ligation of death receptors, including TNFR1, Fas (CD95) or DR4/5 (TRAIL1/2) receptors with corresponding ligands, leads to trimerization of receptors and further recruitment of cytosolic adaptor proteins through hydrophilic interaction mediated via the conserved intracellular death domains (Figure 3) [52]. Adaptor proteins, Fas-associated protein with death domain (FADD) and TNF receptor-associated death domain (TRADD), enable the cell death signalling transduce from the exterior stimuli to the interior signalling cascade via homotypic proteins interactions [53,54].

In CD95L-induced apoptosis, FADD is preassembled to Fas and in turn recruits procaspases (caspase 8, 10) through their homotypic DED-DED (death effector domain) interaction and form the death inducing signalling complex (DISC) (Figure 3) [55]. DISC thereby elevates the local amount of inactive procaspases 8 and subsequently leads to its activation through self-cleavage driven upon dimerization. Active caspase 8 releasing from the DISC complex is capable of activating downstream effector caspases, mainly caspase 3 and 7. Consequently, active effector caspases proteolytic cleave targeted cellular proteins (PARP-1) and finally ring the bell of cell death. In addition to proteolysis target proteins, caspase 3 is able to cleave X-linked inhibitor of apoptosis (XIAP), which synergistically strengthen the cell death procedure because of establishing a positive feedback loop of self-activation [56,57].

### 1.3.1.3 The intrinsic apoptosis pathway

The intrinsic pathway (or mitochondria-mediated pathway) of apoptosis, as its name suggests, requires the involvement of mitochondria. The intrinsic apoptosis can be initiated by a wide variety of stress stimuli that include irradiations, DNA damage agents, abnormal redox potential, growth factor deprivation, and virus infection [58,59]. These various stress stimuli can be sensed by related intra-organellar molecules and transduced to mitochondria leading to mitochondrial membrane adjustment (Figure 3). The main alterations of mitochondria are characterized with changes of mitochondrial outer membrane permeabilization (MOMP) which is tightly regulated by Bcl-2 (B-cell lymphoma 2) family proteins especially Bax and Bak. Increased MOMP enables release of soluble mitochondrial proteins residing between the outer and the inner mitochondrial membrane into the cytosol, including cytochrome *c*, second mitochondria-derived activator of caspases (Smac, also known as Diablo, direct IAP-associated binding protein with low pI), apoptosis inducing factor (AIF), high temperature requirement A2 (HtrA2) (Figure 3) [60-63]. Once released into cytosol, cytochrome *c* interacts with the adaptor molecule Apaf-1 (apoptosis protease activating factor) and further triggers the conformational change and subsequent oligomerization of Apaf-1. Oligomerized Apaf-1 recruit cytochrome *c* and caspase 9 through the CARD domain resulting in a cart-wheel shaped heptameric complex formation, named as apoptosome (Figure 3). Caspase 9 is cleaved and activated within the apoptosome. Consequently, active caspase 9 dissociates from the apoptosome and activate effector caspases (3, 6, and 7) which collectively orchestrate the execution of apoptosis [64-66]. In addition to cytochrome *c*, Smac, as natural inhibitor of IAPs through binding to functional baculovirus inhibitor repeat (BIR) motif in the cytosol, synergistically promotes caspase activation and apoptosis [67,68]. Furthermore, release of HtrA2 from mitochondria boosts apoptosis via inhibiting IAPs activities through its four most N-terminal amino acids [59]. Moreover, cytosol AIF, releasing from the mitochondrial membrane, and finally translocalizes to the cell nucleus where AIF promotes complete condensation and fragmentation of chromosomes to initiate

apoptosis (Figure 3) [59].

Even though the stimuli and most molecules involved in the intrinsic and the extrinsic apoptotic pathways are distinct, both pathways final converge at the activation of effector caspases. In addition, formation of DISC complex and caspase 8 activation lead to cleavage of Bid (tBid) and subsequent induction of intrinsic mitochondrial amplification loop. In the meanwhile, intrinsic pathway mediated release of Smac and HtrA2 increases death receptor-mediated apoptotic pathway through synergistically inhibition of XIAP and cIAPs [69-71]. Understanding the mechanism of apoptosis and its molecular mechanisms is important as it will help develop more effective therapeutic strategies against melanoma through increase pro-apoptotic proteins and inhibition of ant-apoptotic molecules.

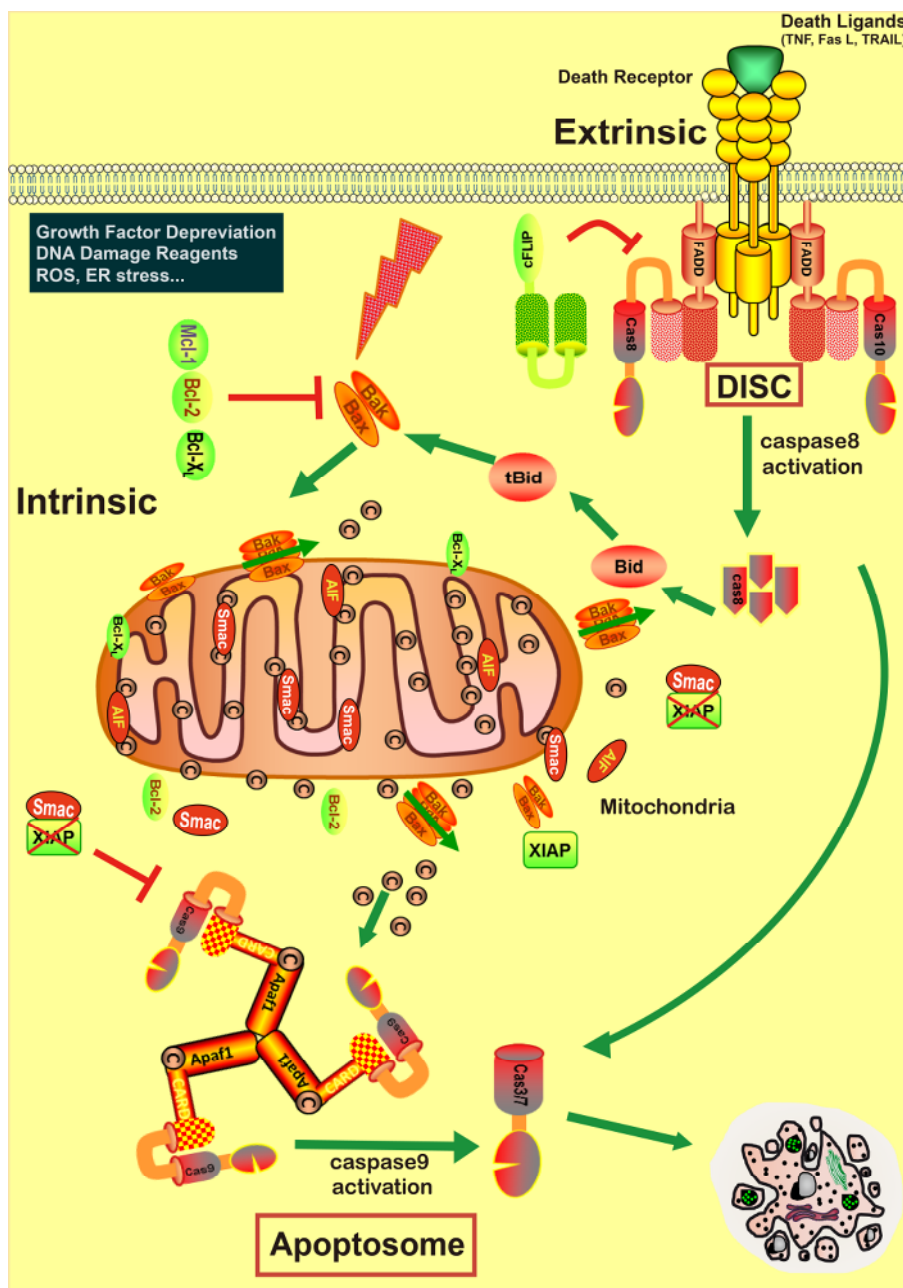


**Figure 3 Molecular mechanisms of the crosstalk between intrinsic and extrinsic**

**signalling pathways in apoptosis.** The extrinsic cell death pathway is mediated by binding of cytokines (TRAIL, CD95L, TNF) to the respective death receptors followed by formation of intracellular protein signalling platforms (DISC or TNF-R1 complex I). Activated caspase 8 within the DISC promotes cleavage of Bid to a truncated Bid protein (tBid) that links both cell death signalling pathways. The intrinsic pathway is further induced via diverse intracellular stress signals that lead to release of cytochrome *c* and formation of the apoptosome that finally promotes effector caspases activation.

### 1.3.2 Necroptosis

Necrosis had been regarded as a form of accidental and passive cell death that resulted from external injury until recently. Accumulating evidences suggest that a cell can initiate demise program through necrosis in a regulated manner under extrinsic or intrinsic stimuli. As an alternative form of programmed cell death, programmed necrosis was firstly proposed in 1988 in which TNF was found able to induce both apoptosis and necrosis depending on cell types [72]. The existence of regulated necrosis was further confirmed with the discovery of serine/threonine kinase RIPK1 dependence in CD95L-induced necrosis of Jurkat cells [73]. In addition, Chan, *et al.* in 2003 introduced the term “programmed necrosis or necroptosis” to depict the role of TNFR2 in anti-viral response. Another milestone in comprehension of the process of regulated necrosis is the revelation of RIPK3 and MLKL which are the determinant factors for necroptosis induction [74-77]. Necroptotic cells share common morphological characteristics with necrotic cells, including increased cell volume, swelling of organelles, and disruption of the plasma membrane and release of the intracellular components. Unlike apoptosis, although the nuclei of necroptotic cells remain intact instead of breakdown into small bodies, the integrity of nuclear membranes is disrupted [78,79].

#### 1.3.2.1 Stimuli for Necroptosis

Tumour necrosis factor (TNF) is most frequently used stimuli for necroptotic cell death induction and its mechanism investigation. Whenever caspase 8 is blocked by its chemical inhibitors or gene deletion, TNF is able to induce necroptosis in a wide variety of cell lines and primary cells. Moreover, antagonists of cellular inhibitor of apoptosis proteins (cIAPs) can notably improve the necroptotic cell death [80-82]. In addition to TNF, ligation of CD95, TRAILR to their respective ligands can induce necroptosis in ways quite similar to TNF [73,83]. Moreover, double-stranded viral RNA and lipopolysaccharide (LPS) as ligands for Toll-like receptor 3 and 4 (TLR3/4) respectively are able to trigger the necroptosis in macrophages when caspase 8 is suppressed by caspase inhibitors [76,84]. Interferons have also been proved to possess the ability to induce necroptosis in different cell types [85-87]. In addition to biological stimuli, some physical or chemical stress can also promote necroptosis, including ionic radiation, photodynamic therapy, calcium overload and anti-cancer chemicals as obatoclax, doxorubicin and etoposide [88,89].

### 1.3.2.2 Molecular mechanism of necroptosis

RIPK1 and RIPK3, as receptor-interacting serine/threonine kinases (RIPKs), are critical regulators for necroptosis execution. In respect of molecular structure, RIPK1 and RIPK3 share common characteristics: an N-terminal homologous kinase domain and a RIP homotypic interaction motif (RHIM). Exclusively in RIPK1, there contains a C-terminal death domain that is responsible for RIPK1 interaction with TRADD and cIAPs [90,91].

The most well studied model of necroptosis is mediated by TNF stimulation. Upon ligation with TNF, TNFR1 changes its conformation for trimerization and further recruits TRADD, which in turn interacts with TNF receptor-associated factor 2 (TRAF2) and TRAF5, RIPK1, and cIAP1/2, termed as TNF complex I [92-95] (Figure 4). In complex I, RIPK1 is K63-polyubiquitinated by cIAP1/2 without weakening its kinase activity. Poly-ubiquitinated RIPK1 in turn serves as a scaffold for the assembly of the transforming growth factor- $\beta$ -activated kinase-1 (TAK1)-TAK-1 binding protein 2 and 3 (TAB2/3) complex, which primarily leads to the activation of the transcription factor nuclear factor  $\kappa$ B (NF- $\kappa$ B) [96,97]. When the K63-ubiquitination of RIPK1 is removed or blocked by deubiquitinases cylindromatosis (CYLD) or IAP antagonist, complex I dissects from plasma membrane and internalized into cytoplasm and form TNF Complex IIa, containing TRAF2, RIPK1, TRADD, caspase 8, cFLIP and FADD [92,98]. On the other hand, Feoktistova, *et al.* and Tenev, *et al.* propose that loss of IAPs is sufficient to promote the other complex formation in absence of death ligands, termed as Ripoptosome, (Figure 4) which includes RIPK1, caspase10, caspase-8, cFLIP and FADD to induce apoptosis [99,100]. Moreover, initiation of TLR signalling enables the interaction of RIPK1 and TRIF as a cell death inducing complex. If RIPK3 expresses normally, it will be integrated into both complexes though interaction with RIPK1 [73,74,101].

In the absence of caspase 8 activity, RIPK1 and RIPK3 keep intact from caspase 8 mediated cleavage and interact through the RHIM domain to assemble a complex with MLKL (mixed lineage kinase-domain like), named as necrosome (Figure 4). In necrosome, RIPK1 and RIPK3 utilize kinase activity to phosphorylate each other and phosphorylated RIPK3 subsequently initiates the phosphorylation of MLKL. MLKL contains a C-terminal pseudokinase domain and an N-terminal four-helix bundle (4HB) domain connected by brace domain [102]. Once phosphorylated, the pseudo kinase domain performs a conformational change of MLKL resulting in exposure of the  $\alpha$ -helix of 4HB domain and promotes MLKL oligomerization through the brace domain. Oligomerized MLKL is translocated to plasma membrane to disrupt the membrane integrity [103,104]. Several explanations have been made to uncover the molecular mechanism for how MLKL oligomer induces necroptosis. Cai and his colleagues hold that MLKL oligomerization activates the calcium channel protein (Tpm7) and cause calcium influx [105]. Chen, *et al.* prove the role of increased sodium influx in necroptotic cell death [106]. Several studies also establish the connection between the oligomerized MLKL and ability to bind

negatively charged lipids in the membrane, which facilitates the disintegration of plasma membrane [107-109].

Due to their essential role of RIP kinases (RIPKs) in propagation and regulation of programmed necrosis, several RIPKs specific inhibitors have been developed, including Necrostatin-1, 7-Cl-O-Nec-1, GSK'481, GSK'963 as RIPK1 inhibitors [110] and GSK'840, GSK'843, GSK'872 as RIPK3 inhibitors [111]. These inhibitors allow us to explore the role of necroptosis in various physiological process and diseases, including cell death resistance, inflammation, infection ischemia-reperfusion damage, and degenerative diseases and cancer.

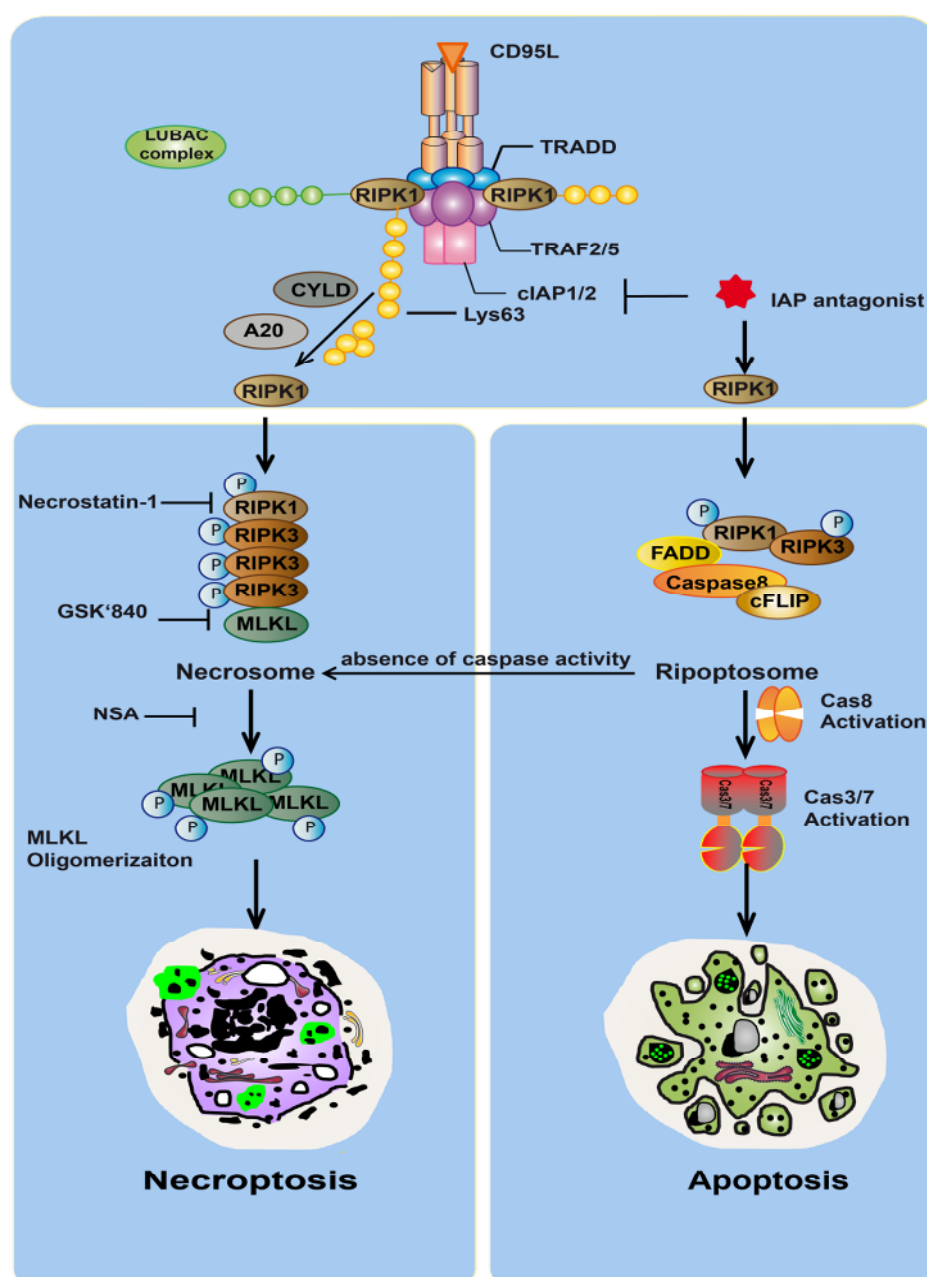


**Figure 4** The role of molecular signalling platforms for transmission of

**apoptotic and necroptotic cell death.** In absence of cIAPs, membrane-associated complex I dissects into cytosol and promotes necrosome formation to induce necroptosis. IAP antagonist initiate Ripoptosome assemble and initiated apoptosis and necroptosis in absence of caspases activities.

### 1.3.3 Regulatory effect of IAPs on programmed cell death

Melanoma has acquired death resistance during the process of development and metastasis. IAP proteins are initially identified as cell death inhibitors in baculovirus since they are able to inhibit virus induced apoptosis and allow viral amplification in their host cells. With the assistance of bioinformatics, 8 human IAP proteins are uncovered, including XIAP, cIAP1, cIAP2, NAIP, Survivin, ML-IAP, Apollon and ILP2 [112]. XIAP, cIAP1 and cIAP2, which share structural similarities, are well-studied in IAP family. Structurally, there exist an N-terminal three copies of ~70 amino acids zinc-binding baculovirus IAP repeat (BIR) that is required for interaction with caspases and other pro-apoptotic proteins to execute its inhibitory effect. In C-terminal there is a carboxyl-terminal RING domain that is characterized with E3 ubiquitin protein ligase activity. An ubiquitin associated (UBA) domain enables XIAP and cIAPs associate with mono-ubiquitin and poly-ubiquitin chains and add ubiquitin chains to target proteins for proteasome-mediated degradation. In addition, the cIAPs possess a caspase-recruitment domain (CARD) that is responsible for the interaction with adaptor proteins and caspases [113-116].

As the nature always keeps balance for adjustment of dominant cellular procedures, the natural inhibitor of IAP proteins, Smac/Diablo is found by XIAP co-immunoprecipitation [117,118]. Smac interacts with the groove in the BIRs of XIAP and cIAP1 via its N-terminal motif to restrain the inhibitory effect of IAPs on caspases [119]. This mechanism is applied in designing Smac mimetics, such as compound A (Figure 5). Compound A has an amino terminal methyl alanine and equivalent binding affinity to XIAP and cIAP1 in the picomolar range. Compound A promotes degradation of cIAP1 and cIAP2, and block XIAP activity without influencing its expression [120]. In addition to inhibitory effect on IAPs, Compound A is able to induce TNF-dependent cell death in some cell lines [120-122].

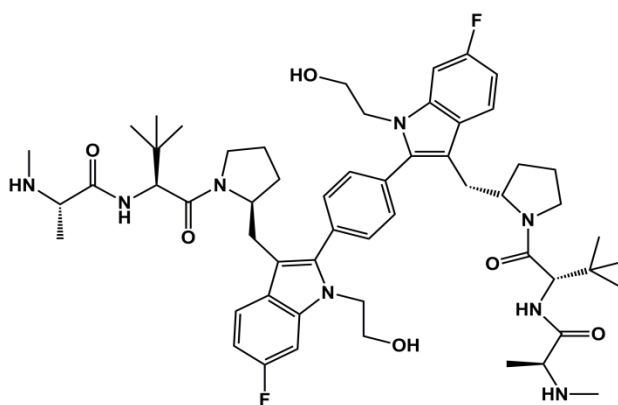


**Figure 5** Chemical structure of Compound A

## 1.4 Suppression of gene expression and cell death via DNA methylation

DNA methylation as one common form of epigenetic modification was firstly proposed in 1980s [123,124]. During mammalian development, DNA methylation is involved in the X chromosome inactivation, genomic imprinting and silencing of repetitive DNA [125]. Approximately 28 million CpGs are estimated in the human genome and 60–80% of them are methylated [126]. When DNA methylation occurs abnormally, it results in various human diseases, including cancer, imprinting disorders, centromeric instability, immunodeficiency, facial anomalies syndrome, Beckwith-Wiedemann syndrome, Prader-Willi syndrome, and Angelman syndrome [127].

During the process of eukaryotic DNA methylation, methyl groups of S-adenosine-methionine (SAM) are added to the cytosine nucleotides of DNA by DNA methyltransferases (DNMTs). The modified cytosine residues usually become adjoining to a guanine nucleotide and lead to methylation of cytosine residing diagonally on opposing DNA strand [128]. Functionally, DNA methylation serves as an epigenetic tool to lock genes in the “off” position. In terms of tumours, their genome displays global hypo-methylation and promoter hyper-methylation of specific genes. Global hypo-methylation frequently at repetitive genomic regions results in weakening genomic stability. Hyper-methylation of tumour suppressor genes leads to expression suppression [129]. In melanoma, more than 70 abnormal hyper-methylated genes have been identified via direct CpG islands methylation screen [130]. It has been demonstrated that *de novo* methylation happens in the early phase of carcinogenesis and can be detected in sputum, serum and urine. *PTEN*, *SOCS1/2*, *CDKN2a*, *RASSF1a* and *MGMT* are reported with aberrant methylation detected from peripheral blood of melanoma patients [131-133]. Furthermore, level of DNA methylation is considered to be related with melanoma progression [134]. These breakthroughs might initiate DNA methylation as a promising marker for melanoma detection and prognosis.

When it comes to the detection of DNA methylation, modifications of DNA samples is a prerequisite to differentiate normal cytosine from its methylated counterpart. Restriction enzyme digestion in combination with high-performance capillary electrophoresis (HPCE) or high-precision liquid chromatography (HPLC) is used to estimate the global content of methylation. Methylated DNA immunoprecipitation using 5mC-specific antibodies is applied to enrich the methylated DNA for further sequencing. Methylation specific PCR (MSP) and sequencing were developed to detect locus-specific DNA methylation after bisulfite converted unmethylated cytosine into uracil without change of methylated cytosine. Introduction of microarray technologies makes simultaneous analysis of thousands of regions of interest accessible. Technological advances in the past two decades have rendered comprehensive understanding of DNA methylation. [135].

Since hyper methylation is responsible for silencing of tumour suppressor genes, effort has been made to investigate DNA methylation inhibitors as anticancer drugs. 5-azacytidine (Vidaza) and 5-aza-2'-deoxycytidine (Dacogen) were approved by the Food and Drug Administration as epigenetic anticancer agents in 2004 and 2006 respectively. Solid tumour size reduction was observed upon 5-azaC treatment in breast and spleen tumour mouse models [136,137]. Lindner, *et al.* also reported the anti-vascularization as well as the anti-proliferative ability of 5-azadC in melanoma [138]. In brief, demethylation reagents are indispensable in comprehension of DNA methylation and clinical cancer treatment.

## 1.5 Regulation of programmed cell death by NF- $\kappa$ B signalling pathway

### 1.5.1 NF- $\kappa$ B signalling pathway

The nuclear factor- $\kappa$ B (NF- $\kappa$ B) transcription factor family has been known as principal regulator in responses to a variety of endogenous and exogenous stimuli. Mammalian NF- $\kappa$ B is consisted of five homologous proteins including RelA (p65), RelB, c-Rel, NF- $\kappa$ B1 p105/p50, and NF- $\kappa$ B2 p100/p52. All NF- $\kappa$ B members share a highly conserved Rel homology domain (RHD) at the N-terminus which is responsible for homo- or hetero-dimerization, nucleus translocalization, consensus DNA sites binding. The RHD domain also enables interaction with inhibitory I $\kappa$ B proteins. In addition, RelA, RelB, and c-Rel share a C-terminal transactivation domain (TAD) that renders them ability to activate target genes expression [139,140]. The activation of NF- $\kappa$ B cascades are characterized into canonical and non-canonical pathway in response to various stimuli.

The canonical pathway is usually initiated by pro-inflammatory and mitogenic stimulants such as death ligands, lipopolysaccharides (LPS), interleukin-1 (IL-1). In the TNF $\alpha$ -mediated NF- $\kappa$ B activation, RIPK1, cIAP1/2, TRAF2/5, and TRADD are recruited to TNFR1 to assemble complex I at the plasma membrane. Within complex I, cIAP1/2 add K63-linked ubiquitin chains to RIPK1 serving as a docking site for TAK1 and TAB2/3. Different stimuli for NF- $\kappa$ B activation converge at activation of a 700-900 kDa trimeric serine-specific I $\kappa$ B kinase (IKK) complex comprised of the catalytic subunit IKK $\alpha$  and IKK $\beta$  and the regulatory subunit IKK $\gamma$  (NEMO). The activation of IKK complex by phosphorylation results in phosphorylation of I $\kappa$ B $\alpha$  allowing its K48-linked ubiquitination and subsequent proteasome degradation [141,142]. When cells are in resting state, cytosolic NF- $\kappa$ B p50/p65 dimers are binding to inhibitory I $\kappa$ B $\alpha$  leading to mask the nuclear translocation signal. Dissociation of I $\kappa$ B $\alpha$  from p50/p65 complex enables entry of this complex into the nucleus and its binding to NF- $\kappa$ B DNA sites, which consequently promotes transcriptional activation of a wide variety of genes involved in immune and inflammatory responses, cell survival and death [143].

A collection of genetic evidence lead to the discovery of the non-canonical NF- $\kappa$ B pathway that is usually triggered by a subset of TNFRS members, including B cell activating factor receptor (BAFF-R), CD40, Fn14, receptor activator of NF- $\kappa$ B (RANK) and TNF-related weak inducer of apoptosis (TWEAK) receptor [143,144]. NIK, known as a constitutive kinase, is usually degraded because of coordinated activity of TRAF2/3 and cIAP1/2 [145,146]. The non-canonical NF- $\kappa$ B signalling requires NIK stabilization and subsequent activation of IKK $\alpha$  to phosphorylate p100, which is in turn ubiquitinated and proteasomal processed into p52. Together with RelB, p52 translocates to the nucleus and drives the transcription of a panel of genes.

### 1.5.2 Regulatory effect of NF- $\kappa$ B on programmed cell death

NF- $\kappa$ B, as a family of transcription factors, is involved in cell death regulation by initiating related genes expression among other targets.

Initially, NF- $\kappa$ B activation is considered as negative regulatory signalling for cell death. It has been demonstrated by several studies that NF- $\kappa$ B activation is able to inhibit cell death induced by distinctive stimuli in a wide variety of cells. NF- $\kappa$ B activation exerts its inhibitory effect on cell death by inducing the transcription of anti-apoptotic genes or genes that negatively regulate cell death. NF- $\kappa$ B activation promotes expression of pro-survival Bcl-2 members, including A1, Bcl-xL, Bcl-2 [143]. In addition, NF- $\kappa$ B blocks cell death through repression of pro-apoptosis proteins, such as Bax and Bim in some cells. IAPs, cFLIP, TRAF1 and TRAF2, as inhibitory components for both apoptosis and necroptosis, are upregulated when NF- $\kappa$ B activates. In addition, NF- $\kappa$ B activation also increases expression of ubiquitin-edit enzymes including A20 and CYLD. By expression of direct cell death inhibitors or indirect cell death regulators, NF- $\kappa$ B protects cells from death [139,147,148]. Moreover, a variety of studies have proved that activation of nuclear factor-kappa B (NF- $\kappa$ B) is involved in the tumour progression and metastasis of melanoma [148-151].

Although NF- $\kappa$ B mainly exhibits inhibitory effect on cell death in most cases, it can behave in an anti-survival manner in some instances. Cytokines and chemokines production including interleukins, interferons, TNF, TRAIL and Fas ligand which are tightly related with immune response are increase upon NF- $\kappa$ B activation [152].

## 2. Materials and Methods

### 2.1 Chemicals and Buffers

Table 1 Chemicals for buffer solution

Chemicals	Company	Catalog No.
4-(2-Aminoethyl)-benzene sulfonyl fluoride (AEBSF) hydrochloride	AppliChem	A1421
Ampicillin sodium salt	Roth	K029.1
Aprotinin	Roth	A162.3
Bis-Tris	AppliChem	A1025,0500
Bovine serum albumin (BSA)	Santa Cruz	sc 2323A
Bromophenol blue	Sigma-Aldrich	B8026
Calcium chloride dihydrate ( $\text{CaCl}_2 \cdot 2\text{H}_2\text{O}$ )	Sigma-Aldrich	C3306
cOmplete™ protease inhibitor cocktail tablets	Roche	11836145001
Crystal violet	AppliChem	A0691.0250
di-Sodium hydrogen phosphate dihydrate	Roth	4984.1
Dithiothreitol (DTT)	AppliChem	A2948.0025
Ethanol denatured ( $\geq 99.8\%$ )	Roth	K928.4
70% Ethanol denatured	Roth	T913.2
FACS shutdown solution	BD Biosciences	334224
FACS flow sheath fluid	BD Biosciences	342003
Glycerin ROTIPURAN®	Roth	3783.2
HEPES	Sigma-Aldrich	H3375-1KG
Hoechst 3342	Polysciences	09460-100
Methanol analaR NORMAPUR®	VWR	20847.360
MOPS for buffer solutions	AppliChem	A1076,1000
Leupeptin	Sigma-Aldrich	L2884
Potassium dihydrogen phosphate ( $\text{KH}_2\text{PO}_4$ )	Roth	3904.1
Potassium chloride (KCl)	Roth	6781.3

Propidium iodide (PI)	Sigma-Aldrich	81845-100MG
SDS Pellets	Roth	CN30.3
Skim milk powder	Sigma-Aldrich	70166-500G
Sodium chloride (NaCl)	Roth	3957.2
Sodium citrate dihydrate (C <sub>6</sub> H <sub>5</sub> Na <sub>3</sub> O <sub>7</sub> ·2H <sub>2</sub> O)	Sigma-Aldrich	W302600
Sodium hydroxide (NaOH) solution (5M)	Roth	KK71.1
Sodium orthovanadate (Na <sub>3</sub> VO <sub>4</sub> )	Sigma-Aldrich	S6508
SYTOX <sup>®</sup> Green nucleic acid stain	Life technologies	S7020
Tris ultrapure	AppliChem	A1086,1000
Triton X-100	AppliChem	A1388,0500
Tween 20	Roth	9127.3
β-Glycerophosphate disodium salt hydrate	Sigma-Aldrich	G9422-10G
β-Mercaptoethanol	Merck Millipore	805740
LB-Agar (Lennox)	Roth	X965.2
LB-Medium (Lennox)	Roth	X964.2

Table 2 Buffer composition

Buffer	Ingredients
<b>10X Annexin V binding Buffer</b>	0.1 M HEPES (pH 7.4), 1.4 M NaCl, 25 mM CaCl <sub>2</sub> solution
<b>Blocking Buffer</b>	5% (w/v) non-fat dry milk, 3%(w/v) BSA in 1X T-PBS
<b>Crystal violet staining solution</b>	0.5% (w/v) crystal violet powder, 20% (v/v) methanol
<b>2X HBS Buffer (pH7.05)</b>	280 mM NaCl, 50 mM HEPES, 1.5 mM Na <sub>2</sub> HPO <sub>4</sub>
<b>5X Laemmli Buffer</b>	60 mM Tris-HCl (pH 6.8), 2% (w/v) SDS, 10% (v/v) Glycerol, 5% (v/v) β-Mercaptoethanol, 0.01% (w/v) Bromophenol blue
<b>Lysis Buffer</b>	30 mM Tris-HCl (pH 7.5), 120 mM NaCl, 10% (v/v) Glycerol, 1% (v/v) Triton X-100, 2 tablets Complete protease Inhibitor cocktail per 100 ml
<b>1X PBS Buffer (pH 7.4)</b>	2.7 mM KCl, 1.5 mM KH <sub>2</sub> PO <sub>4</sub> , 137 mM NaCl, 8 mM Na <sub>2</sub> HPO <sub>4</sub>

<b>1X PBS-T</b>	1X PBS, 0.1%(v/v) Tween
<b>MOPS Buffer (pH 7.7)</b>	50 mM MOPS, 50 mM Tris-base, 0.1% (w/v) SDS, 1 mM EDTA
<b>Triton lysis buffer for phosphoprotein assays</b>	20 mM Tris (pH 7.4), 1% (v/v) Triton X-100, 10% (v/v) glycerol, 137 mM NaCl, 2 mM EDTA, 50 mM $\beta$ -Glycerophosphate disodium salt hydrate, 1mM sodium orthovanadate; Before use, added, 1 mM ABSF, 5 $\mu$ g/ml aprotinin, 5 $\mu$ g/ml Leupeptin hemisulfate salt, 5 mM benzamidine.

Table 3 Reagents and Kits

<b>Reagents and Kits</b>	<b>company</b>	<b>Catalog No.</b>
Agarose (low melt)	Roth	6351.5
Blood & Cell culture DNA Mini kit	QIAGEN	13323
dNTPs mix (10 mM)	Thermo Scientific	R0193
GeneRuler 1 kb DNA ladder	Thermo Scientific	SM0312
GeneRuler 100 bp DNA ladder	Thermo Scientific	SM0242
iBlot 2 Transfer stacks	Life technologies	IB24001
KAPA SYBR FAST Universal	Peqlab	07-KK4600-03
Luminata Forte Western HRP substrate	Merck Millipore	WBLUF0500
Nancy-520	Sigma-Aldrich	01494
NuPAGE Novex 4-12 % Bis-Tris Protein Gels	Invitrogen	NP0329BOX
PerCP/Cy5.5 Annexin V	Biolegend	640936
PageRuler prestained protein ladder	Life technologies	26617
Pierce ECL Western Blotting substrate	Thermo Scientific	32106
Protein Assay Reagent A	Bio-Rad	5000113
Protein Assay Reagent B	Bio-Rad	5000114
Protein Assay Reagent S	Bio-Rad	5000115
Protein G agarose beads	Roche	05015952001
Restore Western Blot stripping buffer	Thermo Scientific	21063
RNaseOUT recombinant ribonuclease inhibitor	Invitrogen	10777-019

SuperScript II reverse transcriptase	Invitrogen	18064-071
E.Z.N.A. FastFilter plasmid Maxi kit	OMEGA	D6924-04
Microlance™ needles (No.27G)	Becton Dickinson	BD300645
EZ DNA METHYLATION™ kit	ZYMO Research	D5001

## 2.2 Methods

### 2.2.1 Cell culture

Human melanoma cell lines: A375, PM-WK, RPM-MC, RPM-EP, SK-MEL28, PREYER, MeWo, IGR, MM-RU, MM-AN, MM-LH, WM1346;

Spontaneously transformed aneuploid immortal keratinocyte cell line: HaCaT;

Human Primary melanocytes: #19, #20;

Human Primary nevus cells: #5, #8;

Murine melanoma cell lines: Ret1, Ret2, HcMel3, HcMel12, HcMel31;

Murine immortalized keratinocytes

Table 4 Cell culture medium and related reagents

Medium and Reagents	Company	Catalog No
Dimethyl sulfoxide (DMSO)	Sigma-Aldrich	H7904
Dulbecco's Modified Eagle Medium (DMEM), GlutaMax, high Glucose	Gibco	61965-059
Dulbecco's phosphate-buffered salines (DPBS)	Gibco	14040-174
Ethylenediaminetetraacetic acid (EDTA)	Merck Millipore	L2113
Fetal bovine serum (FBS)	Gibco	10270-106
HEPES solution (1 M, pH 7.0-7.6)	Sigma-Aldrich	H0887
Hygromycin B	A&E Scientific	P21-014
Lipofectamine® 2000 Transfection Reagent	Invitrogen	11668-019
Melanocyte Growth Medium (Ready-to-use)	Promocell	C-24010
PCT Epidermal Keratinocyte Medium	CELLnTEC	CnT-07
Opti-MEM® I Reduced Serum Medium	Gibco	31985-047

Polybrene (Hexadimethrine bromide)	Sigma-Aldrich	H9268-5G
Puromycin dihydrochloride	Gibco	A11138-03
RPMI1640 medium	Gibco	21875-091
Sodium pyruvate	Gibco	11360-088
Trypsin (2.5%, 10X)	Invitrogen	15090-046
Zeocin™ selection reagent	Gibco	R250-01
(Z)-4-Hydroxytamoxifen (4-HT)	Sigma-Aldrich	H7904

Human melanoma cells and transformed keratinocytes were cultured in DMEM medium containing 10% FBS, 1% HEPES, 1% sodium pyruvate, and 1% MEM amino acids at 37°C in 5% CO<sub>2</sub>. Human primary melanocytes and nevus cells were cultured in melanocytes growth medium with its supplement medium at 37°C in 5% CO<sub>2</sub>. Murine Melanoma cell lines were cultured in RPMI 1640 medium containing 10% FBS, 1% HEPES, 1% sodium pyruvate, and 1% MEM amino acids at 37°C in 5% CO<sub>2</sub>. Murine immortalized keratinocytes were cultured in PCT epidermal keratinocyte medium containing respective supplements and 10% chelex treated FBS at 37°C in 5% CO<sub>2</sub>.

Cells were trypsinized for further subculture or experimental purposes. Cells were washed by DPBS and detached using 2.5% trypsin for 5 minutes. Medium containing 10% FBS was used to neutralize trypsin and make homogenous cell suspension. To collect cell pellets, cell suspension was spun down at 400 x g for 5 minutes at room temperature. Following discarding supernatant, cell pellets were resuspended with fresh medium for culturing or experimental use.

### 2.2.2 Cell death assay

Cells were pretreated or treated with following reagents alone or in combinations as indicated. Then cell death was analysed with following methods:

Table 5 Cytokines and inhibitors

Item	Source	Catalog No.
CD95L-Fc	M. Feoktistova [153]	
z-Val-Ala-DL-Asp-fluoromethylketone (zVAD-fmk)	Bachem	N15100025
5-Aza-2'-deoxytidine	Sigma-Aldrich	A3656-10MG
Necrostatin-1	Sigma-Aldrich	N9037-25MG

---

Necrosulfonamide (NSA)	Merck Millipore	480073-25MG
Compound A (IAP antagonist)	Tetralogics	
GSK'481	Glaxo Smith Kline	
7-Cl-O-Nec-1	Glaxo Smith Kline	
GSK'840	Glaxo Smith Kline	
GSK'872	Glaxo Smith Kline	
Dabrafenib	Selleckchem	S2807
Vemurafenib	Selleckchem	S1267

---

### 2.2.2.1 Crystal Violet staining

Crystal violet solution was used to stain attached, living cells following stimulation.  $1 \times 10^4$  cells were seeded into 96-well plates one day before stimulation. Then cells were treated with the indicated concentrations of stimulating agents in absence or presence of inhibitors in 96-well plates overnight. Before staining, plates were gently washed with PBS twice. Subsequently, 50  $\mu$ l of crystal violet staining solution (Table 2) were added per well and the plates were stained on a shaker for 30 minutes at room temperature. After incubation, plates were washed with water to remove the non-intercalated crystal violet. Plates were air dried, and then 200  $\mu$ l methanol (Table 2) was added per well followed by 30min incubation at RT to solve the incorporated dye. The optical density (OD) of the samples was measured with Victor<sup>3</sup>™ Multilabel Reader (Perkin Elmer). The OD of control (cells treated with diluents) was normalized to 100% and compared with stimulated cells. For statistical analysis, the Standard Error of Mean (S.E.M.) was determined for at least of medium of three independent experiments of each cell line and stimulatory condition.

### 2.2.2.2 Annexin V/PI staining

To detect the externalization of phosphatidylserine to the outer plasma membrane and change of permeability of nuclear membrane during cell death, Annexin V/PI dual staining was used. Firstly,  $2 \times 10^5$  cells were seeded into 6-well plate per well. Cells stimulated with indicated reagents as described. After overnight stimulation, cells were collected by trypsinization, washed twice in 1X PBS (Table 2), and resuspended in 100  $\mu$ l Annexin V binding buffer (Table 2) at a cellular concentration of  $1 \times 10^6$  cells/ml. 5  $\mu$ l Annexin V-Cy5 and 5  $\mu$ l PI (Table 2) were added to cell suspension and incubated for 15 min at RT in the dark after mixing. 400  $\mu$ l Annexin binding buffer was added to the samples before they were analysed via flow cytometry and the FACSCanto™ II (BD Biosciences).

### 2.2.2.3 Hoechst 33342 and SYTOX<sup>®</sup> Green dual staining

To detect the nuclear morphology and the integrity of the plasma membrane,  $5 \times 10^4$  cells of the respective cell lines were seeded per well into a 12-well plate. Next day, cells were stimulated as indicated concentrations overnight. 8 hours later, cells were stained with Hoechst 33342 (5  $\mu\text{g/ml}$ ) and SYTOX<sup>®</sup> Green (5 pM) (Table 1) for 15min at 37°C and then visualized with phase contrast Axio Observer Z1 (Zeiss) fluorescence microscopy.

### 2.2.3 Plasmid transformation and isolation

To expand the amount of plasmids of interest (Table 6), chemically competent TOP10 *E.Coli* cells were incubated with plasmids for 30 minutes. Then the mixture was heat shocked at 42°C for 45 seconds and put back in ice again for 3 minutes. Followed by adding 500  $\mu\text{l}$  SOC medium without antibiotic, competent cells/DNA mixture was further cultured in shaking incubator at 37°C for 45 minutes. Transformation product was plated on pre-warmed LB agar plates containing appropriate antibiotics at 37°C overnight. After successful transformation, single colony were picked and further cultured in Erlenmeyer flask containing 200 ml LB medium (Table 1) with antibiotics 37°C overnight. Plasmid was isolated and purified with the E.Z.N.A Fastfilter Plasmid Maxi Kit (Omega) according to the manual. The concentration of plasmid was measured using a NanoDrop 2000<sup>™</sup> (ThermoFisher SCIENTIFIC) spectrophotometer.

Table 6 Plasmids

Vector	Antibiotic	Inserts
pCFG5-IEGZ	Ampicillin, Zeocin	RIPK3; RIPK3KD
pFGEV16-Super-PGKHygro	Ampicillin, Hygromycin B	
pF 5 $\times$ UAS W SV40 Puro (L27)	Ampicillin, Puromycin	IKK2EE; IKK2KD

### 2.2.4 Ca-phosphate mediated transfection of lentiviral or retroviral DNA and virus production

HEK293T cells or  $\Phi\text{NX-AMPHO}$  cells (amphotrophic producer cell line) were grown into 10 cm plates with  $3 \times 10^6$  cells per plate. Then the medium was freshened with 6 ml of respective medium containing 25  $\mu\text{M}$  Chloroquine per plate at 37°C in 5%  $\text{CO}_2$ . To generate Ca-Phosphate-DNA complex precipitates, 20  $\mu\text{g}$  retroviral DNA or 10  $\mu\text{g}$  lentiviral with 3  $\mu\text{g}$  pMD2.G, 7.5  $\mu\text{g}$  pSPax2, and 3  $\mu\text{g}$  pcDNA3.1/p35 were mixed up with  $\text{CaCl}_2$  respectively to 500  $\mu\text{l}$  as final volume per plate. The formed complex mix was dropwise added into the 500  $\mu\text{l}$  2X HBS buffer (Table 2) with air blowing. Followed by 30 minutes incubation at RT, the mix was dropwise added to

the cells and incubated over night at 37°C in 5% CO<sub>2</sub> atmosphere. The supernatant containing lentiviral or retroviral particle of 48 hour and 72 hour post-transfection were collected, filtered (0.45 µm), shock frozen by liquid nitrogen and stored at -80°C for future use. All steps described were completed according to the safety class 2 requirements.

### 2.2.5 Retroviral and lentiviral transduction

The supernatants containing viral particles (from method 2.2.4) and 5 µg/ml polybrene (Table 4) were added to cells of interest. Target cells were spin-transfected at 2300 rpm for 90 minutes at 30°C. Next day cells were washed and freshened with new medium. Stable cell lines were selected with respective antibiotics. For the inducible protein expression the transduced cells were stimulated with 100 nM 4-HT (4-Hydroxytamoxifen, Table 4) for 24h. Western blot analyses were performed to confirm ectopic expression of the respective molecules.

### 2.2.6 CD95 Receptor staining

2x 10<sup>5</sup> cells of interest were seeded in 6-well plates and incubate for 24 hours. Cell pellets were harvested by trypsinisation. Then cells pellets were washed once with PBS and resuspended with 100 µl FACS buffer followed by addition of anti-CD95 primary antibody (Table 7) to 10 µg/ml for 1 h at 4 °C. The cells were washed with PBS and resuspended with 100 µl FACS buffer containing 1 µl of the secondary antibodies (anti-mouse IgG1-Biotin). Samples were incubated for 30 min at 4 °C and again washed with PBS. Then, 100 µl FACS buffer containing 1µl of the tertiary staining reagent (PE-Cy5 Streptavidin) was added to the cells and the samples were incubated for 30 min at 4 °C. Cells were again washed with PBS, dissolved in 500 µl FACS buffer, and measurement was performed via flow cytometry and the FACS Canto II as described above.

### 2.2.7 Western blot analysis

#### 2.2.7.1 Cell lysate preparation

For generation of total cell lysates, cells were collected by trypsinisation, washed twice with ice-cold 1X PBS and lysed for 1 hour on ice by the addition of cell lysis buffer (Table 2). Cellular debris was removed by centrifugation at 20,000 x g for 30 min at 4°C. The total amounts of isolated cell proteins were quantified by Bradford assay as described below. 5 µg of total cellular proteins was supplemented with 5X Laemmli sample buffer (Table 2) and denatured at 95°C for 5-10 min.

For analysis of phosphorylated proteins, the respective cells were starved in serum free medium for 6 h to get rid of the basal phosphorylation activated by addition of FBS. Then the cells were scraped from the plate and resuspended in phosphor-lysis buffer containing phosphatase inhibitors (Table 2). To quickly disrupt the cell membranes the lysates were homogenized by pushing three times through a syringe

with 0.4 mm Microlance needle, followed by 20,000 x g centrifugation for 30min.

### 2.2.7.2 Protein concentration determination

Protein concentration was measured using the DC™ Protein Assay (BioRad) according to instructions. In brief, 5 µl protein lysate was added to a 96-well plate. Then 25 µl reagents S' (A:S 50:1) were added to each cell followed by addition of 200 µl reagents B. The plate was mixed at room temperature and measured at 750 nm using VICTOR<sup>3</sup>™ 1420 Multilable Reader (Perkin Elmer).

### 2.2.7.3 Western Blot analysis

Total lysates were loaded on NuPAGE 4-12% BisTris gradient gels (Table 2) and proteins were separate using MOPS running buffer (Table 2). PageRuler prestained protein ladder (Table 3) was loaded on the same gel as a standard for protein separation and molecular weight.

Proteins were transferred to PVDF (polyvinylidene difluoride) membrane using iBlot2 Transfer Stacks (Table 2) according to the manual. Membranes were blocked for 1 h in blocking buffer (Table 2) and incubated with primary antibodies (Table 7) overnight. Subsequently, membranes were washed 4 times in 1X T-PBS for 10min, and then incubated with corresponding HRP-conjugated isotype-specific secondary antibody (Table 7) diluted in 5% non-fat milk for 1 hour at RT. After 4 times washing with 1X T-PBS, the blots were visualized with Pierce ECL Western Blot substrate (Table 3) or Luminata Forte Western blot HRP (Table 3) and films (AGFA Curix HT and GE Hyperfilms). Films were developed with Curix 60 (AGFA) developing machine.

Table 7 Primary and secondary antibodies

Antibody	Isotype	Source	Catalog No.
A20 (TNFAIP3)	Mouse IgG1	Imgenex	IMG-161
β-Actin	Mouse IgG2a	Sigma Aldrich	A2228-100UL
Caspase-8	Mouse IgG2b	Provided by P.H. Krammer	
Caspase-8	Goat IgG	Santa Cruz	sc-6136
CD95	Mouse IgG1	Provided by P.H. Krammer	
cIAP1	Rat	provided by J. Silke	
cIAP2	Rat	provided by J. Silke	
cFLIP(NF6)	Mouse IgG1	Enzo Life Science	ALX-804-961-0100
ERK2 (C-14)	Rabbit	Santa Cruz	sc-14
phosph-ERK1/2	Mouse IgG	Santa Cruz	sc-16982
FADD	Mouse IgG1	BD Biosciences	F36620

IκBα	Rabbit IgG	Santa Cruz	sc-371
Phospho-IκBα	Rabbit IgG	Cell Signaling	9246
IKKα/β	Rabbit IgG	Santa Cruz	sc-7607
MLKL	Rat	Provided by James Murphy	
Phospho-MLKL(S158)	Rabbit IgG	Abcam	ab187091
RIPK1	Mouse IgG2a	BD Biosciences	R41220
Phospho-RIPK1(S166)	Rabbit IgG	Provided by P.Gough	
RIPK3	Rabbit IgG	Imgenex	IMG-5846A
NF-κB2 p100/p52	Rabbit IgG	Cell Signaling	4882S
XIAP	Mouse IgG1	BD Biosciences	H62120
<b>Secondary Antibodies</b>			
Mouse IgG1	Goat/HRP	SouthernBiotech	1070-05
Mouse IgG2a	Goat/HRP	SouthernBiotech	1080-05
Mouse IgG2b	Goat/HRP	SouthernBiotech	1090-05
Mouse IgG	Goat/HRP	SouthernBiotech	1030-05
Mouse IgG1-Biotin	Goat	SouthernBiotech	1030-08
rabbit	Goat/HRP	SouthernBiotech	4030-05
Rat	Goat/HRP	SouthernBiotech	3030-05

### 2.2.8 Caspase-8 Co-immunoprecipitation

For the precipitation of caspase 8-bound proteins,  $2 \times 10^7$  cells were seeded and incubated overnight. Cells were washed once with medium at 37°C and pre-incubated with zVAD-fmk (10 μM) for 1h and followed by addition of IAP antagonist (100 nM) at 37°C. After 4 hours stimulation, cell pellets were harvested by trypsinisation, centrifugation and washing. Subsequently cells were lysed in 1ml lysis buffer by gently shaking with tube rotator at 4°C. 1hour later, the lysates were centrifuged two times at 20,000 x g for 30min to discard cellular debris. A minor fraction of these clear lysates were used as control for the input of the respective proteins (total lysates) and prepared as indicated in method 2.2.7.1. Meanwhile, a total amount of 3mg protein was used and mixed well with 1 μg caspase 8 antibody (Table 7). The caspase 8 containing complexes were precipitated from the lysates by co-incubation with 60 μl protein G-beads (Roche) for 16-24h on a tube rotator at 4°C. Beads were washed 4 times with cold lysis buffer before the protein complexes were eluted from dried beads by addition of standard reducing Laemmli buffer and boiling

at 95°C for 10 min. Finally the total lysate and IP samples were analysed by western blot as indicated in method 2.2.7.3.

### 2.2.9 RNA isolation and reverse transcription

RNeasy Mini Kit (Table 3) was used for isolation and purification of total RNA from adherent cell lines according to the manual. Firstly, the cell pellets were disrupted and homogenized with 1%  $\beta$ -mercaptoethanol containing RLT buffer and QIAshredder (Qiagen). Then the samples were washed and purified by using spin column. Last, total RNA was eluted from the columns by RNase free water. RNA quality and quantity were determined using the NanoDrop 2000™ (ThermoFisher SCIENTIFIC) spectrophotometer.

For the reverse transcription reaction, 1-2  $\mu$ g RNA of each sample was used. 1  $\mu$ l dNTP (10 mM), 1  $\mu$ l random nonamers (100  $\mu$ M), 0.2  $\mu$ l oligodT primer (100  $\mu$ M) and RNase free water were mixed with RNA to a final volume of 12  $\mu$ l and incubated in a thermocycler for 5 min at 65 °C.

Afterwards, 4  $\mu$ l 5X First Buffer, 2  $\mu$ l DTT (0.1 M), 0.5  $\mu$ l RNaseOUT and 0.5  $\mu$ l Superscript® II reverse transcriptase (Table 3) were added into the reaction tubes. The samples were further incubated in a thermocycler for 2 min at 42 °C, 12 min at 25 °C, 50 min at 42 °C, and finally 15 min at 70 °C. cDNA samples were collected from the reaction tubes and diluted to a final concentration of 10 ng/ $\mu$ l for qPCR.

### 2.2.10 Quantitative real time polymerase chain reaction (qPCR)

Primers listed in Table 8 were designed with Primer3 software. qPCR experiments were performed in triplicates using KAPA SYBR® FAST Master Mix (2X) Universal as following Table 9

Table 8 qPCR primers

Primer	Forward	Revers
<i>RIPK3</i>	CAAGATCGTAAACTCGAAGG	CCTGGTATGACAACGAATTT
<i>TNF</i>	GGCAGTCAGATCATCTTCTC	TGGTTATCTCTCAGCTCCAC
<i>GAPDH</i>	GTGAGGGTCTCTCTTCCCT	CCGTTCTCCATGAATTTAGT

Table 9 Reaction components for PCR

Component	Volume( $\mu$ l)/ rxn	Final Conc.
PCR grade water	Up to 20 $\mu$ l	N/A
2X KAPA SYBR® FAST qPCR Master Mix	10	1X
Forward Primer (10 $\mu$ M)	0.4	200nM
Reverse Primer (10 $\mu$ M)	0.4	200nM
Template cDNA	100ng	5ng/ $\mu$ l
50X ROX Low	0.4	1X

Table 10 Thermal cycling profile for qPCR

Temperature	time	cycles
95 °C	15 min	1
95 °C	30 s	40
60 °C	30 s	40
72 °C	30 s	40
95 °C	60 s	1
60 °C	30 s	1
95 °C	30 s	1

Melting curve analysis was used to confirm the specific amplification of a single product of the expected size for gene of interest. Furthermore, all primers used for qPCR studies have been tested before by cDNA dilution curves to show efficiency within 80-110 %. In addition, all samples were tested to have a low variance in the housekeeping gene (*GAPDH*) expression (< 2 cycles). Serial dilutions of cDNA (1, 1/5, and 1/25) were amplified for the construction of a standard curve and used for the estimation of the pPCR efficiency using MxPro software (Agilent Technologies). The relative quantification was calculated after dividing the standard curve value of the respective genes by that of the housekeeping gene (*GAPDH*) for each individual sample using Excel.

### 2.2.11 Genomic DNA isolation

Blood & Cell Culture DNA Mini Kit (Table 3) was used for isolation and purification of genomic DNA from adherent cell lines according to the manual. Briefly, cells were harvested using trypsin and washed with cold PBS. Then cells were resuspended with cold PBS to a final concentration of  $10^7$  cells/ml and lysed with lysis buffer. Protein was removed by addition of Protease K for incubation 45 minutes. DNA was purified and collected with Genomic-tip (Qiagen). The quality and quantity of DNA were determined using NanoDrop 2000™ (ThermoFisher SCIENTIFIC) spectrophotometer.

### 2.2.12 Bisulfite conversion of DNA and Methylation specific PCR (MSP)

Methylation specific PCR (MSP) was used to determine the locus specific methylation of genes of interest. Firstly, purified genomic DNA was treated with bisulfite sodium (EZ DNA Methylation™ Kit) to convert unmethylated cytosine into uracil without alteration of methylated ones. Bisulfite modified DNA was collected with zymo-spin™ columns used for further PCR analysis. Once converted, the methylation profile of the DNA can be determined by PCR amplification with specific primers. In this study, two pairs of primers recognize the original sequence and the rest two are specific to the modified sequences with predictive methylation locus (Table 11) [154]. M indicates primers recognising methylated sequences and

U indicates primers recognising unmethylated sequences. The MSP reaction was performed under following conditions:

Table 11 *RIPK3* primers for MSP

Primer	Forward	Revers
<i>RIPK3</i> M1	TAATTCGGAAAAAGGGTAATAATTC	ATAAATATCGAAAACTACGATCGAC
<i>RIPK3</i> U1	AATTTGGAAAAAGGGTAATAATTTG	ATAAATATCAAAAACTACAATCAAC
<i>RIPK3</i> M2	AGGTTATGGTAAGTTTGGATAACGA	CAACAAACGACAAAAAACGAC
<i>RIPK3</i> U2	AGGTTATGGTAAGTTTGGATAATGA	CTTCAACAAACAACAAAAAACAA

Table 12 Reaction components for PCR

Component	Volume( $\mu$ l)/ rxn	Final Conc.
DreamTaq DNA polymerase	1	1X
5X DreamTaq Green buffer	5	1X
Forward Primer (10 $\mu$ M)	0.5	200 nM
Reverse Primer (10 $\mu$ M)	0.5	200 nM
Template cDNA	40 ng	1.6 ng/ $\mu$ l
PCR grade water	Up to 25 $\mu$ l N/A	N/A

Table 13 Thermal cycling profile for MSP

Step	Temperature	time	cycles
1. Initial denaturation	95 °C	10 min	1
	95 °C	30 s	45
2. Annealing	56 °C	30 s	45
3. Elongation	72 °C	30 s	45
	72 °C	10 min	1

### 3. Aim of the thesis

Malignant melanoma is the most dangerous form of skin cancers due to its aggressiveness and resistance to existing therapies. Genetic and epigenetic abnormalities of specific genes and inadequacy of the intracellular signal transduction resulted in aggressiveness of melanoma cells. Development of melanoma is highlighted by activation of molecular mechanisms that directly influence regulation of cell death, cell proliferation and cell survival processes.

The resistance to cell death stimuli is one of the hallmarks of tumour cells to escape host specific elimination. Melanoma cells are easily gaining resistance to either extrinsic or intrinsic cell death stimuli during its development. Inhibitor of apoptosis proteins (IAPs) are such negative regulators of cell death. Therefore overcoming cell resistance by antagonising or downregulation of IAPs has been advocated as a effective strategy for tumour therapy. In view of these facts of cell death and melanoma, the project will be started with the investigation of the role of IAPs in cell death resistance in melanoma. To identify the regulatory proteins in melanoma, CD95 ligand (CD95L), as a death ligand, will be firstly used to study the basal cell sensitivity and forms of cell death in melanoma. Apoptosis and necroptosis, as main forms of cell death, will be investigated in melanoma. The possible cell death forms will be characterized by biochemical and morphological analysis. To conclude the role of IAPs in melanoma cell death, the expression profile of IAPs in melanoma will be screened and its function will be confirmed by usage of its antagonist. Application of specific inhibitors will further support the regulatory effect of proteins on melanoma cell death.

In addition to cell death resistance, acquired gene mutations and epigenetic modifications can also be responsible for cell death resistance of melanoma cells. To identify if such epigenetic modifications influence the regulation of programmed cell death, we will check the methylation status of DNA of genes involved in apoptotic and necroptotic cell death responses in melanomas. Here we will perform overexpression to reconstitute expression of methylated genes to confirm their function in programmed cell death. In addition, knockdown or chemical inhibitors of the specific molecules will be performed for further verification.

Since NF- $\kappa$ B is involved in transcriptional regulation of proteins that control cell proliferation, cell survival and cell death resistance, the regulatory impact of NF- $\kappa$ B activation in melanoma cell death will be evaluated. To investigate the role of the NF- $\kappa$ B signalling for cell death responses in melanoma, we will firstly identify anti-apoptotic proteins, of which expression and modifications are influenced by NF- $\kappa$ B, by artificial generation of melanomas with constitutive active or inactive IKK2. Subsequently, the effect of NF- $\kappa$ B-mediated protein expression on cell sensitivity will be screened and analysed in melanomas.

## 4. Results

### 4.1 Identification of regulatory proteins for programmed cell death in melanomas

Escape from intrinsic self-check mechanism for programmed cell death is one hallmark of tumours [155]. Primary or acquired cell resistance render melanoma cells ability for survival and metastasis. Previous studies have confirmed the negative role of IAPs in cell death regulation [97,117,153]. Therefore, it was proposed that IAPs could be negative regulators for cell death in melanoma. In addition, RIPK1-RIPK3-MLKL platform mediates programmed necrosis under specific stimulation conditions [79,105,156]. Accordingly, the regulation of necroptosis will be studied in melanoma.

#### 4.1.1 Loss of IAPs sensitizes human melanoma cells to CD95L-induced cell death

Melanoma acquires death resistance during development and metastasis. IAP proteins are initially identified as cell death inhibitors through weakening caspases activity and other proteins required for cell death execution. Therefore IAPs play as negative regulators of cell death and related with cell death resistance. To identify the effect of IAPs on regulation of CD95L-induced cell death, endogenous expression levels of cIAP1, cIAP2 and XIAP of melanoma cell lines from different tumour stages were firstly compared with primary melanocytes, primary nevus cells, and spontaneously transformed aneuploid immortal keratinocyte cell line (HaCaT) (Figure 6A). cIAP1 was expressed in all cell lines but with relatively low level in PREYER, MeWo and MM-LH cells. Moreover, one additional band with higher molecular weight of cIAP1 was detected in primary melanocytes, nevus cells (#5, #8), as well as in SK-MEL 28 and MM-AH melanoma cells, suggesting that in these cells cIAP1 might be modified post translation. On the contrary, cIAP2 was only detectable in A375, RPM-EP and HaCaT cells but not in other cell lines. XIAP, which was absent in HaCaT cells, was expressed more in human melanoma than melanocytes or nevus cells (Figure 6B). In summary, cIAP1 and XIAP both were expressed normally in cultured human melanomas and primary cells, which suggested the potential relationship between IAPs expression and cell death resistance.

Furthermore, to further confirm the relevance of IAPs expression and negative regulatory effect on melanoma cell death, the IAP antagonist (Compound A, Figure 5) was used to downregulate the intrinsic cIAPs levels and to suppress XIAP activity. Compound A was sufficient to downregulate both endogenous expression of cIAP1 and cIAP2 with low concentrations in 1 hour. Moreover, Compound A showed relatively significant inhibitory effect on cIAP1 expression compared with cIAP2. Meanwhile, Compound A blocked XIAP activity without altering its protein

expression (Figure 6B). Our results indicated that whenever expression or activity of IAPs was blocked by Compound A, melanoma cells exhibited increased cell sensitivity to CD95L *in vitro* (Figure 6A). To investigate if this observed decrease of cell viability was caspase-dependent apoptosis or RIPK1-dependent necroptosis, the effect of pan-caspase inhibitor zVAD-fmk and the RIPK1 inhibitor Necrostatin-1 on cell death was analysed by Annexin V/Propidium iodide (PI) dual staining (Figure 6D). In our study, caspase inhibitor but not RIPK1 inhibitor protected melanoma cells from CD95L/IAP antagonist-induced cell death, which indicated that caspase-dependent apoptosis was the dominant cell death form in melanoma cells. Our results confirmed that IAPs, especially cIAP1 and XIAP were negative regulatory elements for CD95L-mediated cell death in melanoma cell lines. In addition, CD95L dominantly induced caspase-dependent apoptosis but not unmasked RIPK1 dependent necroptotic cell death in melanoma *in vitro* indicating that the molecules involved in necroptosis could be absent in melanomas.

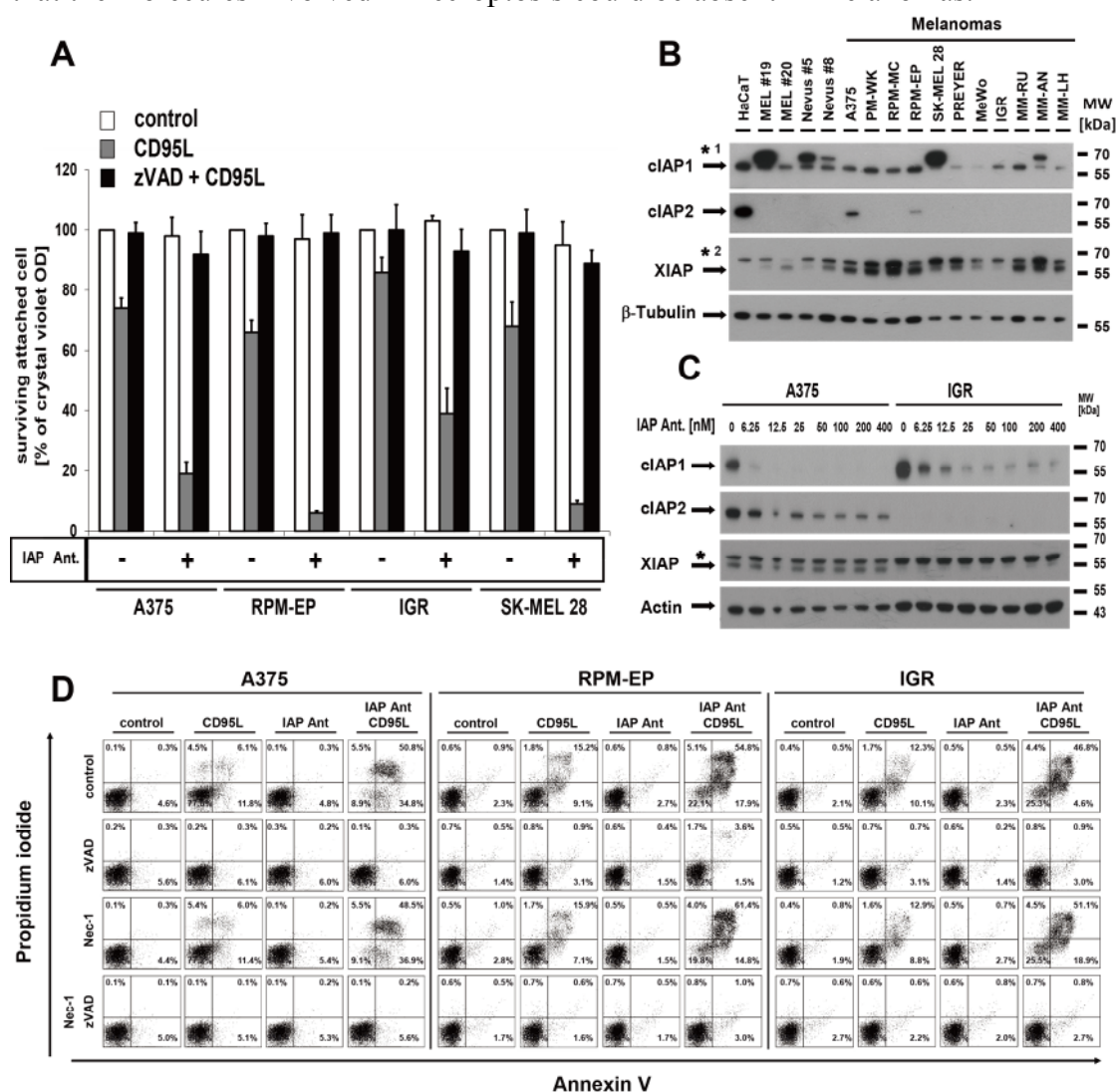


**Figure 6 Loss of IAPs sensitizes melanoma cell lines to CD95L-mediated apoptotic cell death.** A A375, RPM-EP, IGR, SK-MEL 28 cells were pre-treated with zVAD-fmk (10  $\mu$ M) or Compound A (100 nM) alone or in combination for 1 h

and subsequently stimulated with CD95L (0.5 U/ml) for 18-24 h. Cell viability was quantified with crystal violet staining. Summary of three independently performed experiments including the S.E.M. of the whole set of experiments is shown. **B** Endogenous expression of respective proteins in human keratinocytes (HaCaT), primary melanocytes (Mel #19, Mel #20), nevus cells (Nevus #5 and #8), and melanoma cell lines was analysed by western blot. \*1 describes an unknown band, \*2 described an unspecific band.  $\beta$ -tubulin or actin were served as loading control. One representative experiment of two independently performed experiments is shown. **C** A375 and IGR cells were stimulated with Compound A (100nM) for 1hour. cIAP1, cIAP2 and XIAP expression was analysed by western blot. Actin was served as loading control. One representative experiment of two independently performed experiments is shown. **D** A375, RPM-EP and IGR melanoma cells were either pre-stimulated with zVAD-fmk (10  $\mu$ M), Nec-1 (50  $\mu$ M), IAP antagonist (100 nM) alone or in combinations as indicated for 1 h and subsequently stimulated with CD95L (0.5 U/ml) for further 14 h. The externalization of phosphatidylserine as well as the amount of death cells were analysed by Annexin V/PI double staining. One representative experiment of two independently performed experiments is shown.

#### 4.1.2 Necroptosis is limited by absence of RIPK3 expression in melanoma cells

The essential role of RIPKs in necroptotic cell death via necrosome assemble has been confirmed by recent studies. Since melanoma cells failed to be killed by CD95L through necroptotic cell death *in vitro*, endogenous expression of main necrosome components was examined and compared between melanoma cells to primary melanocytes, primary nevus cells, and HaCaT keratinocytes. Of interest, RIPK3 expression was relatively low or absent in melanoma cell lines compared with primary melanocytes (Mel #20 but not Mel #19), nevus cells, and HaCaT cells. While RIPK1 and MLKL were expressed as normally in most of melanoma cells with exception of PREYER, MeWo, and MM-AN cells as in melanocytes, nevus cells and HaCaT keratinocytes (Figure 7A). To exclude the possibility that absence of RIPK3 in melanomas was unique phenomenon in human, RIPK3 expression in five murine melanoma cells lines, which were isolated from two transgenic murine melanoma models, were also compared with murine immortalized keratinocytes. Consistent with human melanomas, RIPK3 was also low expressed in murine melanoma cells, especially in *RET* model melanoma cell lines (Figure 7A). The expression pattern of RIPK3 in melanoma cell lines suggested that absence of RIPK3 expression was a potential explanation for necroptosis resistance of melanomas.

To identify if deficiency of RIPK3 in melanomas was mediated by transcription repression, its mRNA level was quantified by qPCR. Consistent with western blot results, RIPK3 was below detection level in all tested melanoma cell lines. On the



### 4.1.3 Reconstitution of RIPK3 promotes MLKL phosphorylation and allows for CD95L-induced necroptosis in malignant melanomas

Since RIPK3 was low expressed in melanoma cells, the role of RIPK3 and its kinase activity on necroptotic cell death in melanomas was subsequently investigated by overexpression of RIPK3 or its kinase inactive mutant (RIPK3 D160N) [74] in three human melanoma cell lines (A375, IGR, RPM-EP) via retroviral transduction. Of interest, successful overexpression of RIPK3 but not its kinase dead mutant led to spontaneous phosphorylation of MLKL in all tested melanoma cell lines (Figure 8A). This result indicated MLKL, as a part of the necroptosis signalling machinery because of RIPK1 and RIPK3 activation, was RIPK3 downstream substrate via phosphorylation.

The role of RIPK3 on cell death was firstly investigated in A375 and IGR melanoma cells carrying with RIPK3 overexpression were compared with vector control or RIPK3 KD overexpressing cells. Of interest, RIPK3 expression increased melanoma cell sensitivity to CD95 ligand, suggesting RIPK3 activity was involved in cell death regulation, which was consistent with previous results. Furthermore, whenever the expression of cIAPs was depleted by Compound A, cells became more sensitive to CD95L induced cell death which was in line with the result of parental cell lines (Figure 8B, C). In summary, reconstitution of RIPK3 sensitized A375 and IGR cell to CD95L stimulation, which confirmed the regulatory impact on cell death.

As reconstitution of RIPK3 was sufficient to induce spontaneous phosphorylation of MLKL in melanoma cells, effect of RIPK3 on necroptosis regulation was next studied. To block caspase-dependent apoptosis, A375 and IGR cells with vector control, RIPK3 or RIPK3 KD were pretreated with the caspase inhibitor zVAD-fmk for 1 hour. Uniquely in RIPK3 overexpressing melanoma cells, caspase-independent necroptotic cell death was remarkably revealed upon CD95L stimulation (Figure 8B, C). On the contrary, caspase inhibitor protected vector control or RIPK3 KD melanoma cells from CD95L-induced apoptosis as the same as parental melanoma cells. In addition, antagonization of IAPs by using Compound A also sensitized RIPK3 overexpressing cells to CD95L-mediated necroptosis (Figure 8B, C), which verified the inhibitory function of IAPs in necroptosis. These results demonstrated the critical function of RIPK3 in melanoma necroptosis.

In summary, melanoma cells were resistant to necroptotic cell death potentially resulting from lack of RIPK3 expression. Reconstitution of RIPK3 via retroviral transduction in melanoma cells initiated spontaneous phosphorylation of MLKL and subsequently unveiled CD95L-induced necroptosis that can be sensitized by IAP antagonist.

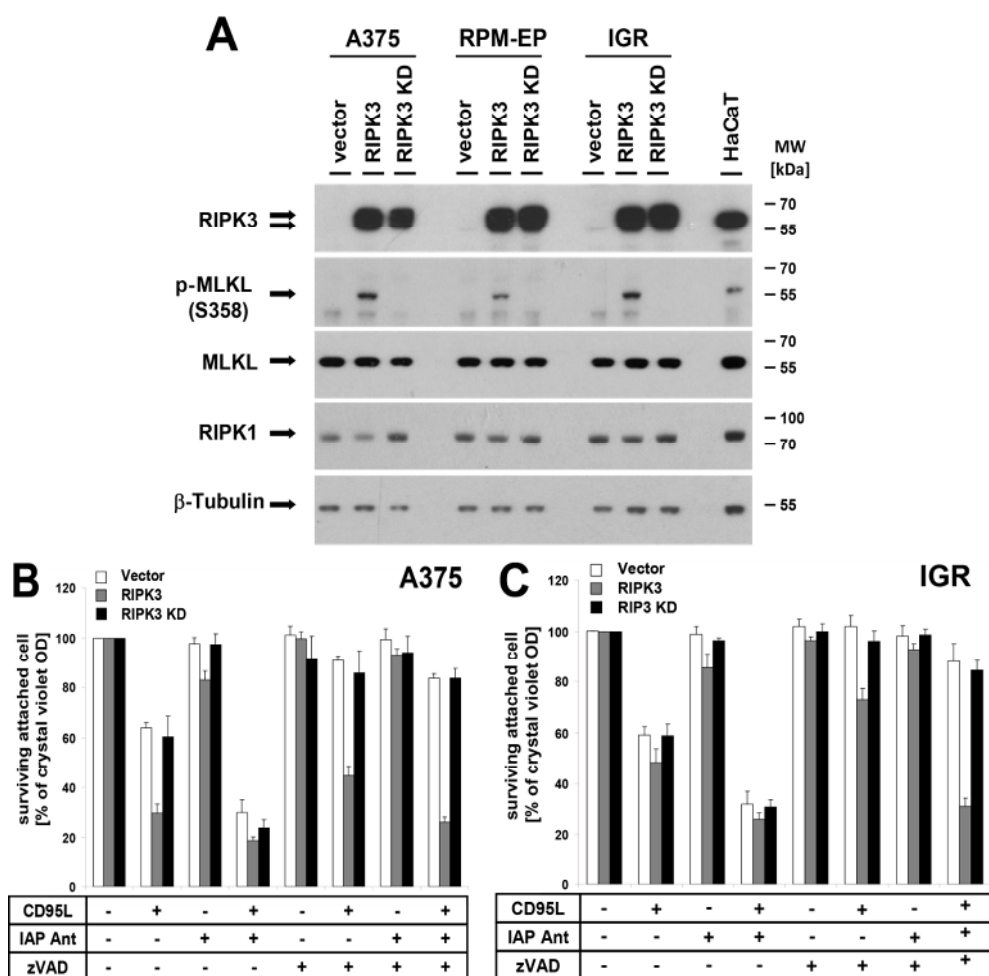


**Figure 8 Overexpression of RIPK3 promotes spontaneous phosphorylation of MLKL and CD95L-induced necroptotic cell death.** **A** A375, RPM-EP, and IGR cells were transduced with retroviruses containing vector control, cDNA for human RIPK3 or its kinase dead mutant (RIPK3 KD). RIPK3 overexpression, as well as for p-MLKL, MLKL, RIPK1 were analysed by western blot after transduction and selection.  $\beta$ -tubulin was served as loading control. One representative experiment of two independently performed experiments is shown. **B,C** A375 (**B**) cells or IGR cells (**C**) with expression of vector (control), RIPK3, and RIPK3 KD were pre-treated with zVAD-fmk (10  $\mu$ M) or Compound A (100 nM) alone or in combination for 1 h and subsequently stimulated with CD95L (0.5 U/ml) for 18-24 h. Cell viability was quantified with crystal violet staining. Summary of three independently performed experiments including the S.E.M. of the whole set of experiments is shown.

Reconstitution of RIPK3 could open the door for necroptosis execution in melanomas *in vitro*. For a detailed description of the quantity of the observed cell death, the externalization of phosphatidylserine and the change of membrane permeability were further investigated in RIPK3 reconstituted melanoma cells by Annexin V/PI dual staining followed by FACS analysis and Hoechst/SYTOX<sup>®</sup> green staining by fluorescence intensity analysis. During the process of necroptosis,

externalization of phosphatidylserine from inner plasma membrane was confirmed by Annexin V staining positivity. In addition, increase of nuclear membrane permeability via PI positivity also characterised with necroptosis in RIPK3 overexpressing melanoma cells (Figure 9A, B).

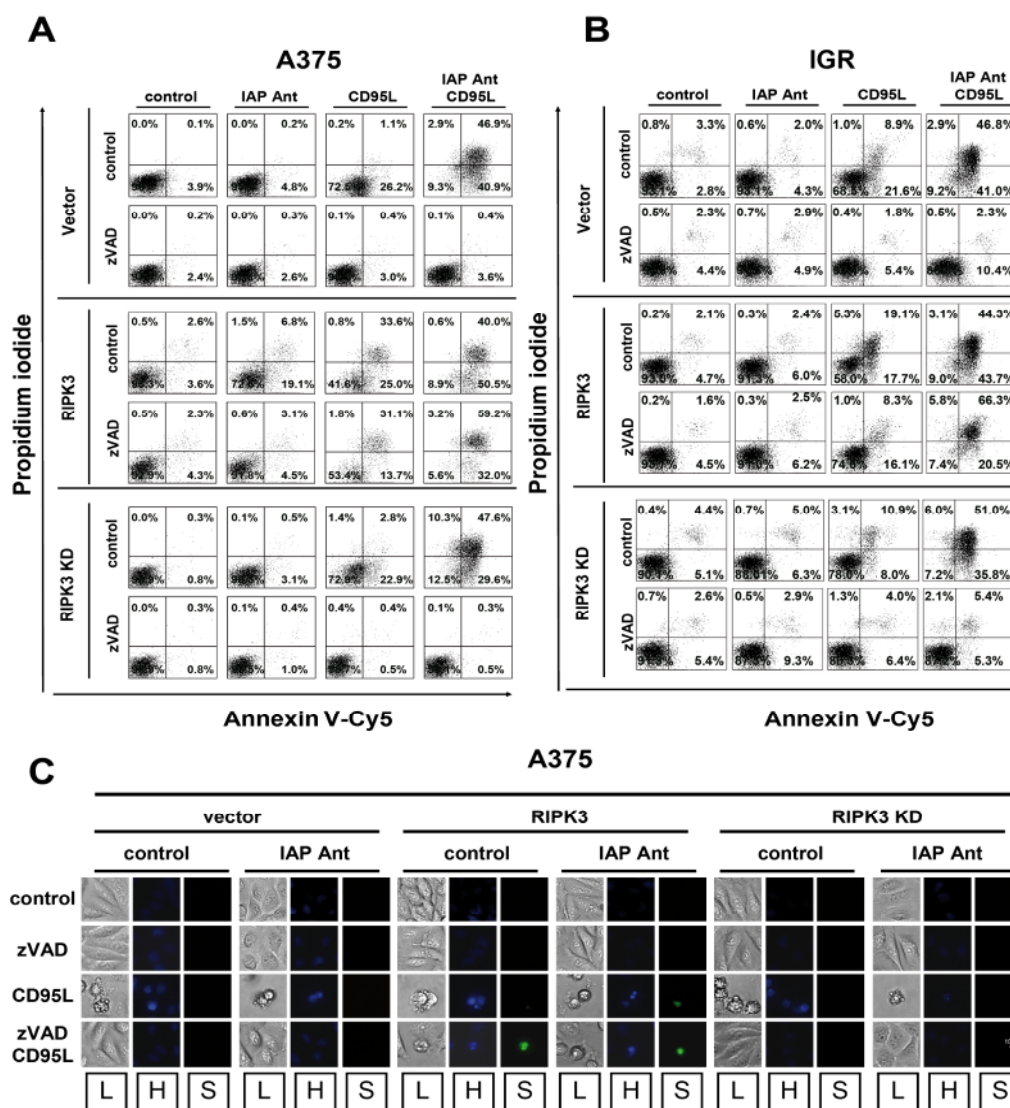


**Figure 9 RIPK3 overexpression promotes CD95L-mediated necroptosis in melanoma cells.** A375 (A) cells or IGR cells (B) with expression of vector (control), RIPK3, and RIPK3 KD were pre-treated with zVAD-fmk (10  $\mu$ M) or Compound A (100 nM) alone or in combination for 1 h and subsequently stimulated with CD95L (0.5 U/ml) for 14 h. The externalization of phosphatidylserine as well as the amount of dead cells were analysed by FACS following Annexin V/PI staining. One representative of two independently performed experiments is shown. C A375 cells with respective expressions stimulated as described in A were dual stained with Hoechst 3342 and SYTOX<sup>®</sup> Green followed by fluorescent microscopy analysis. One representative experiment of two independently performed experiments is shown (L, Light; H, Hoechst3342 staining; S, SYTOX<sup>®</sup> Green staining).

In addition, CD95L-mediated necroptosis was further characterized by Hoechst 3342 and SYTOX<sup>®</sup> green staining. In presence of caspase activity, CD95 ligand or in combination with IAP antagonist stimulation resulted in apoptosis morphology in all cells, including cell shrinkage and condensed nucleus (Figure 9C). While, altered cell death morphology was only observed in RIPK3 overexpressing cells whenever the activity of caspases was blocked by zVAD-fmk. During necroptotic death, cells became rounded shape, accompanying with a swollen cytoplasm and disintegrated nuclei (Hoechst 3342 and SYTOX<sup>®</sup> green dual positivity) (Figure 9C). During the process of necroptosis, phosphatidylserine became externalized from the inner cellular membrane which was confirmed by the Annexin V staining. Even though cells remained intact during the process of necroptosis, the plasma membrane were disrupted that enabled big molecules enter into nucleus. The positivity of PI and SYTOX<sup>®</sup> confirmed the increased plasma membrane permeability in the process of CD95L-induced necroptosis.

#### 4.1.4 RIPK3 promotes CD95L-induced necroptosis without altering CD95 expression

The CD95 (also named as Fas, Apo-1) is known as death receptor expressing on cell surface to initiate programmed cell death. In our study, since reconstitution of RIPK3 resulted in increased cell sensitivity to CD95 ligand in melanomas *in vitro*, the impact of RIPK3 overexpression on CD95 receptor expression was studied. Compared with vector control, receptor surface expression pattern of CD95 was unchanged after RIPK3 overexpression both in A375 and IGR cells (Figure 10). Reconstitution of RIPK3 in melanoma did not alter surface expression pattern of CD95, which excluded the possibility that the increased cell sensitivity to CD95L of melanoma cells was related with gain of CD95 surface expression. The other way round, without altering death receptor expression, RIPK3 was directly involved in programmed cell death and its regulation.

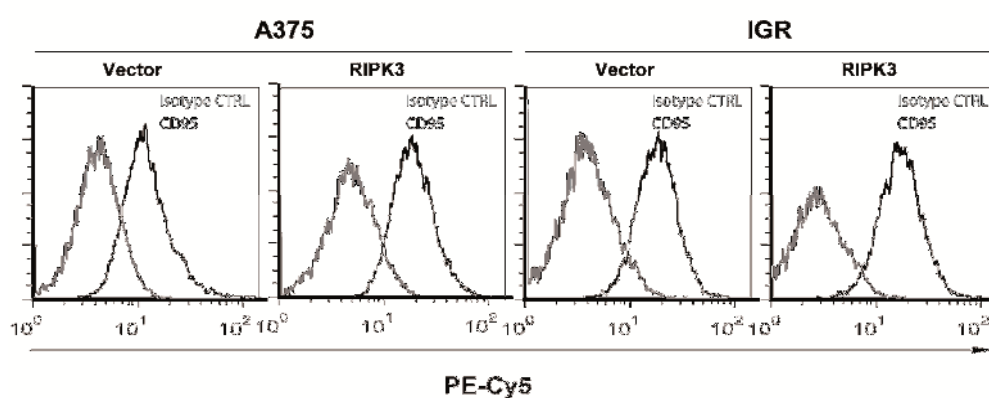


**Figure 10 RIPK3 reconstitution does not alter CD95 surface expression.** Surface expression of CD95 in A375 or IGR cells overexpressing vector or RIPK3 were

stained with CD95 specific antibody and quantitatively analysed by flow cytometry. Isotype control was used to exclude the unspecific staining of CD95 antibody. One representative experiment of two independently performed experiments is shown.

#### **4.1.5 CD95L-mediated apoptosis and necroptosis in RIPK3 overexpressing A375 cells are independent of IAP antagonist-mediated autocrine TNF activation.**

To address the possibility that IAP antagonist induced autocrine TNF production and therefore the TNF-dependent cell death signalling in RIPK3 overexpressing cells, the recombinant TNFR2-Fc was used to study the TNF dependency in IAP antagonist-mediated cell sensitivity in CD95L-induced cell death. Similar with above observed results, loss and inhibition of IAPs by Compound A resulted in increasing cell sensitivity to both apoptotic and necroptotic death in A375 RIPK3 cells (Figure 11A). Whereas, in RIPK3-reconstituted A375 melanoma cells, CD95L-induced neither apoptosis nor necroptosis was interfered by addition of recombinant TNFR2-Fc in presence of IAP antagonist (Figure 11A). The same result was also acquired in IGR-RIPK3 cells (data not shown). In addition, Annexin V/PI dual staining was used for further qualification and quantification of autocrine TNF-dependency in IAP antagonist-induced cell sensitivity. FACS analysis demonstrated that recombinant TNFR2-Fc failed to prevent RIPK3 overexpression cells from CD95L-mediated apoptosis and necroptosis in presence of Compound A which was consistent with crystal violet assay results (Figure 11B). To assure the activity of TNFR2-Fc used in our study, HaCaT cells carrying IKK2 kinase mutant form (IKK2 KD) which can be killed in TNF-dependent manner were used as positive control. Compared with vector control cells, whenever IKK2 kinase was mutated in HaCaT, cells became remarkably sensitive to TNF and were blocked by addition of recombinant TNFR2-Fc (Figure 11C). These result confirmed the bioactivity of our recombinant TNFR2-Fc.

Taken together, IAP antagonist sensitized RIPK3 overexpressing melanoma cells to CD95L-mediated apoptotic and necroptotic cell death, which confirmed the inhibitory role of IAPs in programmed cell death. Inability of recombinant TNFR2-Fc to protect melanoma cells from death ligand-induced cell death excluded the dependency of TNF activation resulted from IAP antagonist in cell sensitivity of RIPK3 reconstituted melanomas.

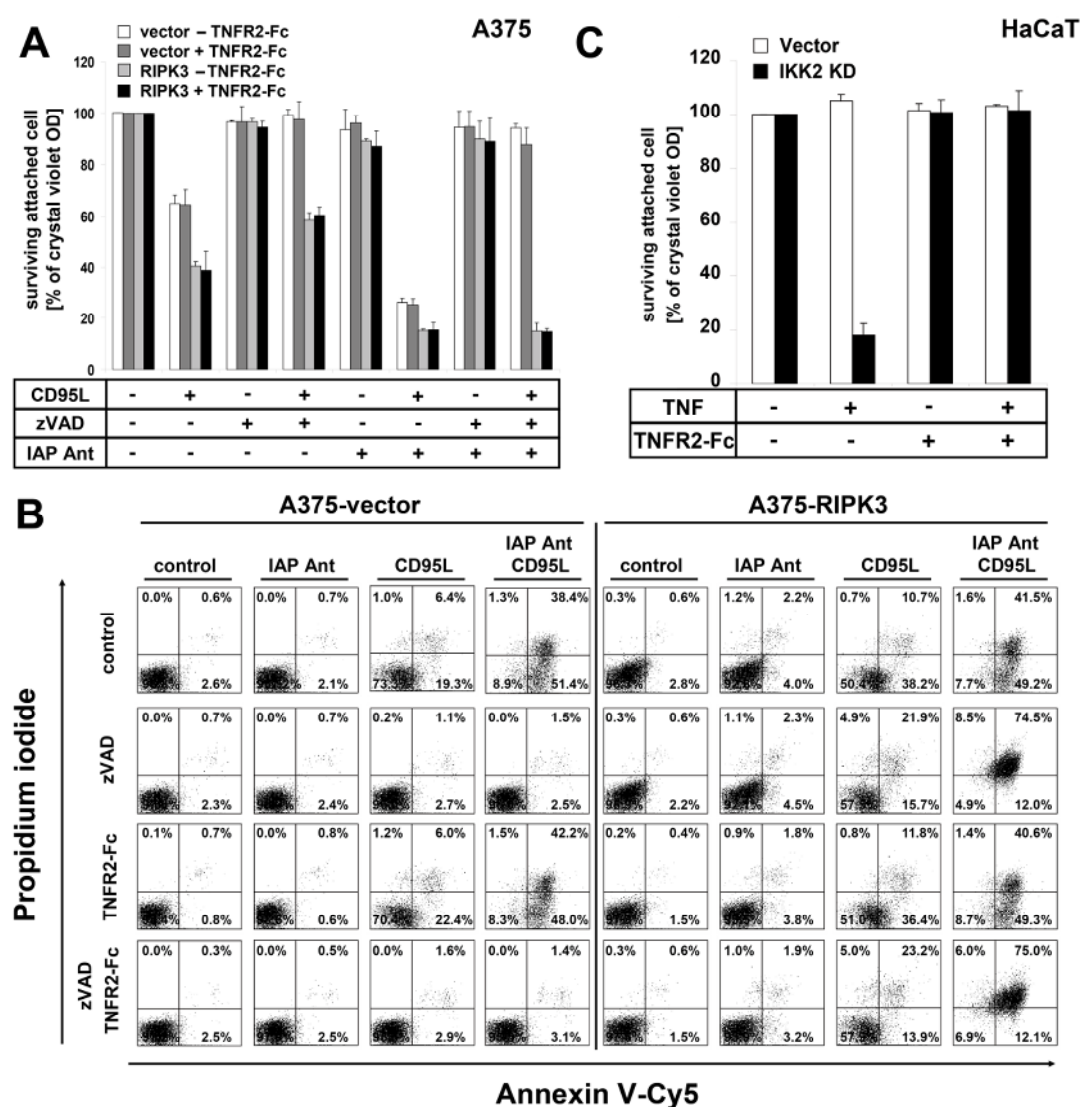


**Figure 11 CD95L-induced apoptosis and necroptosis in A375-RIPK3 cells are independent from Compound A-mediated TNF signalling.** **A, B** A375 cells with expression of vector (control), RIPK3, and RIPK3 KD were pre-treated with zVAD-fmk (10  $\mu$ M) or Compound A (100 nM) or TNFR2-Fc (10 mg/ml) alone or in combinations for 1 h and subsequently stimulated with CD95L (0.5 U/ml) for 18-24 h (A) or 14h (C) followed by analysis with crystal violet staining or Annexin V/PI staining. Summary of three or two independently performed experiments including the S.E.M. of the whole set of experiments is shown. **C** HaCaT cells with vector control or IKK2KD were either non-stimulated or pre-stimulated with TNFR2-Fc (10  $\mu$ g/ml) for 1h and subsequently stimulated with recombinant TNF (10 ng/ml) for 18-24 hrs followed by crystal violet staining. Summary of two independently performed experiments including the S.E.M. of the whole set of experiments is shown.

### 4.1.6 Death ligands promote MLKL phosphorylation during the process of necroptosis in RIPK3-reconstituted melanoma cells

During the process of necroptosis, RIPK1 and RIPK3 bind to each other through the RHIM domain and further form a amyloid complex where RIPK3 executes auto-phosphorylation at its serine 227 residue, which is critical for the interaction with MLKL. Upon necroptosis induction, MLKL is recruited to serine 227 phosphorylated RIPK3 and is subsequently phosphorylated by RIPK3 at the threonine 357 and serine 358 residues [157,158].

In our study, RIPK3 but not its kinase inactive mutant reconstitution led to spontaneous phosphorylation at serine 358 residue of MLKL in melanoma cell lines (Figure 8A). To further elucidate the role of RIPK3 kinase activity in MLKL phosphorylation during necroptosis execution (zVAD-fmk/Compound A/CD95L), the status of MLKL phosphorylation was further analysed by western blot. A375 cells with vector control, RIPK3 or RIPK3 KD were non-stimulated or stimulated under necroptotic induction conditions within different time kinetic. The phosphorylation of MLKL (Ser358) was increased within 3 hours upon necroptosis induction and upregulated in a time-dependent manner exclusively in RIPK3 overexpressing A375 cells (Figure 12A). In addition, phosphorylation of MLKL was also compared between CD95L, TRAIL and TNF. CD95L, led to relatively significant phosphorylation of MLKL (Figure 12B). In our study, death ligands of TNF superfamily uniquely initiated necroptosis in RIPK3 overexpressing melanoma cells. During the process of necroptosis, MLKL was phosphorylated by RIPK3. MLKL phosphorylation and subsequent necroptosis execution confirmed the indispensable role of RIPK3 and its kinase activity in death ligand-induced necroptotic cell death initiation in melanoma cells *in vitro*.

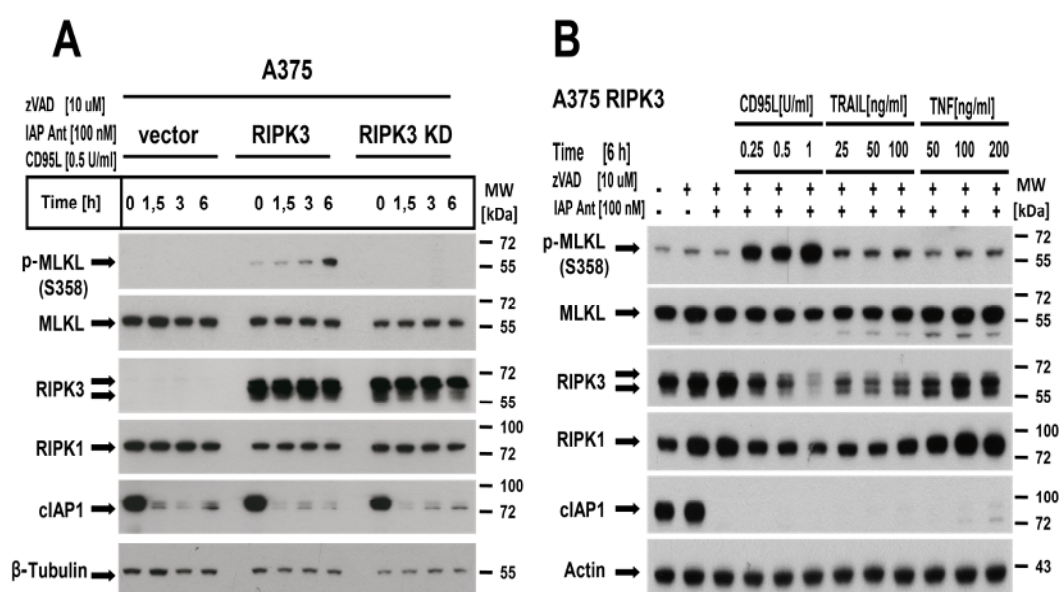


**Figure 12 MLKL is phosphorylated during the death ligand-mediated**

**necroptosis in RIPK3 overexpressing A375 cell.** **A** A375 cells with expression of vector (control), RIPK3, and RIPK3 KD were non-treated or pre-treated with zVAD-fmk (10  $\mu$ M) and Compound A (100 nM) in combination for 1 h and subsequently stimulated with CD95L (0.5 U/ml) for indicated time. Protein expression of p-MLKL (S358), MLKL, RIPK3, RIPK1 and cIAP1 was analysed by western blot.  $\beta$ -Tubulin was served as loading control. One representative experiment of two independently performed experiments is shown. **B** A375 cells with respective overexpression were non-treated or pre-treated with zVAD-fmk (10  $\mu$ M) or Compound A (100 nM) alone or in combination for 1 h and subsequently stimulated with CD95L (0.25, 0.5, 1 U/ml), TRAIL (20, 50, 100 ng/ml) or TNF (50, 100, 200 ng/ml) for 6 hours. Protein expression of p-MLKL (S358), MLKL, RIPK3, RIPK1 and cIAP1 was analysed by western blot. Actin was served as loading control. One representative experiment of two independently performed experiments is shown.

#### **4.1.7 RIPK1 and RIPK3 kinase activity are determinant for MLKL phosphorylation in CD95L induced necroptosis.**

Intriguingly, recent research demonstrated that upon TNF stimulation, RIPK1 and RIPK3 form a functional amyloid complex. There consists of RHIM domain of RIPKs in the amyloid core, and their kinase domain might flank the core for necroptosis signalling transduction [159]. Considering the decisive role of RIPK1 and RIPK3 playing in necroptosis, the effect of newly reported RIPKs specific inhibitors on cell death was scrutinized. The toxicity of RIPKs inhibitors was firstly examined in A375 cells. Both RIPK1 and RIPK3 inhibitors exhibited minor toxic or proliferation inhibitory effect at the concentration of 10  $\mu$ M which concentration was used for further study (Figure 13A). Notably, RIPK3 specific inhibitors (GSK'840 and GSK'872) [160,161] pre-treatment remarkably protected RIPK3 overexpressing cells from zVAD-fmk/Compound A/CD95L-induced necroptosis, while did not influence the apoptotic cell death (Figure 13B). To ascertain that the inhibitory effect of RIPK3 inhibitors on necroptosis was via depression RIPK3 kinase activity, the phosphorylation of MLKL was next measured by western blot. RIPK3 inhibitors down regulated both spontaneous phosphorylation by RIPK3 overexpression and CD95L-induced phosphorylation of MLKL (Figure 13C). Compared with RIPK3 inhibitors, RIPK1 inhibitors (7-Cl-O-Nec-1 and GSK'481) [110,111] and Necrostatin-1 (Nec-1) only partially prevented RIPK3 reconstituted A375 cells from necroptotic death and did not change the quantity of apoptosis (Figure 13B). Similar with RIPK3 inhibitors, the inhibitory effect of RIPK1 inhibitors was related to their negative regulatory influence on MLKL phosphorylation (Figure 13C). On the contrary, MLKL inhibitor Necrosulfonamide (NSA) was not able to prevent RIPK3 A375 cells from apoptosis or necroptosis (Figure 13B). Moreover, NSA did not demonstrate inhibitory influence on MLKL phosphorylation during necroptosis which explained NSA inability on necroptosis protection (Figure 13C). Taken

together, in the study of respective necroptosis inhibitors, we found the inhibition of respective necroptotic active proteins and necroptosis execution was correlated with extent of MLKL phosphorylation. RIPK1, indirectly regulating MLKL phosphorylation via interaction with RIPK3 only was only partially involved in CD95L-induced necroptosis. In respect of RIPK3, RIPK3 inhibitors completely protected melanomas from necroptosis through decrease MLKL phosphorylation. Suppressive effect of RIPK3 inhibitors on RIPK3 kinase activity and subsequent MLKL phosphorylation, and in turn necroptosis inhibition further affirmed the imperative role of RIPK3 in necroptosis execution.

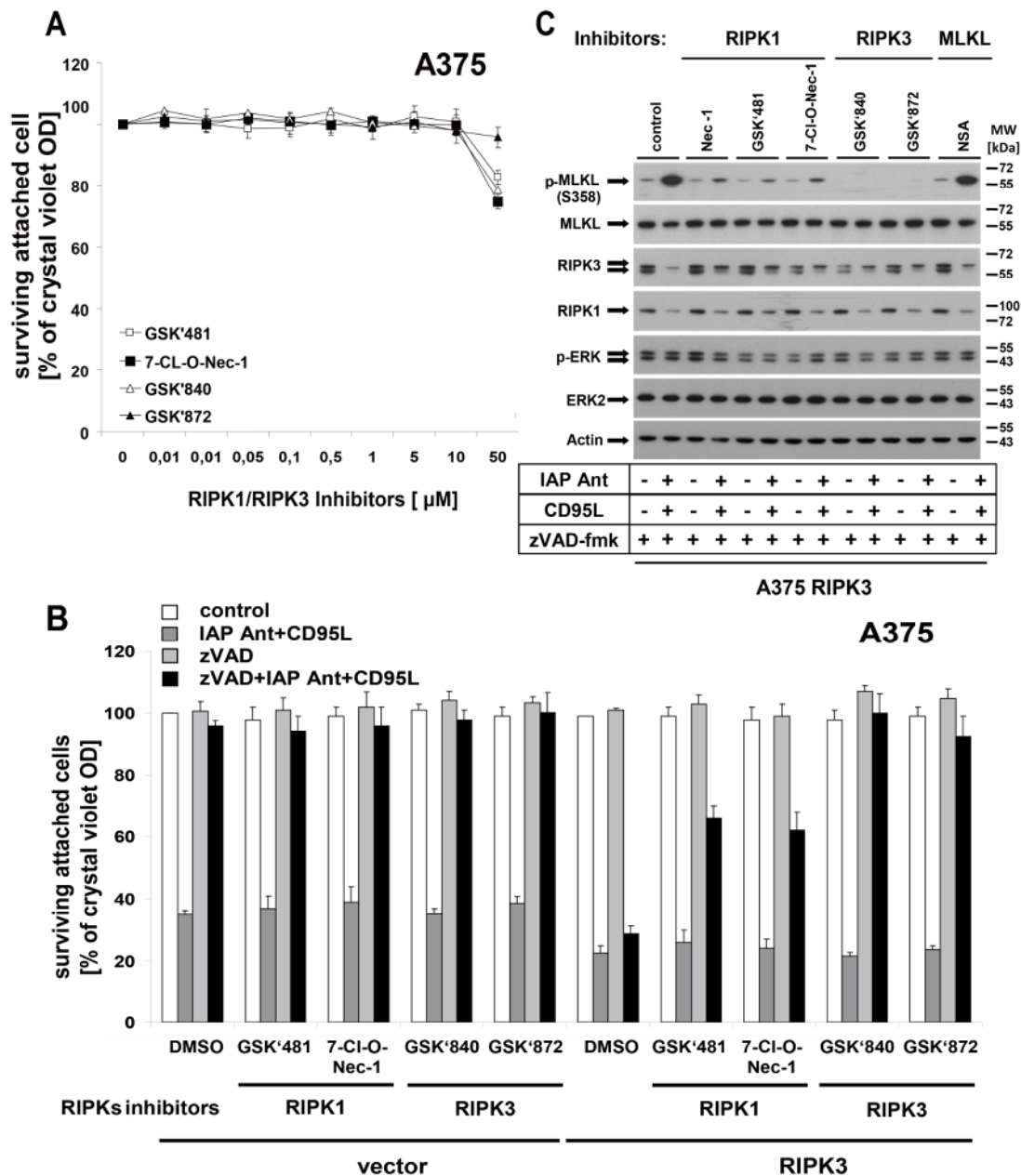


**Figure 13 RIPK3 and partially RIPK1 is required for MLKL phosphorylation mediated necroptosis.** A A375 cells were stimulated with RIPK1 specific inhibitors (7-Cl-O-Nec-1 and GSK'481; 10 µM each), RIPK3 specific inhibitors (GSK'840

and GSK'872) for 18-24 hours followed by crystal violet staining. Summary of three independently performed experiments including the S.E.M. of the whole set of experiments is shown. **B** A375 cells with expression of vector (control), RIPK3, and RIPK3 KD were pre-treated with zVAD-fmk (10  $\mu$ M), Compound A (100 nM), RIPK1 specific inhibitors (7-Cl-O-Nec-1 and GSK'481; 10  $\mu$ M each), Nec-1 (50  $\mu$ M), RIPK3 specific inhibitors (GSK'840 and GSK'872) or MLKL inhibitor NSA (10  $\mu$ M) alone or in indicated combinations for 1 h and subsequently stimulated with CD95L (0.5 U/ml) for 18-24 hours followed by crystal violet staining. Summary of three independently performed experiments including the S.E.M. of the whole set of experiments is shown. **C** A375 cells with expression of vector (control), RIPK3, and RIPK3 KD were pre-treated with zVAD-fmk (10  $\mu$ M), Compound A (100 nM) Nec-1 (50  $\mu$ M), RIPK1 specific inhibitors (7-Cl-O-Nec-1 and GSK'481; 10  $\mu$ M each), RIPK3 specific inhibitors (GSK'840 and GSK'872) or NSA (10  $\mu$ M) alone or in indicated combinations for 1 h and subsequently stimulated with CD95L (0.5 U/ml) for 6 hours. Protein expression of p-MLKL (Ser358), MLKL, p-ERK, ERK2, RIPK3 and RIPK1 was analysed by western blot. Actin was served as loading control. One of two independently performed experiments is shown.

#### 4.1.8 Inhibition of RIPK3 kinase activity promotes TNF-complex II formation

Ligation of death ligands to corresponding receptors is able to induce the complex assembly in absence of cIAPs activity using IAP antagonists and subsequently induce apoptosis or necroptosis [99,100]. Since RIPK3 inhibitors prevented RIPK3 reconstituted A375 cells from necroptosis, the effect RIPK3 inhibition on caspase 8-bound protein complex formation was analysed via using caspase 8 antibody coimmunoprecipitation. Upon TNF ligation, FADD, cFLIP, and RIPK1, RIPK3, and MLKL were recruited to caspase 8, namely complex II formation. In addition, phosphorylated RIPK1 (Ser166) and phosphorylated MLKL (Ser358) were also detected in the caspase 8-containing complex (Figure 13). When RIPK3 kinase activity was suppressed by RIPK3 inhibitor GSK'840, the amount of FADD and cFLIP within the complex II were elevated (Figure 13). Furthermore, interaction of RIPK3, RIPK1 and p-RIPK1 with caspase 8 were also increased in presence of GSK'840 (Figure 13). These results displayed that inhibition of RIPK3 activity promoted TNF complex II assembly. On the contrary, MLKL and its phosphorylation were less recruited to the complex when RIPK3 activity was restrained by GSK'840 (Figure 13).

Under TNF stimulation, RIPK3 reconstitution uncovered necroptosis through MLKL phosphorylation in melanoma cells, while RIPK3 repression by kinase inhibitor restrained CD95L-induced necroptosis via downregulating phosphorylation of MLKL. In RIPK3 overexpressing A375 cells, TNF-complex II

was assembled upon TNF ligation in absence of cIAPs and was locally increased by RIPK3 inhibitor (Figure 14). Inhibition of RIPK3 increased TNF complex II components interaction with caspase 8 but decrease of MLKL and its phosphorylation (Figure 14). These results indicated that Necrosome, which was composed of RIPK1, RIPK3 and MLKL, was potential part of complex II and dissected from complex II to initiate necroptosis execution. Inhibition of RIPK3 potentially stabilized TNF-complex II and prevented the necrosome dissociation.

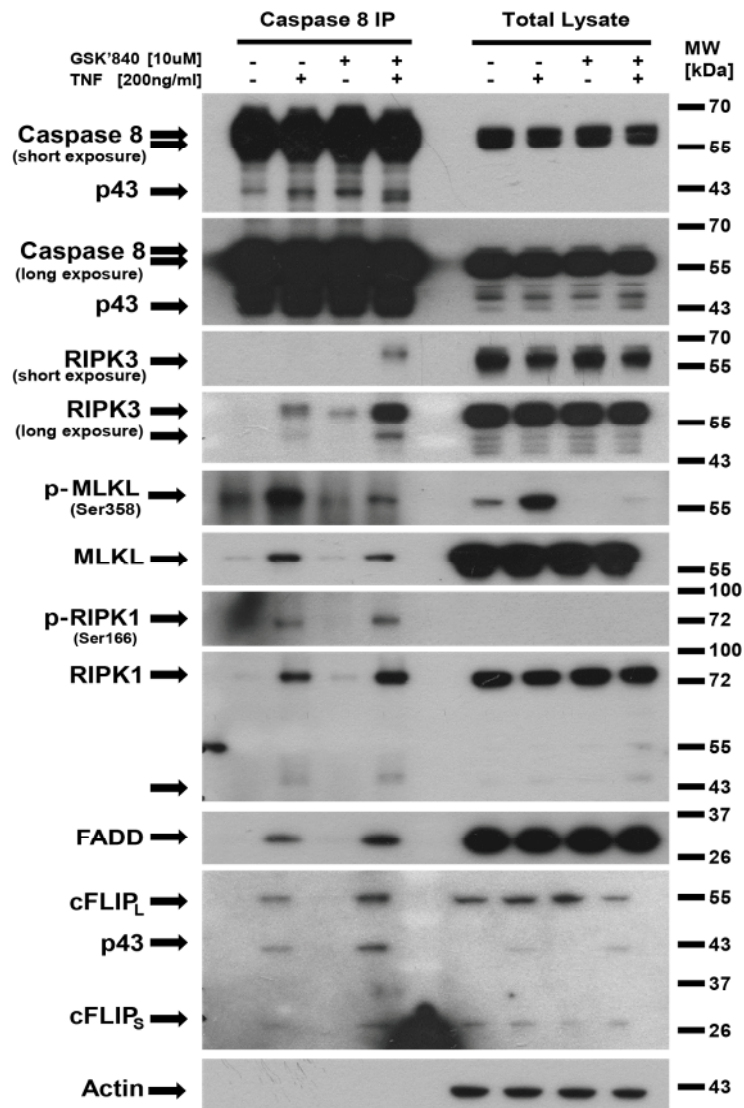


**Figure 14 RIPK3 inhibitor increased assembly of TNF-complex II formation.** A375 RIPK3 overexpressing cells were pretreated with zVAD-fmk (10  $\mu$ M) and Compound A (100 nM) in absence or presence of RIPK3 inhibitor GSK'840 (10  $\mu$ M) for 1 hour and subsequently stimulated with TNF (200 ng/ml) for 4 hours. TNF complex II was co-immunoprecipitated from total lysate using caspase 8 antibody. Respective proteins were subsequently analysed with western blot. One representative experiment of two independently performed experiments is shown.

### 4.1.9 DNA-Demethylation by DAC reconstituted RIPK3 expression in both human and murine melanoma cells

DNA methylation is one form of post-transcriptional modifications which add methyl groups to cytosine residues of DNA. 5-aza-2'-deoxytidine (Dacogen, DAC), as a cytidine analogue, is able to decrease methylation by restricting the activity of DNA methyltransferases. Since the mRNA expression level of RIPK3 is low or absent in melanoma cell lines, the causality between epigenetic DNA methylation and expression silence of RIPK3 was studied with application of demethylation reagent DAC.

Initially, human melanoma cell lines (A375, MM-LH, MM-RU and PM-WK) were cultured in medium with 2  $\mu$ M DAC for four days and the medium with DAC was freshened every day. Remarkably, RIPK3 expression was upregulated both at protein and mRNA level after demethylation via addition of DAC in human melanoma cells (Figure 14A, B). To confirm the general effect of DAC on RIPK3 expression in melanoma, murine melanoma cell lines (Ret1, 2 and HcMel3, 12), of which RIPK3 was also low expressed, were cultured with the same demethylation method as used for human melanoma cell lines. Analogously, RIPK3 expression was restored after demethylation in murine melanomas cell lines four days after treatment (Figure 14A). However unlike ectopical overexpression, reconstitution of RIPK3 via demethylation failed to induce spontaneous phosphorylation of MLKL (data not shown). In summary, demethylation reagent 5-aza-2'-deoxytidine was able to restore RIPK3 expression without altering other necroptosis-related proteins in human and murine melanoma cells *in vitro*, which indicated that hyper methylation was one potential mechanism for deficiency of RIPK3 and necroptosis resistance in melanomas.

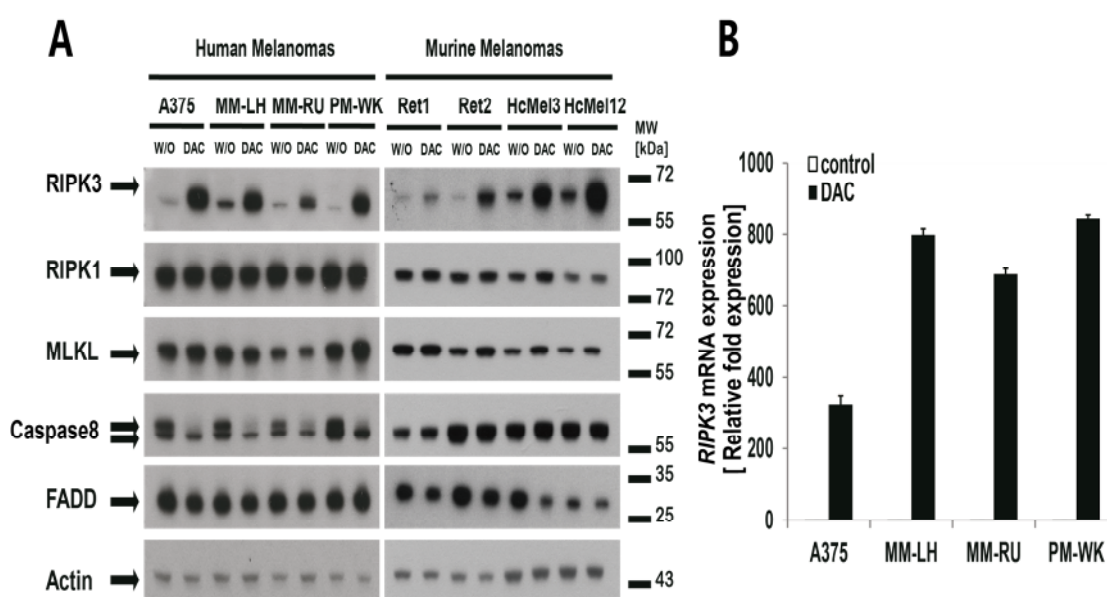


**Figure 15** DNA demethylation by 5-aza-2'-deoxytidine (DAC) was able to restore RIPK3 expression in melanomas. A Human melanoma cell lines (A375,

MM-LH, MM-RU and PM-WK) and murine melanomas cell lines (Ret1, Ret2, HcMel3 and HcMel12) were cultured with respective medium containing DAC (2  $\mu$ M) and medium with DAC were freshened every day. In the fourth day, cell pellets were collected to analyse RIPK3, RIPK1, MLKL, caspase 8 and FADD expression by western blot. Actin was served as loading control. One representative experiment of two independently performed experiments is shown. **B** Total mRNA from human melanomas cultured as described above was isolated and reverse transcribed to cDNA. *RIPK3* mRNA was quantified with qPCR. Summary of two independently performed experiments including the S.E.M. of the whole set of experiments is shown.

Based on the information available on DBTSS (database of transcription start sites, <http://dbtss.hgc.jp/>), there are predictive CpG islands prone to methylation residing in the promoter zone and exon 1 of *RIPK3* (Figure 16A). To further certify that the methylation status of *RIPK3* promoter, two specific primers for methylation specific PCR (MSP) as described in methods part were applied to qualification specific locus methylation of *RIPK3*. Compared with control group, DAC treatment decreased the methylation of *RIPK3* promoter in four human melanoma cell lines (Figure 16B). In addition to promoter methylation, methylation was detectable in the region of *RIPK3* exon2 as predicted. In brief, *RIPK3* promoter was methylated and its methylation was responsible for gene silence.

In both human and murine melanomas cells, *RIPK3* expression was low at the transcription level which suggested the potential epigenetic modification in *RIPK3* gene promoter. Addition of demethylation reagent DAC successful restoration *RIPK3* protein expression without changing *RIPK1* and *MLKL* further indicated that methylation was reason for lack of *RIPK3* expression. Methylation PCR results affirmed the methylation status of *RIPK3* gene promoter zone.

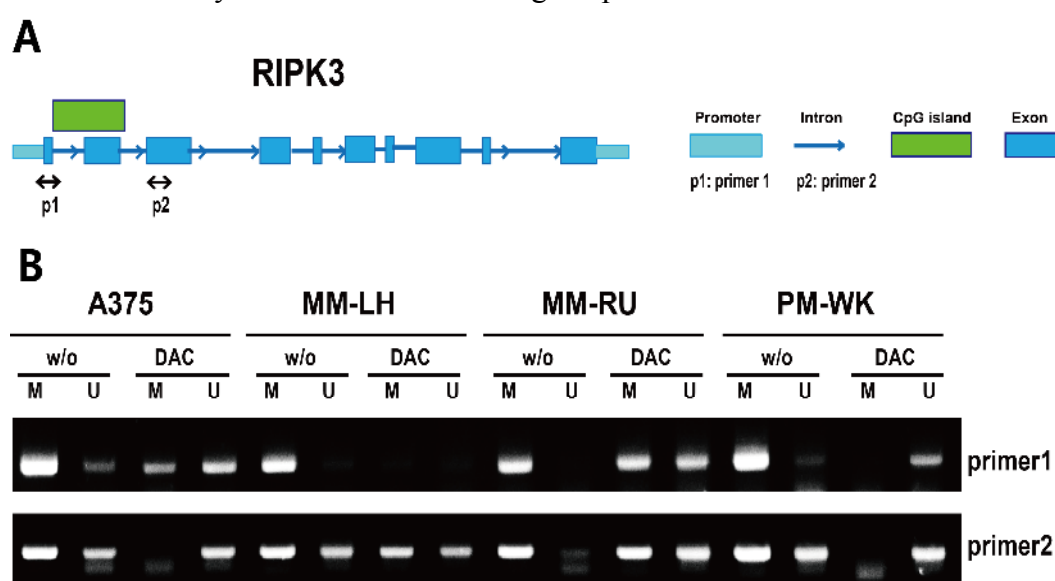


**Figure 16** *RIPK3* promoter is methylated in human melanoma cell lines. **A**

Schematic representation of *RIPK3* gene organization. **B** Human melanoma cells (A375, MM-LH, MM-RU and PM-WK) were cultured with respective medium containing 5-aza-2'-deoxytidine (2  $\mu$ M). Medium with DAC were freshened every day. In the fourth day, cell pellets were collected for genomic DNA isolation. DNA was modified with denaturation and sodium bisulfite treatment based on the protocol described in the methods part followed by PCR analysis. Methylation status was compared with methylated (M) *RIPK3* or unmethylated (U) *RIPK3* specific primers. One representative experiment of two independently performed experiments is shown.

#### 4.1.10 Demethylation-mediated *RIPK3* restoration is not competent for necroptosis execution

Since demethylation was sufficient to recommence *RIPK3* expression in melanoma cell lines, effect of demethylation-mediated *RIPK3* restoration on cell death was subsequently investigated. Human melanoma cell lines, of which *RIPK3* was reconstituted after demethylation treatment, were stimulated under apoptotic (CD95L) condition or necroptotic (zVAD-fmk/CD95L) condition in absence or presence of IAPs respectively. Of interest, whenever DNA methylation was prevented by DAC, metastatic melanoma cells (MM-LH, MM-RU) became more sensitive to CD95L-induced apoptosis and further sensitized by IAP antagonist (Figure 17). Nonetheless, CD95L failed to induce caspase-independent necroptosis in DAC-treated melanoma cells as ineffective as in parental melanoma cells (Figure 17). In the murine melanoma cells, demethylation-mediated *RIPK3* restoration was also not sufficient to induce necroptosis (data not shown).

We found that lack of *RIPK3* expression conferred necroptosis resistance in melanoma cell lines which was mediate by hyper methylation of *RIPK3* promoter. Demethylation of *RIPK3* by DAC treatment reconstituted its expression without altering *RIPK1* and *MLKL*. Although demethylation successfully reconstituted *RIPK3* in some melanoma cell lines, cells cannot be killed in necroptotic manner. Not as strong as ectopic *RIPK3* overexpression, demethylation failed to initiate *MLKL* phosphorylation, which can partially explained the incompetence of demethylation of *RIPK3* in necroptosis induction. In a meanwhile, RPM-EP melanoma cells in which *RIPK3* was absent were resistant to DAC-mediated *RIPK3* reconstitution (data not shown). This result suggested potential *RIPK3* mutation and other existed unknown regulatory elements were involved in *RIPK3* expression and in regulation of necroptosis execution in melanomas.

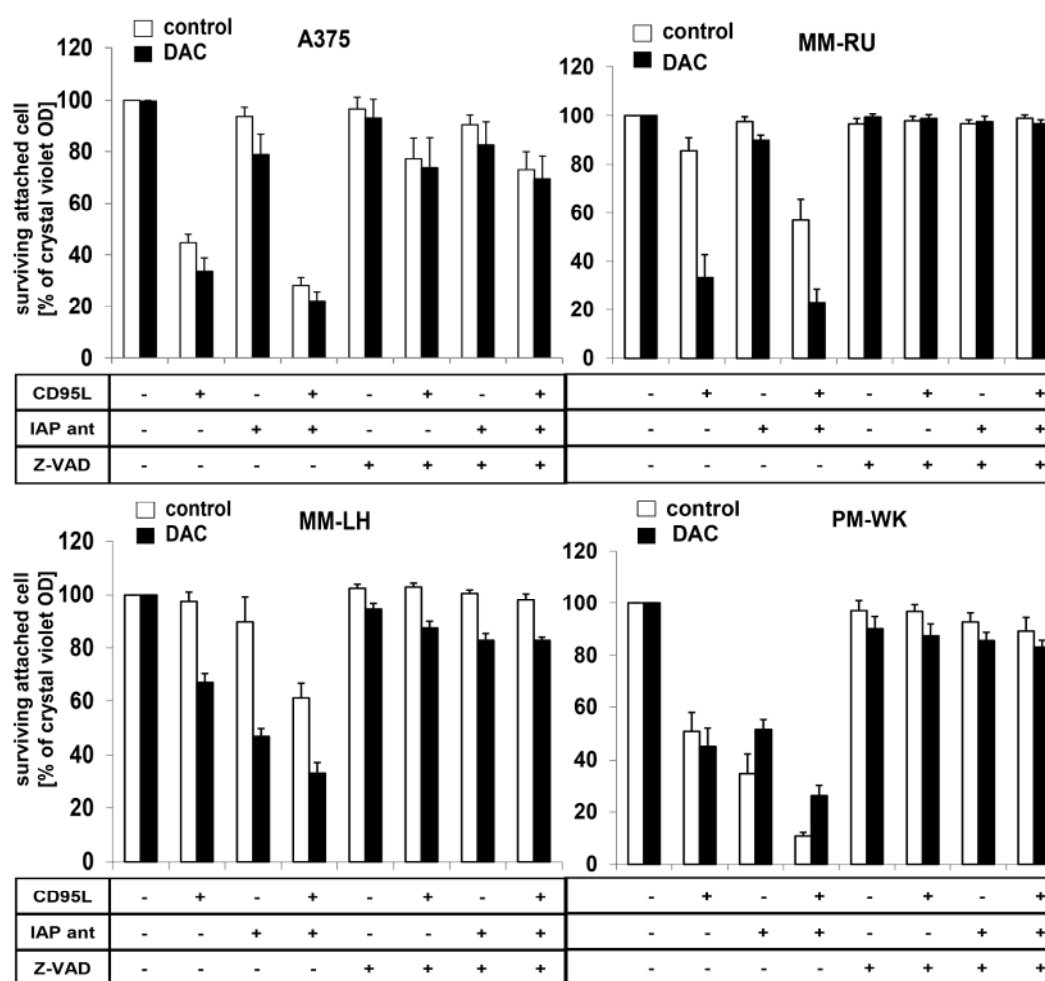


**Figure 17 Reconstitution of RIPK3 by demethylation is not sufficient to induce CD95L-mediated necroptosis.** Human melanoma cell lines (A375, MM-LH, MM-RU and PM-WK) were cultured with respective medium containing DAC (2  $\mu$ M) for four days. Medium with DAC were freshened every day. In the fourth day control or DAC treated cells were seeded into 96-well plate. Next day, cells were pre-treated with zVAD-fmk (10  $\mu$ M), Compound A (100 nM) alone or in combination for 1 h and subsequently stimulated with CD95L (0.5 U/ml) for 18-24 hours followed by crystal violet staining. Summary of three independently performed experiments is shown including the S.E.M. of the whole set of experiments.

#### 4.1.11 Dabrafenib blocks necroptotic cell death through inhibition of RIPK3 kinase activity

Since activating *BRAF* mutations account for more than 50 percent of melanoma patients, BRAF inhibitors are as an important class of anticancer drugs for melanoma targeted therapy [162]. Appealingly, Li, *et al.* reported that BRAF<sup>V600E</sup> inhibitor Dabrafenib is a potent RIPK3 inhibitor [163]. To investigate the effect of BRAF inhibitors effect on different death ligands-induced cell death, melanoma cells

carrying with vector control or RIPK3 were pre-treated Dabrafenib. In a meanwhile, effect of another BRAF inhibitor Vemurafenib on cell death was also used to compare with Dabrafenib. Consistent with reported results, Dabrafenib protected RIPK3 overexpressing cells from death ligands-mediated necroptosis but not apoptosis in our study (Figure 18A, B). Different from Dabrafenib, Vemurafenib did not exhibit any inhibitory impact on necroptosis in melanoma cells (Figure 18A, B).

Dabrafenib and Vemurafenib, as targeted therapeutic strategy against melanoma exhibited significantly clinical effectiveness for melanoma treatment. While Dabrafenib but not Vemurafenib protected RIPK3 reconstituted melanoma cells from death ligands-induced necroptosis. Considering the off-target effect of Dabrafenib on RIPK3 and necroptosis inhibition, Vemurafenib was potentially more promising without weakening necroptosis as an alternative form for tumour cell death.

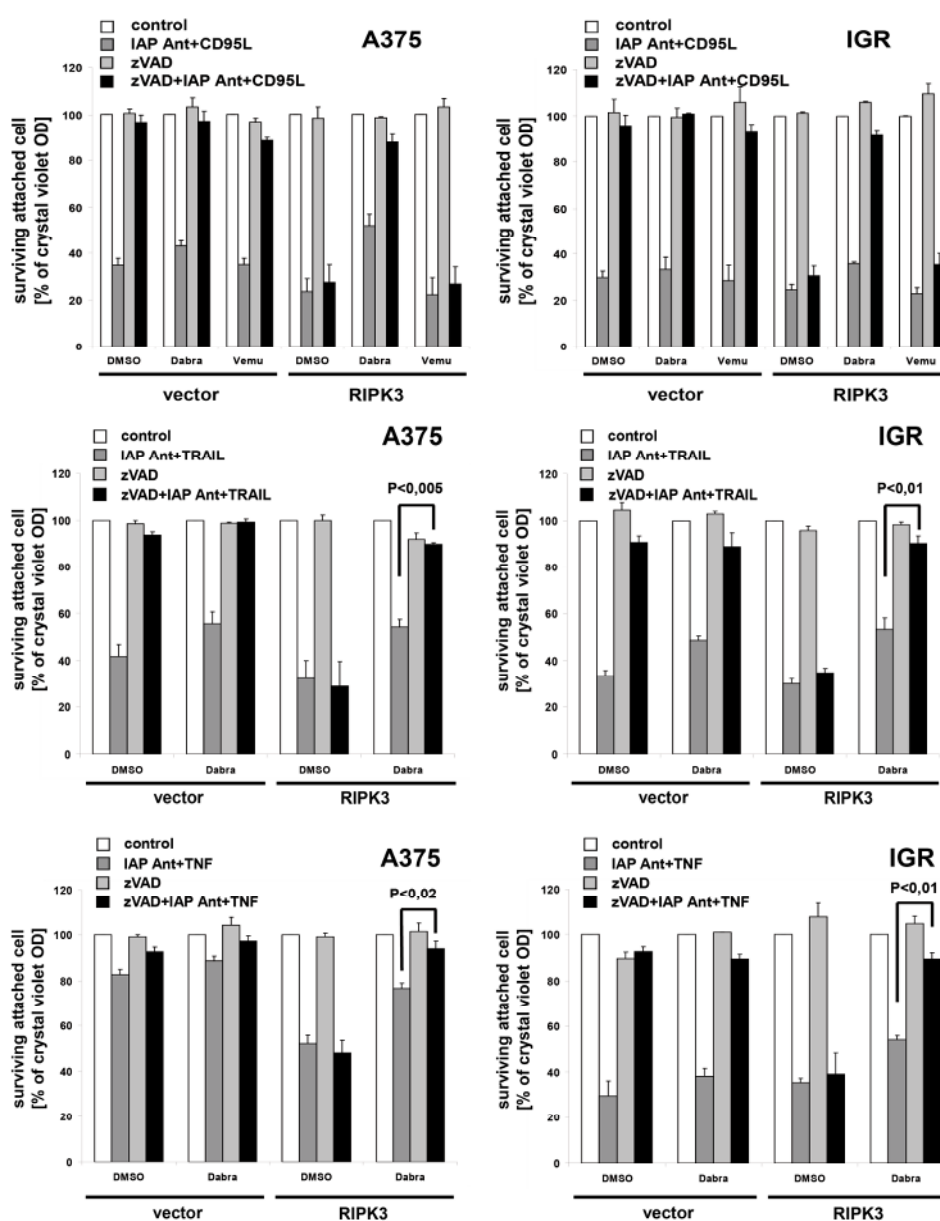


**Figure 18** BRAF inhibitor Dabrafenib but not Vemurafenib prevent A375

**RIPK3 overexpressing cells from death ligand-mediated necroptosis.** A375 (A) or IGR (B) cells with vector (control) or RIPK3 overexpression were pre-treated with zVAD-fmk (10  $\mu$ M), Compound A (100 nM) alone or in combination in absence or presence of respective BRAF inhibitors (10  $\mu$ M) for 1 h and subsequently stimulated with CD95L (0.5 U/ml) or TRAIL (100 ng/ml) or TNF (200 ng/ml) for 18-24 hours followed by crystal violet staining. Summary of three independently performed experiments including the S.E.M. of the whole set of experiments is shown.

Above results confirmed the inhibitory effect of Dabrafenib on necroptosis as off-target effect. To further investigate inhibitory function of Dabrafenib in necroptosis, phosphorylation of MLKL was next analysed. Both in A375 and IGR RIPK3 reconstituted cells, Dabrafenib decreased not only the spontaneous but also the necroptosis-induced phosphorylation of MLKL (Figure 19). On the contrary, Vemurafenib did not demonstrated inhibitory effect on necroptosis-mediated phosphorylation MLKL (Figure 19). These results explained that Dabrafenib exercised its inhibitory impact on necroptosis via interfering RIPK3 kinase activity. BRAF inhibitor, Dabrafenib but not Vemurafenib, interfered with necroptotic cell death through decrease phosphorylation of MLKL through restricting RIPK3 activity.

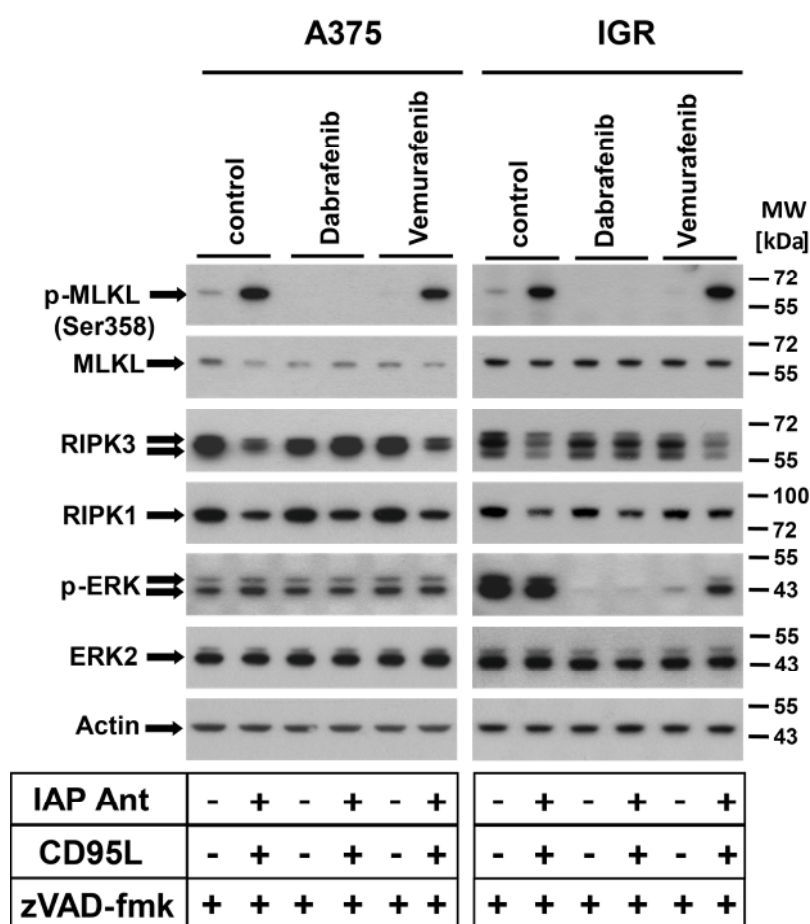


**Figure 19 Dabrafenib negatively regulated necroptosis via inhibition of**

**RIPK3-mediated spontaneous and CD95L-mediated MLKL phosphorylation.**

A375 or IGR cells with vector (control) or RIPK3 overexpression were pre-treated with zVAD-fmk (10  $\mu$ M), Compound A (100 nM) alone or in combination in absence or presence of Dabrafenib (10  $\mu$ M) or Vemurafenib (10  $\mu$ M) for 1 h and subsequently stimulated with CD95L (0.5 U/ml) for 6 hours. Expression of respective proteins were analysed by western blot. One representative experiment of two independently performed experiments is shown.

Both Dabrafenib and Vemurafenib as BRAF inhibitors are effective target therapies against melanoma, while they exhibited different influence on necroptotic cell death. Dabrafenib but not Vemurafenib protected RIPK3-reconstituted melanomas from death ligands mediated necroptosis. Dabrafenib, sharing the common characteristic with RIPK3 inhibitors, exerted its inhibitory impact through restriction of RIPK3 kinase activity and in turn decreasing phosphorylation of MLKL.

In this study, the inhibitory role of IAPs in death ligand-induced cell death was confirmed by chemical IAP antagonist. Loss and inhibition of IAPs by using IAP antagonist increased cell sensitivity, but not promoted melanoma cells from apoptosis into necroptosis when caspase activity was repressed. Lack of RIPK3 expression was identified as the missing link for necroptosis resistance in melanomas *in vitro*. Absence of RIPK3 in melanoma cell lines was the consequence of *RIPK3* DNA promoter hyper methylation. Ectopical expression of RIPK3 unveiled death ligand-induced necroptosis in melanoma cell lines. Mutation of RIPK3 kinase domain and addition of RIPK3 specific inhibitors further confirmed the indispensability of RIPK3 in necroptosis execution. Dabrafenib, which was used as BRAF inhibitor, impaired necroptosis by weakening RIPK3 kinase activity which was critical for phosphorylation of MLKL and necroptosis execution. Therefore, re-expression of RIPK3, either by DNA demethylation or overexpression, can be a strategy for necroptosis based therapeutic intervention against melanoma.

## 4.2 Identification of NF- $\kappa$ B regulatory effect on melanoma cell death

NF- $\kappa$ B signalling cascade activation initiates transcription of a variety of genes including cell death regulators such as cFLIP, Bcl-2 proteins, IAPs [143]. Initially, NF- $\kappa$ B activation is considered as negative regulatory signalling for cell death. It has been demonstrated by several studies that NF- $\kappa$ B activation is able to inhibit cell death induced by distinctive stimuli in a wide variety of cells [143,164]. Therefore, disordered NF- $\kappa$ B activation can induce pro-survival and death resistance signalling in melanomas in different ways. In this study, the impact of NF- $\kappa$ B activation for

cell death regulation in melanoma cells will be studied.

#### **4.2.1 IKK2 activation leads to constitutive activation of both canonical and non-canonical NF- $\kappa$ B pathway**

When the serine 177 and 181 residues of IKK2 are replaced by glutamine (IKK2EE), IKK2 became constitutively active resulting in activation of NF- $\kappa$ B pathway. On the contrary, IKK2 became dominant negative to block NF- $\kappa$ B pathway if the serine residues were mutated with alanine (IKK2 KD) [165]. In order to investigate the regulatory effect of NF- $\kappa$ B on cell death in melanoma, stable melanoma cells lines overexpressing IKK2 EE or IKK2 KD were generated respectively. Initially, IKK2 EE was tried to ectopically constitutively expressed, but it resulted in spontaneous cell death potentially because of cytokines or chemokines production (data not shown). To solve this problem, the overexpression was completed using vectors with tamoxifen inducible system. The different mutation forms of IKK2 were also transduced to cervical carcinoma HeLa cell to exclude the potential melanoma cell line-specific effect.

Successful overexpression of IKK2 was detectable when cells were stimulated with 4-hydroxytamoxifen overnight in both melanoma cell lines and HeLa cells. In addition, upregulation of p-I $\kappa$ B $\alpha$  also confirmed the NF- $\kappa$ B activation via IKK2 EE overexpression (Figure 20). Of interest, canonical NF- $\kappa$ B pathway activation via IKK2 EE overexpression, NF- $\kappa$ B2 p100 and its cleavage product p52 were upregulated in melanoma and HeLa cells which were usually mediated by IKK1 activation in non-canonical NF- $\kappa$ B pathway (Figure 20). Consistent with previous results that NF- $\kappa$ B activation led to upregulation of a variety of genes that exercise anti-apoptotic effect, IKK2 EE overexpression upregulated cFLIP expression in IGR and WM1346 cells (Figure 20). In HeLa cells, expression of cFLIP<sub>S</sub> was increased when NF- $\kappa$ B was activated. Furthermore, cIAP1, cIAP2 and A20 which played essential but reverse roles in the ubiquitination modification were increased in IKK2 EE but not IKK2 KD cells (Figure 20). Necroptosis related proteins, RIPK1, RIPK3 and MLKL were not altered after IKK2 activation. Expression of adaptor protein FADD and caspase 8 that were essential for apoptosis was independent from IKK2 activation status (Figure 20).

In summary, replacement of serine 177 and 181 residues by glutamine resulted in constitutive activation of NF- $\kappa$ B, which was confirmed by phosphorylation and degradation of I $\kappa$ B $\alpha$ . In our study, activation of NF- $\kappa$ B by active IKK2 initiated expression of a variety of proteins related with cell death resistance, including cFLIP, cIAP1, cIAP2 and A20. In addition, overexpression of IKK2 EE resulted in upregulation of NF- $\kappa$ B2 p100 and its partial cleavage fragment p52, which suggested the potential role of canonical NF- $\kappa$ B in non-canonical NF- $\kappa$ B activation. In terms of necroptosis related proteins, NF- $\kappa$ B activation did not display regulatory

effect on RIPK1, RIPK3 and MLKL.

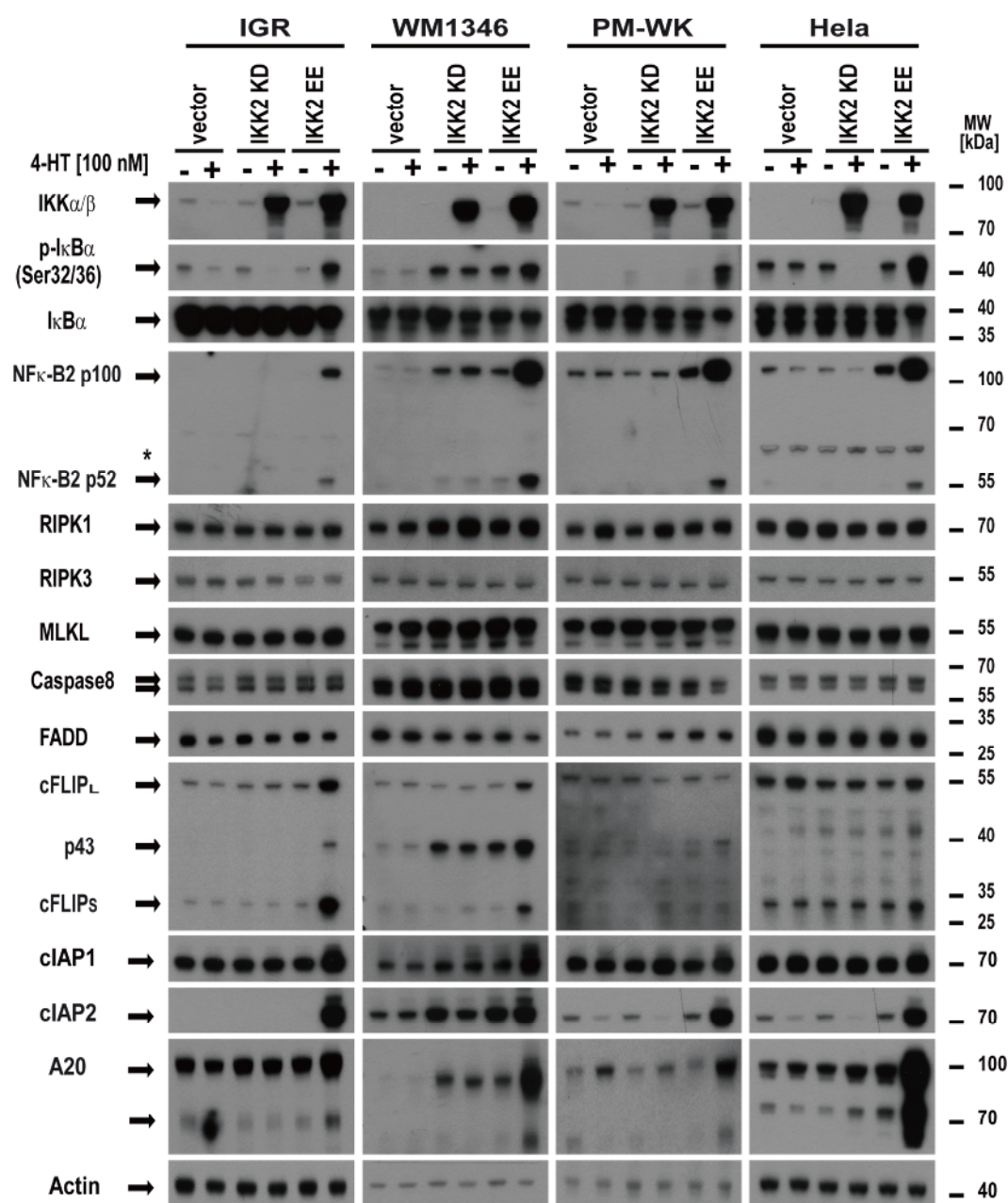


**Figure 20 IKK2 EE overexpression promotes target genes expression and activation of non-canonical NF- $\kappa$ B activation.** Human melanoma cell lines (IGR, WM1346 and PM-WK) and cervical carcinoma Hele cells were transduced with lentiviruses containing vector control, constitutively active IKK2 (IKK2 EE) and dominant negative IKK2 (IKK2 KD). After puromycin selection, cells with respective vectors were incubated with medium containing 4-hydroxytamoxifen (4-HT, 100 nM) overnight. IKK2 overexpression and expression of NF- $\kappa$ B related proteins, RIPK1, RIPK3, MLKL, caspase 8, FADD, cFLIP, cIAP1, cIAP2, A20 were analysed by western blot. Actin was served as loading control. One representative experiment of two independently performed experiments is shown.

## 4.2.2 Constitutive activation of NF- $\kappa$ B renders melanoma cells resistance to TNF-mediated apoptosis

Since overexpression of IKK2 EE resulted in upregulation of proteins that was relevant for cell death resistance in melanomas, the role of NF- $\kappa$ B signalling machinery on cell death regulation was further investigated. Cell sensitivity to TNF was compared between IKK2 EE and vector control or IKK2 KD cells. Consistent with the early results from our group [166], expression of dominant negative IKK2 (IKK2 KD) increased cell sensitivity to TNF stimulation while constitutive IKK2 activation (IKK2 EE) rendered cell resistance to TNF stimulation in melanoma cells *in vitro* (Figure 21). Moreover, blockade of IAPs by IAP antagonist generally and considerably increased cell sensitivity to TNF in melanoma and HeLa cells (Figure 21). Of interest, IKK2 EE overexpression resulted in acquired spontaneous sensitivity to IAP antagonist, which indicated the unusual potential pro-apoptotic effect of NF- $\kappa$ B in absence of IAPs (Figure 21). While TNF-mediated cell death in absence of IAPs activity was restrained by caspase inhibitor, which excluded that NF- $\kappa$ B activation was able to promote necroptosis in melanomas *in vitro*.

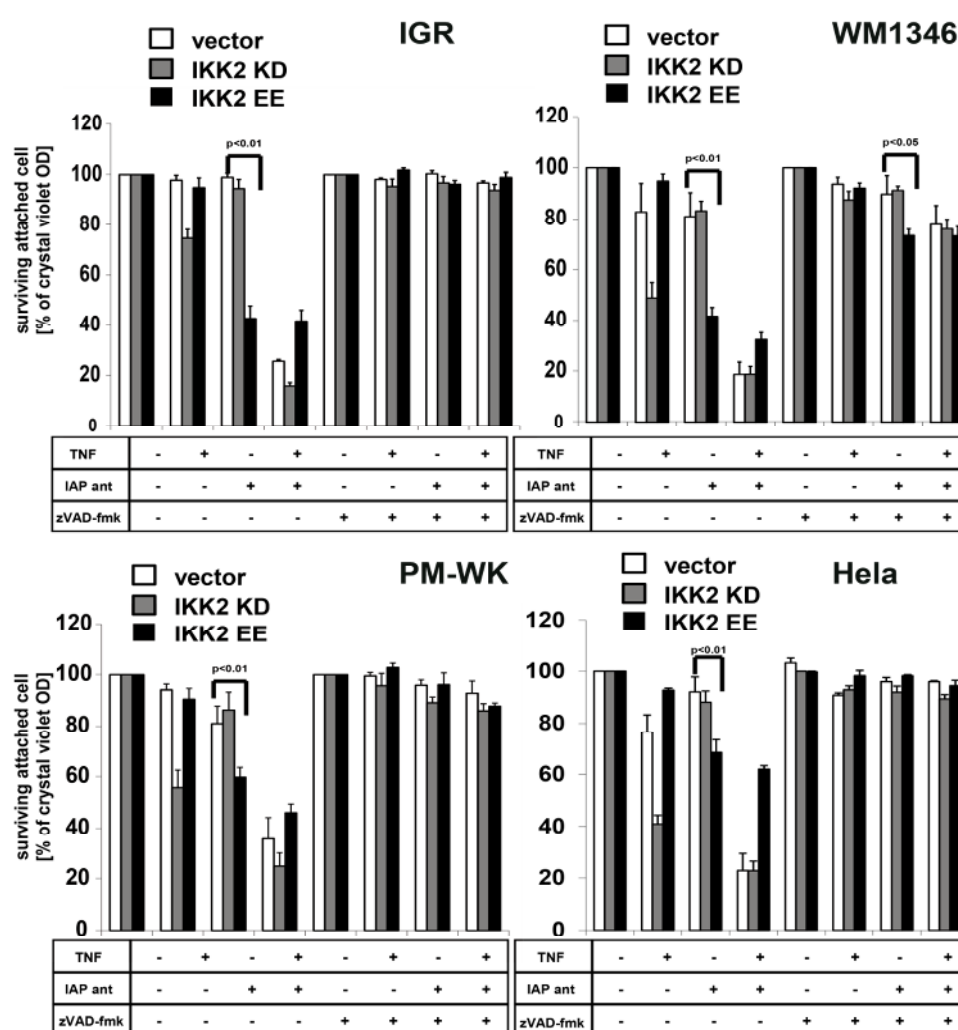


**Figure 21** Overexpression of IKK2 EE increase cell resistance to TNF and

**increased cell sensitivity to IAP antagonist.** Melanoma cells (IGR, WM1346 and PM-WK) or HeLa cells with expression of vector (control), IKK2 EE, and IKK2 KD were incubated with medium containing 4-hydroxytamoxifen (100 nM) overnight. Next day, cells were pre-treated with zVAD-fmk (10  $\mu$ M) or Compound A (100 nM) alone or in combination for 1 h and subsequently stimulated with TNF (100 ng/ml) overnight followed by crystal violet staining. Summary of three independently performed experiments including the S.E.M. of the whole set of experiments is shown.

We found that NF- $\kappa$ B activation resulted in TNF resistance in melanoma cells. On the contrary, overexpression of dominant negative IKK2 render cell sensitivity of melanoma cells to TNF. These results confirmed the general inhibitory effect of NF- $\kappa$ B signalling cascade on melanoma cell death. Moreover, depletion of cIAPs and inhibition of XIAP via chemical IAP antagonist led to spontaneous cell death in IKK2 active melanoma cells. In summary, NF- $\kappa$ B activated melanoma cells were resistant to TNF-mediated cell death but became sensitive to chemical IAP antagonist, which suggested the role of NF- $\kappa$ B in cell death regulation potentially varied because of the specificity of tested cells. In contrast, both IKK2 EE and IKK2 KD cells were protected from TNF-induced cell death when caspases activity was blocked, which suggested inability of NF- $\kappa$ B to induce necroptosis in melanomas.

Since activation of IKK2 resulted in spontaneous cell sensitivity to IAP antagonist in melanomas, molecular mechanism behind the phenomenon was next studied. As transcriptional target genes of NF- $\kappa$ B, both cIAP1 and cIAP2 were upregulated in IKK2 EE overexpressing cells. Particularly, cIAP2, which was generally lower expressed compared with cIAP1 in melanoma cells, remarkably increased whenever NF- $\kappa$ B was activated by inducible IKK2 EE expression (Figure 22). To confirm that IAP antagonist-induced cell death in IKK2 EE cells was related with inhibitory effect on IAPs, expression of cIAP1 and cIAP2 was compared between vector control and IKK2 EE cells in presence of IAP antagonist. As an effective IAP antagonist, Compound A was able to decrease both endogenous expression and IKK2 EE-mediated upregulation of cIAP1. Although Compound A was sufficient to downregulate cIAP2 expression, its inhibitory effect of on NF- $\kappa$ B activation-induced cIAP2 was marginal (Figure 22). In addition, a cleavage product of caspase 8, oligomerized p18 fragment was uniquely detectable in IKK2 EE overexpressing cells upon IAP antagonist treatment. Furthermore, NF- $\kappa$ B2 p52 was accumulated when cIAP1 was depleted in WM1346 cells.

Although NF- $\kappa$ B played negative role in TNF-mediated apoptosis in melanomas, activation of NF- $\kappa$ B by constitutively active IKK2 led to spontaneous cell death when IAPs activity was impaired by IAP antagonist. This unexpected pro-apoptotic impact of NF- $\kappa$ B on melanoma was completed through downregulate cIAP1 and

slightly cIAP2 by addition of Compound A. Moreover, an active fragment of caspase-8 p18 was only detectable in IKK2 EE cells by IAP antagonist stimulation. These results confirmed the pro-apoptotic effect of IKK2 activation in melanoma cells in absence of IAPs activity.

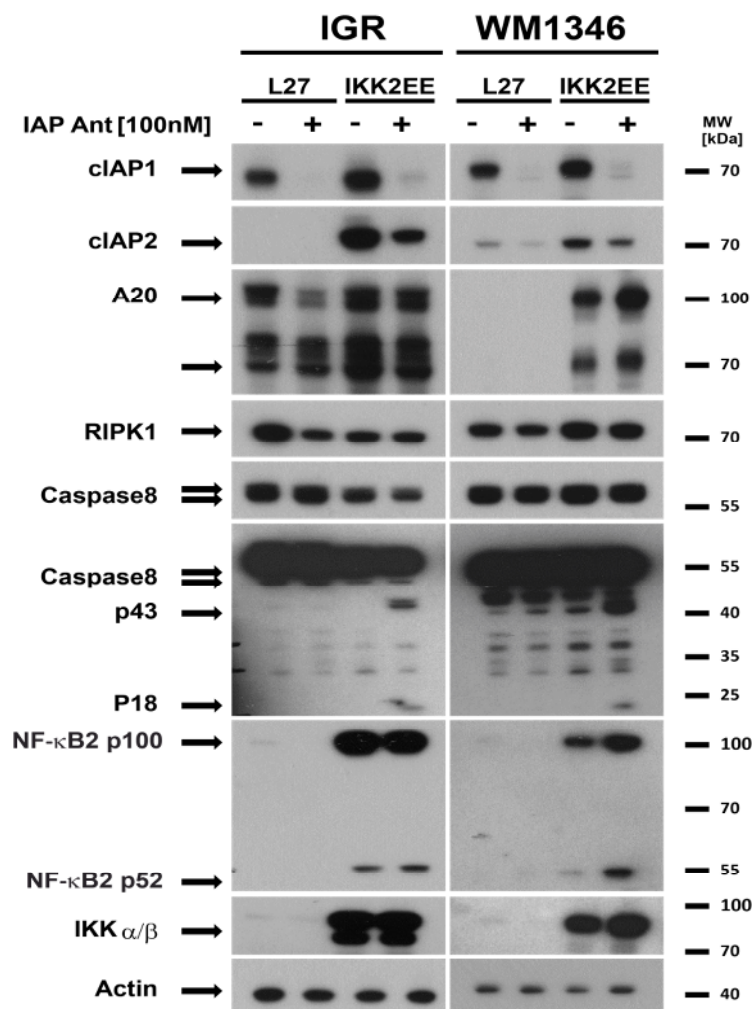


**Figure 22 IAP antagonist decreases cIAP1 and slightly cIAP2 and promotes caspase 8 cleavage to induce apoptosis.** IGR and WM1346 melanoma cells with expression of vector (control) or IKK2 EE, were treated with 4-HT (100 nM) overnight to induce gene of interest to express. Next day, cells were treated by Compound A (100 nM) for 1 h. Total lysate was isolated and respective proteins were analysed by western blot. One representative experiment of two independently performed experiments is shown.

### 4.2.3 Spontaneous apoptosis of IKK2 EE cells in absence of IAPs was independent from IAP antagonist-mediated autocrine TNF activation

Since IAP antagonist was sufficient to induce apoptosis in IKK2 EE cells, dependency of IAP antagonist-mediated TNF activation was investigated to unmask the molecular mechanism behind the cell death. *TNF* mRNA expression was firstly compared between vector control cells and IKK2 EE overexpressing cells in absence of IAP antagonist. As a target gene of NF- $\kappa$ B signalling cascade, *TNF* was increased considerably in IKK2 EE cells compared with vector control. When cIAP1 was depleted by Compound A, *TNF* was marginally increased in mRNA level in the IKK2 EE IGR cells (Figure 23A).

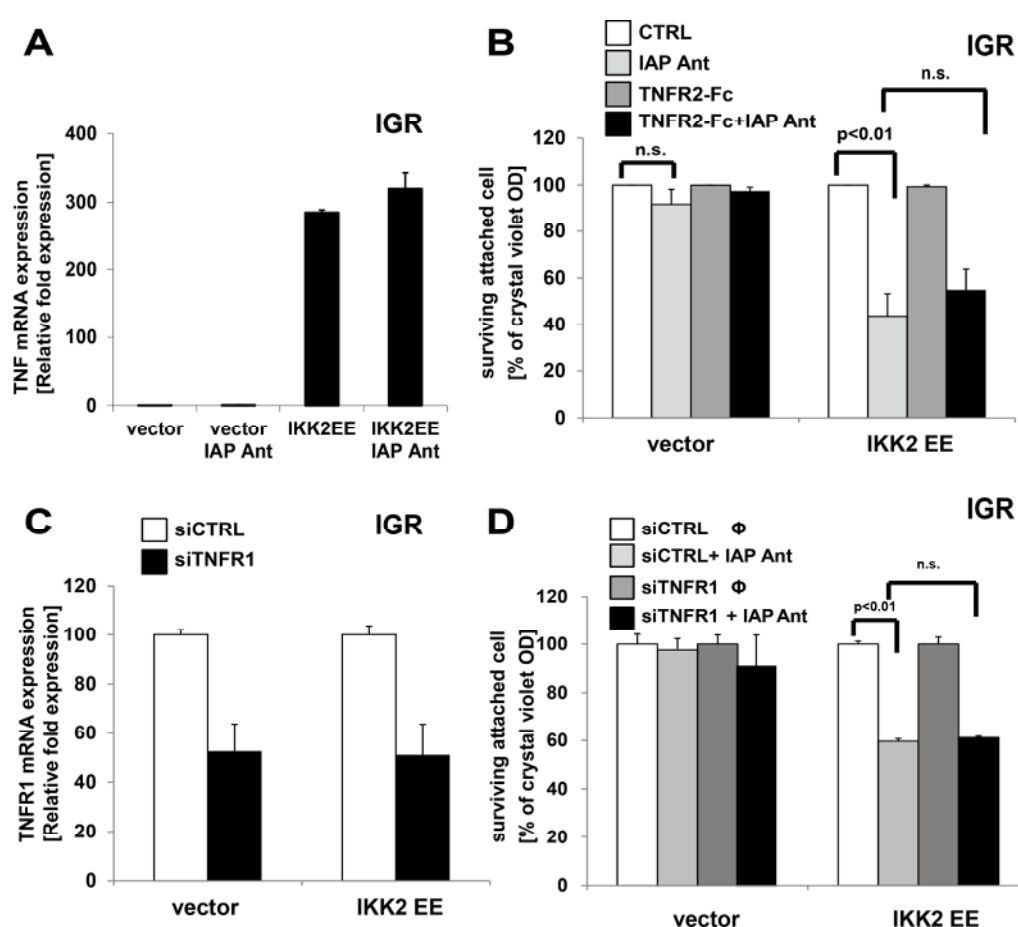


**Figure 23 IAP antagonist-induced apoptosis is independent from IAP antagonist-mediated autocrine TNF activation in IKK2 EE IGR cells.** **A** Vector control or IKK2 EE overexpressing IGR cells were non-stimulated or stimulated with Compound A (100 nM) for 1 hour. Total mRNA was isolated and reverse transcribed to cDNA. *TNF* level was quantified with qPCR. Summary of two independently performed experiments including the S.E.M of the whole set of experiments is shown. **B** Vector control or IKK2 EE overexpressing IGR cells were

pre-treated with recombinant TNFR2-Fc (10  $\mu\text{g/ml}$ ) for 1 h and subsequently stimulated with compound A (100 nM) overnight followed by crystal violet staining. Summary of three independently performed experiments is shown including the S.E.M. of the whole set of experiments. **C** IGR cells were transfected with either siCTRL or siTNFR1 for 48 h. Knockdown effect was quantified with *TNFR1* mRNA qPCR analysis. Summary of two independently performed experiments is shown including the S.E.M. of whole set of experiments. **D** Vector control or IKK2 EE overexpressing IGR cells were transfected with either siCTRL or siTNFR1 for 48 h and subsequently stimulated with compound A (100 nM) overnight followed by crystal violet staining. Summary of three independently performed experiments including the S.E.M. of the whole set of experiments is shown.

To further investigate if this minor upregulation of endogenous TNF by IAP antagonist was sufficient to induce apoptosis in IKK2 EE cells sensitivity, recombinant TNFR2-Fc was used to block the TNF signalling machinery to confirm the effect of IAP antagonist-induced TNF. Interestingly, addition of TNFR2-Fc failed to prevent IKK2 EE cells from compound A-mediated cell death (Figure 23B). To further conclude that apoptosis resulting from loss of cIAP1 in IKK2 EE cells was independent from IAP antagonist-mediated autocrine TNF loop, siRNA of TNFR1 were used to downregulate TNFR1 expression. The knockdown efficiency of TNFR1 was confirmed by qPCR analysis (Figure 23C). Consistently with addition of TNFR2-Fc, knockdown of TNFR1 expression was not sufficient to block Compound A-induced cell death in IKK2 EE overexpression cells (Figure 23D).

In this part of study, NF- $\kappa$ B activation resulted in increase of *TNF* expression at mRNA level that was slightly increased after IAPs inhibition. Blockade of TNF signalling by addition of recombinant TNFR2-Fc failed to protect IKK2 EE cells from IAP antagonist-induced apoptosis suggest the independency of autocrine TNF activation by IAP antagonist in IKK2 EE cell death, knockdown of *TNFR1* was also incompetent to prevent IKK2 EE cells from apoptosis in absence of IAPs. These results demonstrated that the pro-apoptotic effect of IKK2 activation was independent from IAP antagonist-mediated autocrine TNF activation.

#### **4.2.4 Loss of cIAP1 promotes formation of RIPK1-dependent Ripoptosome to induce apoptosis by constitutive NF- $\kappa$ B activation**

It has been confirmed by early results from our group that cIAPs are negative regulators for Ripoptosome formation [99]. To identify the role of loss of cIAPs in apoptosis in IGR IKK2 EE cells, the proteins interacting with caspase 8 were immunoprecipitated following Compound A stimulation and compared with vector

control cells. Of interest, loss of cIAP1 by Compound A stimulation resulted in recruitment of FADD, cFLIP, RIPK1 to caspase 8 in NF- $\kappa$ B inducibly activated IGR cells by addition of 4-HT (Figure 24). These results suggested that decrease of cIAP1 by IAP antagonist was sufficient to induce Ripoptosome formation without exogenous ligands stimulation when NF- $\kappa$ B was activated. In addition, phosphorylated RIPK1, which was difficult to detect in the total lysate samples, was massively recruited to the Ripoptosome complex (Figure 24). These results indicated that RIPK1 especially its phosphorylation was functionally relevant for IAP antagonist-induced cell death in IKK2 EE cells.

NF- $\kappa$ B activation resulted in cIAP1 and cIAP2 expression and inhibition of cIAPs mainly cIAP1 by IAP antagonist led to spontaneous apoptotic cell death in IGR IKK2EE cells. Assembly of Ripoptosome potentially explained the IAP antagonist-induced apoptosis in IKK2 EE melanoma cells. In the complex, phosphorylated RIPK1 was recruited substantially which suggested the indispensable role of RIPK1 in apoptosis of IKK2 EE cell in absence of cIAPs.

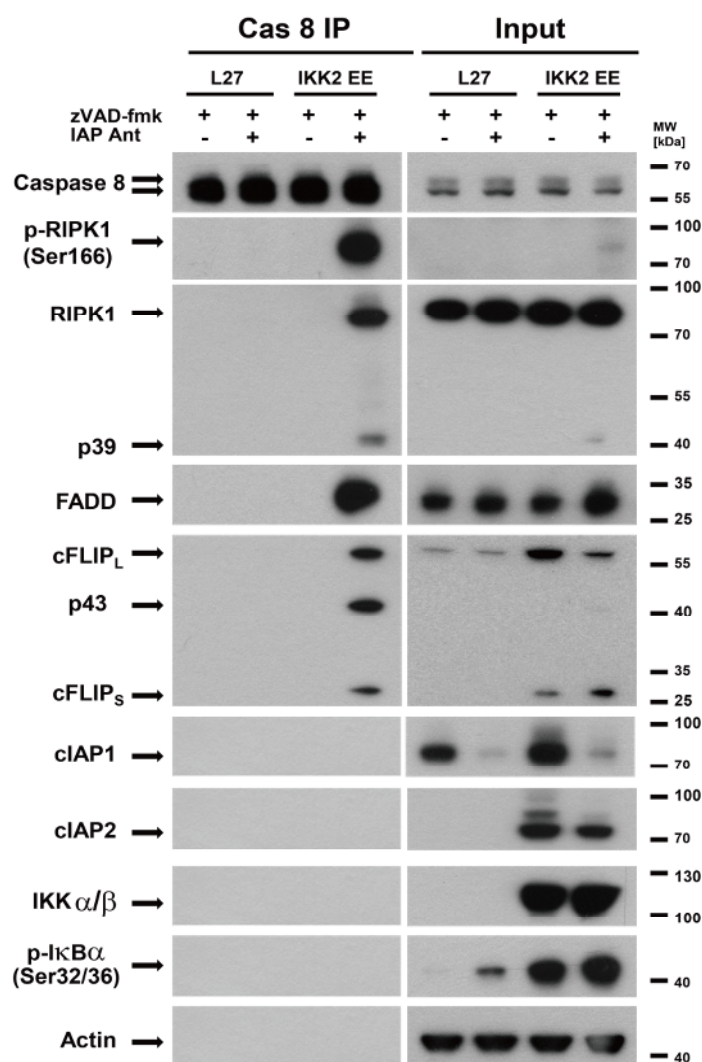


**Figure 24 Loss of cIAP1 promotes Ripoptosome formation in IKK2 EE cells.**

IGR cells with overexpression of vector (control) or IKK2 EE, were treated with 4-HT (100 nM) to induce expression of gene of interest overnight followed by Compound A (100 nM) stimulation for 1 h. Caspase 8 was immunoprecipitated from total cell lysates (Input) as described in the methods part. Respective co-precipitated proteins were analysed by western blot. One representative experiment of two independently performed experiments is shown.

Considerable recruitment of RIPK1 and RIK1 phosphorylation in the Ripoptosome complex led us to investigate the dependency of RIPK1 in IAP antagonist-mediated cell death in IKK2 EE cells (Figure 25A). Compared with vector control, IKK2 constitutive activation leads to spontaneous sensitivity to IAP antagonist which was consistent with previous results. Of interest, RIPK1 inhibitor, Necrostatin-1, largely rescued IKK2 EE cells from cell death. To further confirm the essential role of RIPK1 for cell death in IKK2 EE cells, the role of RIPK1 in Ripoptosome formation was also investigated. As expected, level of FADD and cFLIP recruited to caspase 8 was decreased, namely repression of RIPK1 decreased Ripoptosome formation. Significantly, RIPK1 and its phosphorylation were both downregulated when RIPK1 kinase activity was restrained by its inhibitor (Figure 25B).

In brief, during the study of RIPK1 dependency in IKK2 EE cells apoptosis in absence of cIAPs, we found that RIPK1 activity was required for the cell death. RIPK1 was phosphorylated and recruited to the Ripoptosome complex and further induced IAP antagonist-mediated cell death in IKK2 EE melanoma cells.

In summary, NF- $\kappa$ B activation initiates a variety of genes transcription, including cell death-related proteins. In this study, we confirmed that NF- $\kappa$ B activation resulted in upregulation of IAPs and cFLIP which rendered melanoma resistance to TNF-mediated apoptosis. Inhibition of IAPs via IAP antagonist increased cell sensitivity to TNF stimulation *in vitro*. Different from the general inhibitory impact of NF- $\kappa$ B on cell death, depletion of cIAPs resulted in spontaneous cell death when NF- $\kappa$ B was activated via inducible expression of constructively active IKK2. IAP antagonist-induced apoptosis in IKK2 EE IGR cells was independent from the IAP antagonist-mediated autocrine-TNF activation. The pro-apoptosis effect of IKK2 activation on IAP antagonist-induced cell death was result of RIPK1-dependent Ripoptosome assembly. These results suggested that the pro-survival NF- $\kappa$ B signalling can also transverse into pro-apoptotic cell cascade under specific conditions like IAPs depletion in melanoma cell lines.

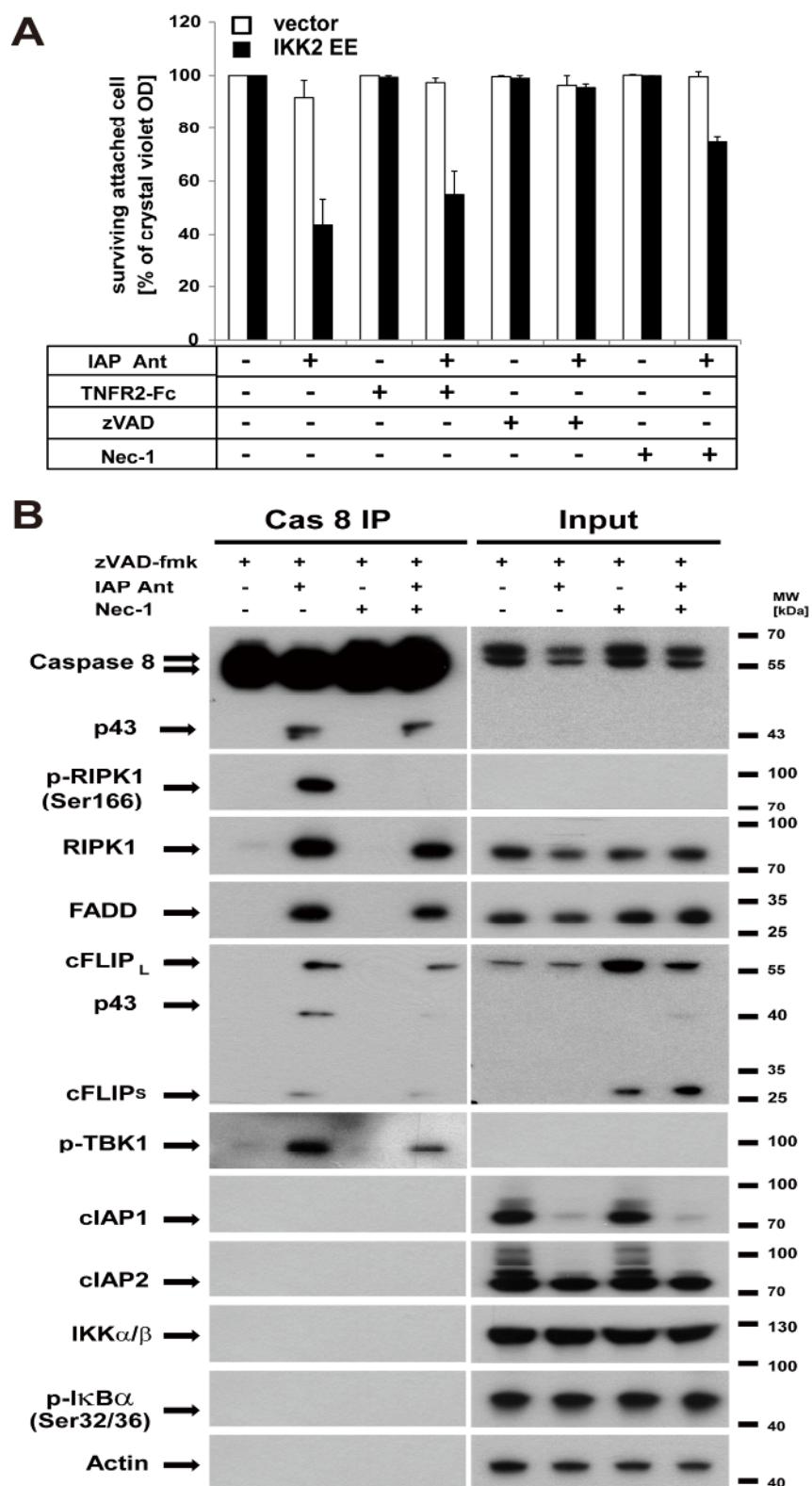


**Figure 25 IAP antagonist-mediated Ripoptosome assembly and apoptosis in IKK2 EE overexpressing cells is RIPK1 dependent.** A IGR cells with overexpression of vector (control) or IKK2 EE, were treated with 4-HT (100 nM) overnight to induce expression of gene of interest. Next day, cells were pretreated

with zVAD-fmk (10  $\mu$ M), or TNFR2-Fc (100 ng/ml) or Necrostatin-1(10  $\mu$ M) alone or in combination and subsequently stimulated with Compound A (100 nM) stimulation overnight followed by crystal violet staining. Summary of three independently performed experiments including the S.E.M. of the whole set of experiments is shown. **B** IGR IKK2EE cells were treated with 4-HT (100 nM) overnight to induce expression of gene of interest. Next day, cells were pretreated with zVAD-fmk (10  $\mu$ M) for 1 hour followed by Compound A (100 nM) stimulation for 4 hours. Caspase 8-bound proteins were immunoprecipitated from total cell lysates (Input) by caspase 8 specific antibody. Expression of respective co-precipitated proteins was analysed by western blot. One representative experiment of two independently performed experiments is shown.

## 5. Discussion

### 5.1 IAPs inhibits CD95L-mediated cell death in melanoma

Melanoma is primarily resistant or acquires resistance to targeted therapeutics such as BRAF inhibitors or in combination with MEK inhibitors [167]. It is worth of investigations to ascertain the resistance mechanism of melanomas and better increase sensitivity to therapeutics and prolong the survival rate of melanoma patients.

In our study, the cell sensitivity to CD95 ligand (CD95L) of human melanoma cell lines from different stages was studied. A375 and RPM-EP cells are originated from primary or recurrent primary cutaneous melanoma, while IGR cells are from lymph node metastasis and SK-MEL 28 cells are from subcutaneous metastasis of melanoma. Compared with primary melanomas, metastatic cell lines were more resistant to CD95 ligand-mediated apoptosis (Figure 6A) which was consistent previous results [168] reported by our lab. Moreover, in RIPK3 reconstituted cells, the metastatic cell line (IGR) was also less sensitive to CD95L-mediated necroptosis compared with A375 RIPK3 cells (Figure 8B, C). These results suggested that melanoma cells have gained the resistance in the process of metastasis and the extent of metastasis were probably relevant for the cellular resistance.

For further understanding of the cell death resistance mechanisms in melanoma, the role of IAPs was studied because of their well-characterized inhibition in regulation of caspases and RIPK1 activities and in turn cell death. An impressive finding was that cIAP1 was uniformly expressed in different stages of melanomas as keratinocytes, melanocytes and nevus cells. In contrast, cIAP2 was only expressed in A375, RPM-EP melanoma cells and HaCaT keratinocytes. Of interest, the level of XIAP expression was higher in melanoma than keratinocytes, melanocytes or nevus cells (Figure 6B). Therefore, cIAP1 and XIAP could play the main role of cell death resistance and inhibition of these proteins might represent a promising strategy for melanoma treatment. The IAP antagonist, Compound A, used in this study is designed to disrupt the function of XIAP and downregulate the endogenous expression of cIAP1 and cIAP2 [120]. In terms of inhibitory effect, the protein level of cIAP1 can be downregulated by Compound A with lower concentration in A375 cells than IGR cells. Compared with cIAP2, the effect of Compound A on cIAP1 was more specific in A375 cells (Figure 6C).

Even though apoptosis and necroptosis regulated the cell death via utilization of different signalling machineries [43], considerably increased cell sensitivity to CD95L-mediated both apoptosis (Figure 6A, D) and necroptosis (Figure 8B, C) was detected when IAP activity was suppressed by Compound A in all tested melanoma cells. These results evidently demonstrated that cIAP1 and XIAP conferred main resistance to CD95L-induced cell death and suggested the less indispensable role of cIAP2 in cell death resistance. As well, early reports of our group confirmed that the

anti-apoptotic effect of cIAP1 was more distinguishable than cIAP2 [166]. In IGR cells which lack of XIAP and cIAP2 expression, Compound A increased its cell sensitivity through downregulation of cIAP1. To ascertain which proteins have more significant regulatory impact on cell death, it has to be noted that the expression level of IAP family members varies among different stages and types of cell lines. It is also reported that IAP antagonist is able to increase the efficiency of radiology in prostate cancer treatment [169] and sensitivity to chemotherapy in glioblastoma [170]. In all, inhibition of IAPs sensitizes melanoma cells to CD95L-mediated cell death. Therefore, a combination of IAP inhibition and death receptor activation could be an effective strategy for elimination of melanoma tumours in patients.

## 5.2 RIPK3 is lost during the development of melanoma because of promoter methylation

When melanoma cell sensitivity to CD95L was screened, it was found that human melanomas were killed by CD95L in an exclusively apoptotic manner (Figure 6A, C). Lack of caspases-independent and RIPKs-dependent necroptosis makes it intriguing to unveil the mechanism of necroptosis resistance in human melanomas. Gene deficient mouse models have confirmed that loss of certain components of necroptosis machinery, especially RIPK3 and MLKL, usually protects different tissues or mice from necroptotic cell death [171-173]. Of interest, compared with normal pigmentation cells and keratinocytes, RIPK3, but not MLKL, was absent in melanoma cells (Figure 7A, B) in our study, which suggested that absence of RIPK3 could be a potential reason for lack of *in vitro* necroptosis in melanomas. In addition to human melanomas, RIPK3 expression level was also low in melanoma cell lines derived from the transgenic melanoma mice (Figure 7A).

In human melanomas, absence of RIPK3 protein expression is a consequence of lack of *RIPK3* expression at transcriptional level (Figure 7B). A general lack of *RIPK3* mRNA can be a result of limited promoter activation controlled by epigenetic modifications such as DNA methylation and histone deacetylation. In both human and murine melanoma cells, demethylation reagent 5-aza-2'-deoxytidine tremendously restored expression of RIPK3 without influencing expression of other cell death related proteins (Figure 15A). Within the availability of genetic information of *RIPK3*, CpG islands near the *RIPK3* transcription start site (TSS) were identified in a variety of human tissue and cancer cells (<http://dbtss.hgc.jp/#chr14:24335619-24341040:->). Methylation specific PCR (MSP) results verified methylation of *RIPK3* promoter and the methylation of RIPK3 was reversible through addition of demethylation reagent 5-aza-2'-deoxytidine (Figure 16B). Furthermore, methylation level of RIPK3 promoter was decreased more significantly in primary melanoma cell lines (A375 and PM-WK) than in the metastatic melanoma cells (MM-RU and MM-LH) after demethylation ( B). On the contrary, in human RPM-EP melanoma cells, 5-aza-2'-deoxytidine was not able to

upregulate RIPK3 expression (data not shown). In murine melanomas, although RIPK3 expression was restored in all murine melanoma cells *in vitro*, melanoma cell lines originated from DMBA-induced *HGF-CDK4R24C*-transgenic melanoma mice were more sensitive to 5-aza-2'-deoxytidine-induced demethylation than cells from *RFP-RET*-transgenic mice (Figure 15A). Koo G.B, *et al.* recently reported that about two thirds of sixty cancer cell lines representing different types and stages of cancers abnormally express RIPK3 as undetectable level including glioblastoma, lung adenocarcinoma, hepatocellular carcinoma, bladder transitional cell carcinoma, breast ductal carcinoma, cervical adenocarcinoma, colorectal adenocarcinoma, and pancreatic adenocarcinoma, prostate adenocarcinoma [154]. In contrast, in terms of cancer cell lines originated from hematopoietic malignancies including acute lymphoblastic T leukaemia, acute myeloid leukaemia, acute monocytic leukaemia, Burkitt's B-cell lymphoma and follicular B cell lymphoma, the expression of RIPK3 is detectable. In summary, RIPK3 is low expressed in a panel of cancer cell lines as well as melanoma and its expression can be reconstituted by demethylation reagent. However, inconsistent expression level and response to demethylation of RIPK3 in melanoma and other cancers cell lines suggest that promoter methylation only can partially explains the silence of RIPK3 and other unknown mechanisms such as gene mutations are required further investigations.

Of interest, DAC treatment increased apoptotic cell sensitivity to CD95L in MM-LH and MM-RU cells (Figure 17), which was potentially related with upregulation of RIPK3 since its facilitative regulatory in apoptosis independent from kinase activity. In the meanwhile, other tumour suppressor genes also restored after demethylation in melanoma.

Although demethylation treatment restored RIPK3 expression to detectable level and increased cell sensitivity to CD95L-mediated apoptosis, it failed to induce CD95L-mediated necroptosis in absence of caspase 8 activity (Figure 17). Unlike RIPK3 overexpressing cells, demethylation of RIPK3 was unable to induce spontaneous phosphorylation of MLKL. Furthermore, phosphorylated MLKL was undetectable under necroptotic induction conditions in demethylated melanoma cells (data not shown). These results suggested demethylation was sufficient to reconstitute RIPK3 expression but insufficient to rescue its kinase activity. Given cells that are resistant to demethylation like RPM-EP, it is quite probable that the other unknown mechanisms exist to regulate RIPK3 expression and its kinase activity.

In contrast with CD95 ligand, both Doxorubicin and Etoposide, as common chemotherapeutics for cancers, are able to induce RIPK3-dependent necroptosis in 5-aza-2'-deoxytidine treated cancer cells [154]. Doxorubicin and Etoposide, as DNA damage reagents, interfere with the process of DNA transcription and generally induce apoptosis via mitochondria-mediated pathway. In the earliest researches for necroptosis, it is believed that mitochondria are required for the induction of necroptosis [174,175]. Recent evidence casts doubt on the idea that the involvement

of mitochondria is essential in necroptotic signalling machinery [102,176,177]. The involvement of mitochondria and its related cell death effectors in necroptosis induction need further experiment proof. In addition to RIPK3 kinase activity, it has been demonstrated by several groups that the interaction between RIPK3 and HSP90 is required for RIPK3 activation and necroptosis induction [178,179]. On the other hand, demethylation reagents decreased the lysine methylation of Hsp90 [180]. Is the effect of demethylation on HSP90 interfere its interaction with RIPK3 needed further experimental proof. These results indicate that ectopical expression of RIPK3 differs from its natural expression because of potential lack of post translational scaffold or modifications. If RIPK3 only performs as a kinase or may also involves in the stoichiometry modulation of proteins within death-inducing complexes by a presumed scaffold function is an intriguing question that needs to be addressed by further studies.

### **5.3 RIPK3 kinase and partial RIPK1 activity is critical for MLKL phosphorylation and necroptosis initiation**

Previous studies have revealed that RIPK3 is imperative in necroptotic cell death regulation during embryonic development [181,182], inflammation [172,183,184], virus infections [185] and cell death upon different stimuli ligation [76,84,99,186]. In our study, RIPK3 but not its kinase inactive mutant ectopical expression allowed for necroptotic cell death which was absent in the parental melanoma cells. Unlike RIPK3, RIPK1 generally was expressed in all the tested melanoma cell lines and its expression and phosphorylation were not altered by RIPK3 overexpression (Figure 7A and Figure 8A). These results indicated that RIPK3 but not RIPK1 expression as a kinase was the missing link for necroptosis initiation in human melanoma.

Although RIPK1 and RIPK3 share common characteristics in structure, RIPK1 possesses an unique C-terminal death domain (DD) for interaction with other proteins containing DD. RIPK1 is recruited to plasma membrane associated complex I upon death ligand ligation and dissected into cytoplasm as a secondary complex when it is deubiquitinated. In the cytoplasmic complex, RIPK1 interacts with RIPK3 as an amyloid-like structure followed by phosphorylation [74]. Within the complex, RIPK1 is auto-phosphorylated at the serine 166 residue that positively contributes to RIPK1 activation and interaction with RIPK3. Auto-phosphorylation at Ser227 residue of RIPK3 is not required for RIPK1/RIPK3 necrosome assembly, but essential for the interaction of RIPK3 with MLKL [157]. When RIPK1 activity was blocked by its inhibitors, CD95L/IAP antagonist-induced necroptosis was only partially protected in our study. While in case of RIPK3 repression, necroptotic cell death under the same stimuli conditions were completely rescued by addition of RIPK3 specific inhibitors (Figure 13). These results suggested that RIPK1 inhibitors disrupted interaction between RIPK1 and RIPK3, in turn resulting in decrease of RIPK3 in the necrosome complex but without affecting its kinase activity. If the

remaining less RIPK3 in the complex is still able to induce necroptosis, this hypothesis needs to be proved by further RIPK1 co-immunoprecipitation.

To date, there is still lack of discriminative biochemical biomarkers for the *in situ* detection of necroptosis *in vitro* and *in vivo*. MLKL is firstly discovered to be involved in necroptosis as searching RIPK3 interacting proteins by using necroptosis inhibitor Necrosulfonamide (NSA) and later confirmed by siRNA library [102]. MLKL interchanges with phosphorylated RIPK3 through its C-terminal pseudokinase domain upon necroptosis induction. Following recruitment, MLKL is phosphorylated by RIPK3 at Thr357 and Ser358 residues. In our study, the overexpression of RIPK3 but not its kinase mutant led to the spontaneous phosphorylation (Ser358) of MLKL as strong as it in HaCaT keratinocytes in which RIPK3 was expressed normally (Figure 8A). The basal phosphorylation of MLKL in RIPK3 overexpressing cells and HaCaT keratinocytes have not led to spontaneous necroptosis, suggesting phosphorylation of MLKL is an essential but not decisive step of necroptosis induction. Phosphorylation of MLKL is believed to induce a conformational change as releasing the N-terminal four-helix bundle domain of MLKL which is indispensable for necroptosis induction. Murphy, *et al.* found that structure-guided mutation of the MLKL pseudo-active site resulted in constitutive, RIPK3 independent necroptosis, indicating that modifications of MLKL is required for initiation of the necroptosis pathway downstream of RIPK1/RIPK3 platform [102]. Even though reconstitution of RIPK3 leads to spontaneous MLKL phosphorylation, it is still not sufficient to induce conformational change compared with the level under necroptotic stimuli conditions. Furthermore, development and application of RIPK1 and RIPK3 inhibitors enable to further prove the role of RIPKs in necroptosis. In our study, RIPKs inhibitors, especially RIPK3 inhibitors, prevented MLKL from phosphorylation (Figure 13B, C). The extent of MLKL phosphorylation is relevant for the percentage of necroptotic cell death which demonstrates that MLKL phosphorylation by RIPK3 is required in the necroptosis.

MLKL is characterized with an N-terminal coiled-coil domain region and a C-terminal kinase-like domain that is responsible for binding to RIPK3. NSA competitively binds to the cysteine 86 in the N-terminal coiled-coil domain of MLKL instead of C-terminal pseudokinase domain [157]. Not as effective as RIPKs inhibitors, NSA is unable to decrease MLKL phosphorylation or CD95L-mediated necroptosis in RIPK3 overexpressing melanoma cells *in vitro* (Figure 13B, C). Structural studies of MLKL identified the Lys219 and Glu343 as functionally indispensable residues for ATP binding of murine MLKL. Site mutations of these two residues (K219M and Q343A) in murine MLKL result in its constitutive activation and necroptosis without stimuli [102]. These principles support our finding that NSA is not sufficient to block CD95L-mediated necroptosis.

In addition to RIPK3 specific inhibitors, Li, *et al.* found that six different *BRAF* inhibitors, Dabrafenib as the most potent one, selectively inhibited RIPK3 kinase activity by competitively binding to its ATP site [163]. In our study, the described

off-target effect of Dabrafenib protected RIPK3-reconstituted melanoma cells from not only necroptotic cell death via inhibition of RIPK3 kinase activity (Figure 18, 19). In addition to hindrance of RIPK3 activity, other unknown molecules involved in cell signalling regulation such as MAPK are potentially influenced by Dabrafenib. On the contrary, alternative BRAF inhibitor Vemurafenib failed to suppress MLKL phosphorylation and necroptosis (Figure 18, 19). The distinctive effect of these two BRAF inhibitors on necroptosis raises further attention to investigate the interaction between BRAF/MAPK mediated proliferation signalling and RIPK3-mediated necroptosis. In terms of therapeutic intervention, the off-target effect of Dabrafenib on cell death mainly on necroptosis should be considered. Since Dabrafenib interferes with the necroptosis via impairing RIPK3 kinase activity, it is not suitable for using it in combined therapy.

#### **5.4 Constitutively active IKK2 EE renders cell resistance to TNF stimulation via expression of anti-apoptotic proteins in melanoma cells**

The first member of the nuclear factor-kappa B (NF- $\kappa$ B) protein family was discovered in 1988. As a family consisted of transcription factor, NF- $\kappa$ B activation leads to a wide variety of genes transcription. According to their functions, target genes of NF- $\kappa$ B can be categorized into cytokines/chemokines and their modulators, immunoreceptors, proteins involved in antigen presentation, cell adhesion molecules, acute phase proteins, stress-related proteins, cell surface receptors, cell death regulators, growth factors and their modulators, transcription factors and their modulators, enzymes [164].

Since the main focus of this study is the regulatory effect of NF- $\kappa$ B on melanoma cell death, stable melanoma cell lines with IKK2 mutations that imitate the constitutively active (IKK2 EE) or dominant negative (IKK2 KD) forms of IKK2 were respectively generated. Initially, IKK2 EE was tried to be ectopically constitutively expressed, but it resulted in spontaneous cell death potentially because of cytokines or chemokines production (data not shown). To solve this problem, the overexpression was completed using vectors with tamoxifen inducible system. Consistent with previous results, successful IKK2 EE overexpression led to the phosphorylation and degradation of I $\kappa$ B $\alpha$  and further the activation of NF- $\kappa$ B signalling machinery (Figure 20). Unlike the canonical NF- $\kappa$ B pathway, activation of NIK (NF- $\kappa$ B-inducing kinase) only requires activation of IKK1, not IKK2 nor NEMO, for leading to phosphorylation and processing of NF- $\kappa$ B2 p100 into p52 [187]. In our study, only IKK2 activation led to upregulation of both precursor NF- $\kappa$ B2 p100 and its partial degradation product p52 (Figure 20). It is known that activation of NF- $\kappa$ B initiates the expression of NF- $\kappa$ B2 in a feedback regulatory circuit [188]. In case of NF- $\kappa$ B2 p52, since the expression level of NIK was not altered after IKK2 activation (data not shown), if active IKK2 was sufficient to

mediate the processing of NF- $\kappa$ B2 p100 or active IKK2 inter-phosphorylated IKK1 resulting in processing of NF- $\kappa$ B2 p100 needed further studies. More and more studies have recognised that canonical and non-canonical NF- $\kappa$ B pathways are not completely independent from each other.

In respect of transcriptional function, NF- $\kappa$ B activation resulted in anti-apoptotic protein expression as previous reported (Figure 20). Both the long and short form of cFLIP, a natural inhibitor of caspase 8, was significantly upregulated in IGR and WM1346 cells after IKK2 activation. However, in PM-WK cells and HeLa cells, the level of cFLIP was not altered significantly post IKK2 activation, which indicated the transcriptional regulatory effect of NF- $\kappa$ B on cFLIP was cell specific (Figure 20). In addition, both cIAP1 and cIAP2 were upregulated in IKK2 active cells (Figure 20). cIAP2 is weakly detectable in most cancer cells including melanomas because of its shorter half-life than cIAP1, which might be due to an increased susceptibility of cIAP2 to spontaneously dimerize, auto-ubiquitinate, and be degraded [122]. Whenever NF- $\kappa$ B was activated, cIAP2 increased remarkably especially in cells that were lack of cIAP2 expression, in turn which suggested cIAP2 played critical role in NF- $\kappa$ B activation (Figure 20). In terms of the ubiquitin-editing enzyme A20, its expression was also elevated by NF- $\kappa$ B activation in all the tested cells regardless of its endogenous expression level. One additional band about 70 kDa was detected and upregulated consistent with the expression pattern of the band near 100 kDa in IKK2 EE cells (Figure 20). Further experiments are needed to confirm the specificity of the lower molecular weight band. A20 is capable of terminating NF- $\kappa$ B activation through degradation of Lys63-linked poly-ubiquitin chains on RIPK1 as a deubiquitinase and further proteasomal degradation of RIPK1 by addition of Lys48-linked poly-ubiquitin chains as an ubiquitin E3 ligase [189]. Hutti JE, *et al.* reported IKK2 activation phosphorylates A20 at its Ser381 residue to increase its inhibitory effect on NF- $\kappa$ B activation [190]. In our study, even though A20 was recruited after NF- $\kappa$ B activation, the inhibitory feedback of A20 was not dominant, potentially because of its modification by IKK2 activation. For the necroptosis related proteins, RIPK1, RIPK3 and MLKL, none of them was changed after IKK2 activation (Figure 20). RIPK3 which was absent in melanoma and HeLa cells was still low expressed, which excluded the possibility that NF- $\kappa$ B activation was required for RIPK3 expression and partially explained the incompetence of NF- $\kappa$ B activation to induce necroptosis.

Since NF- $\kappa$ B activation enabled the upregulation of anti-apoptotic proteins expression, the negative regulatory effect of NF- $\kappa$ B on apoptosis was studied. Cancer cells are generally resistant to TNF because of intrinsic activation of NF- $\kappa$ B. Both vector control and IKK2 EE cells have not responded to TNF stimulation (Figure 21). On the contrary, consistent with previous results that IKK2 inactivation rendered cell sensitivity to TNF [166], melanoma cells overexpressing IKK2 KD became sensitive to TNF (Figure 21). Moreover, when

activity of IAPs was blocked by Compound A, cells became sensitive to TNF, which was because of autocrine TNF-loop induced by IAP antagonist [120]. On the contrary, IAP antagonist-induced apoptosis in IKK2 EE cells were independent from IAP-mediated autocrine TNF activation (Figure 23B, D). In addition, either melanoma cells or HeLa cells were lack of RIPK3 expression, TNF or TNF/IAP antagonist solely induced caspase-dependent cell death (Figure 21). When NF- $\kappa$ B was activated by constitutive IKK2, cells, lack of RIPK3 expression, were still resistant to necroptosis in presence of IAP antagonist. NF- $\kappa$ B activation initiates a variety of genes transcription but not RIPK3, which partially explained the inability of NF- $\kappa$ B for necroptosis induction. In addition, NF- $\kappa$ B activation crosstalks with other pro-survival signalling which potentially antagonize necroptosis machinery. The regulatory effect of NF- $\kappa$ B on necroptosis needed to be further studied within cells that RIPK3 expressed normally like HaCaT keratinocytes.

### **5.5 Constitutive activation of IKK2 promotes melanoma cell death in absence of cIAP1 independent from IAP antagonist-mediated autocrine TNF activation**

When cIAPs were depleted by IAP antagonist, spontaneous cell sensitivity was observed in all tested IKK2 active melanoma cells (Figure 21). As effective as in parental cells, Compound A was able to decrease the endogenous and inducible expression of cIAP1 to the undetectable level (Figure 22). In respect of cIAP2, compound A exhibited less efficient inhibition especially for the NF- $\kappa$ B activation-induced cIAP2. cIAP2, which expression level was low in melanomas, was enhanced by IKK2 activation and remained stable in spite of IAP antagonist treatment. The less responsive reaction of cIAP2 to Compound A can be explained by resistance of its homodimers to Smac mimetics-induced degradation and its characteristic of rapid induction by NF- $\kappa$ B [121,122]. These results demonstrated that NF- $\kappa$ B activation mainly induced cIAP2 expression, while Compound A exercised its cell death induction effect principally through depleting cIAP1 instead of cIAP2 expression. Caspase activation is central to the regulation of apoptotic pathways. In the process of IAP antagonist-mediated apoptosis, the initiator caspase 8 was cleaved and activated as p18 fragment that was consistent with the function of other IAP antagonist in various cancer cells (Figure 22). Because of the inhibitory effect of cIAPs on NIK, addition of IAP antagonist releases NIK into the cytoplasm and promotes the partial degradation of NF- $\kappa$ B2 p100 into p52. Consistent with the known knowledge, IAP antagonist increased the processing of the precursor NF- $\kappa$ B2 p100 into p52 fragment (Figure 22).

It has been confirmed by continuous studies that IAP antagonist is capable of inducing apoptosis in TNF-dependent manner in sensitive cells [120,191].

Activation of NF- $\kappa$ B induces a variety of genes transcription including TNF $\alpha$ , CD95L and TRAIL, IAP antagonist-mediated cell death only can be rescued by TNFR1-Fc [120]. Inconsistent with this general TNF-dependency in IAP antagonist-mediated apoptosis, neither addition of recombinant TNFR2-Fc or knockdown of TNFR1 by siRNA failed to protect IKK2 EE cells from IAP antagonist-induced apoptosis (Figure 23B, D). Unlike IAP antagonist-mediated NF- $\kappa$ B activation, active IKK2 EE led to more forceful and durable NF- $\kappa$ B activation. In turn the amount of cytokine production was more considerable (Figure 23A). When death ligands interact with respective receptors, the signalling commences within complexes formation at the plasma membrane and matures to generate cytoplasmic secondary signalling complexes, which appears to occur not only for TNFR1 but also Fas, TRAILR and TLR [99,153,192,193]. In previous project, the inhibitory effect of recombinant TNFR2-Fc on TNF-mediated apoptosis was confirmed in IKK2 KD HaCaT and melanoma cells. Failure of suppression of TNFR2 to protect IKK2 EE cells from compound A-induced apoptosis suggested the potential existence of other death platforms which were independent from TNF production. Even though TNFR1 siRNA decreased TNF receptor expression, there still remained considerable level of TNFR1. To exclude or confirm the TNF-dependency in IAP antagonist apoptosis, further experiments are needed, such as generation of TNFR1 knockout cell lines by CRISPR, blockade of Fas or TRAIL receptors by its relative antibodies.

## 5.6 Loss of cIAP1 promotes RIPK1-dependent Ripoptosome formation in IKK2 active melanoma cells

In the absence of survival signalling, membrane associated TNF complex I transits to cytoplasm as complex IIa, which mainly contains TRAF2, FADD, caspase 8, and RIPK1, to induce apoptosis. It has been proved loss of cIAP1 promotes the other form of complex assembly in absence of death receptor stimulation, known as Ripoptosome [80,99,153]. In our study, depletion of cIAP1 and downregulate cIAP2 expression led to the spontaneous Ripoptosome complex formation without exogenous death ligands stimulation in IKK2 EE cells. The components of the complex included caspase 8, p-RIPK1 (Ser166), RIPK1, FADD, cFLIP (long, short and p43 forms), and A20 (Figure 24). In terms of the composition of the TNF complex IIa and Ripoptosome, there are no substantial differences. However, the stimuli of both complexes are certainly different. Unlike TNF-induced complex II, Ripoptosome formation can be triggered in the absence of TNF signalling [99,100]. In our study, IAP antagonist promoted complex formation in IKK2 EE cells. Although it did not require extra exogenous TNF $\alpha$  or other TNF family death ligands, IKK2 activation itself resulted in considerable accumulation of endogenous production of TNF and other death ligands. Inability of TNFR2-Fc to protect IKK2 EE cells from IAP

antagonist-mediated cell death suggested the possibility that loss of cIAP1 in IKK2 EE cells advocated the Ripoptosome not TNF complex II assembly. TNFR1 knockout or inhibition of the TNF signalling can be used to confirm the identity of the complex.

RIPK1 dependency for its Ripoptosome formation was substantiated by addition of RIPK1 inhibitor Necrostatin-1 (Figure 25B). Upon TNF $\alpha$  stimulation, RIPK1 was immediately ubiquitinated with K63 poly-ubiquitin chains that can be degraded and converted into K48 poly-ubiquitin chains by A20 [189]. In addition to ubiquitination, phosphorylation of RIPK1 is required for its effect on both apoptosis and necroptosis. In our study, blockade of RIPK1 kinase activity prevented IKK2 EE cells from IAP antagonist-mediated cell death (Figure 25A). Similar with many kinases, auto-phosphorylation of RIPK1 plays a critical role in its activation. RIPK1 is auto-phosphorylated on the Ser161 residue. Of interest, point mutations (S161A and S161E/D) of RIPK1 that predict the conformational change of the RIPK1 T-loop disable the Necrostatin-1 to inhibit RIPK1, suggesting that Nec-1 is an allosteric inhibitor of RIPK1 kinase. X-ray crystallography study confirms that Nec-1 binds to a hydrophobic pocket between the N- and C-lobes of the kinase domain and stabilizes RIPK1 in an inactive conformation [194,195]. In NF- $\kappa$ B constitutively active melanoma cells, Necrostatin-1 partially protected cells from apoptotic cell death resulting from IAP antagonist. Moreover phosphorylation of RIPK1 found in the cytoplasmic complex in response to the IAP antagonist is also decreased because of RIPK1 inhibition. Phosphorylation of RIPK1 is required for its interaction with RIPK1 for necroptosis. However these results indicated RIPK1 kinase activity was required for auto-phosphorylation and apoptosis induction in IKK2 EE cells.

In summary, inhibitors of apoptosis proteins, which were regulated by NF- $\kappa$ B activation, rendered resistance to death ligand-induced cell death in melanoma cells *in vitro* (Figure 26). Inhibition of IAPs by IAP antagonist sensitized melanoma cells to death ligand-mediated apoptosis. In addition, when NF- $\kappa$ B was activated, IAP antagonist was sufficient to induce Ripoptosome formation and subsequent apoptosis which were RIPK1 dependent (Figure 26). Either death ligands or IAP antagonist exclusively induced caspase-dependent apoptosis but not RIPKs-dependent necroptosis in melanoma cell lines. Necroptosis resistance of melanoma cells resulted from lack of RIPK3 expression of which DNA promoter was hyper methylated. Moreover, demethylation reagent restored RIPK3 expression in melanomas but not sufficient to initiate necroptosis. Ectopical expression of RIPK3 via retroviral transduction in melanoma cell lines initiated necroptosis execution through phosphorylation of MLKL (Figure 26). Better understanding of cell death regulation in melanomas provides theoretical basis for melanoma clinical treatment.

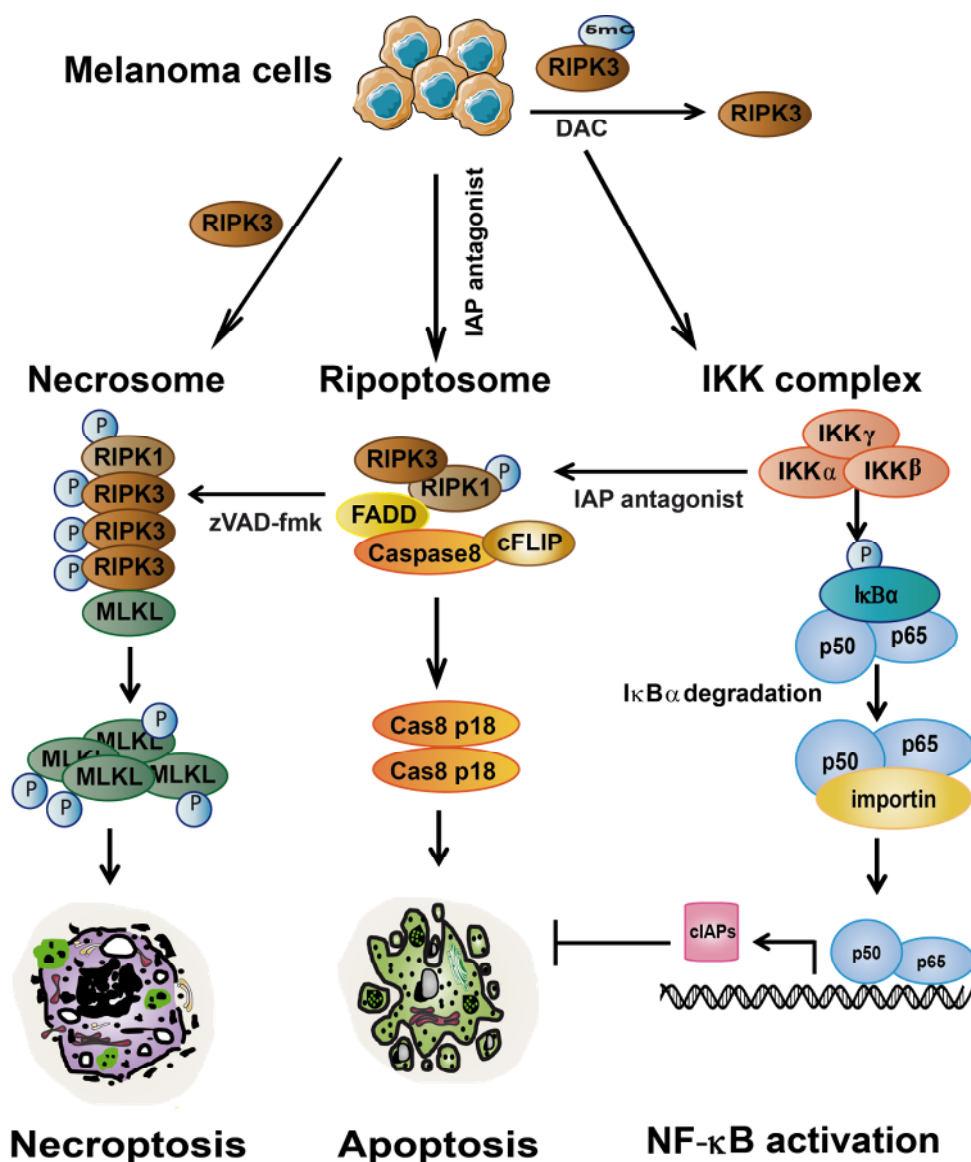


Figure 26 Identification of RIPK3 and NF-κB for melanoma cell death regulation

## References

- [1] Bissett DL. Common cosmeceuticals. *Clinics in dermatology*. 2009;27(5):435-445.
- [2] James WB, Timothy; Elston, Dirk Andrews' *Diseases of the Skin*(10th ed.): Elsevier; 2005.
- [3] McGrath JAE, R.A.; Pope, F.M. *Rook's Textbook of Dermatology* (7th ed.): Blackwell Publishing; 2004.
- [4] Houben E, De Paepe K, Rogiers V. A keratinocyte's course of life. *Skin pharmacology and physiology*. 2007;20(3):122-132.
- [5] Montagna WP, Giuseppe; Kenney, John A. *Black skin: structure and function*: Gulf Professional Publishing; 1993.
- [6] Ginhoux F, Tacke F, Angeli V, et al. Langerhans cells arise from monocytes in vivo. *Nature immunology*. 2006;7(3):265-273.
- [7] Chren MM. Measurement of vital signs for skin diseases. *The Journal of investigative dermatology*. 2005;125(4):viii-ix.
- [8] Dobric I. [Skin changes in rheumatic diseases]. *Reumatizam*. 2005;52(2):9-20.
- [9] Goebeler M, Brocker EB. [Problems and diseases of the aging skin]. *MMW Fortschritte der Medizin*. 2005;147(18):35-38.
- [10] Ferlay J SI, Ervik M, et al. *Cancer Incidence and Mortality Worldwide: IARC CancerBase No. 11*[Internet]. 2013; Lyon, France: International Agency for Research on Cancer; 2013. Available at: <http://globocan.iarc.fr/Default.aspx>.
- [11] Hurst EA, Harbour JW, Cornelius LA. Ocular melanoma: a review and the relationship to cutaneous melanoma. *Archives of dermatology*. 2003;139(8):1067-1073.
- [12] Mooi WJ. Diagnosis of thin melanoma. *Journal of clinical pathology*. 1997;50(3):179-180.
- [13] Mobley AK, Braeuer RR, Kamiya T, Shoshan E, Bar-Eli M. Driving transcriptional regulators in melanoma metastasis. *Cancer metastasis reviews*. 2012;31(3-4):621-632.
- [14] McDonald SL, Edington HD, Kirkwood JM, Becker D. Expression analysis

- of genes identified by molecular profiling of VGP melanomas and MGP melanoma-positive lymph nodes. *Cancer biology & therapy*. 2004;3(1):110-120.
- [15] Tornaletti S, Pfeifer GP. UV damage and repair mechanisms in mammalian cells. *BioEssays : news and reviews in molecular, cellular and developmental biology*. 1996;18(3):221-228.
- [16] Matsumura Y, Ananthaswamy HN. Short-term and long-term cellular and molecular events following UV irradiation of skin: implications for molecular medicine. *Expert reviews in molecular medicine*. 2002;4(26):1-22.
- [17] Behrens T, Lynge E, Cree I, et al. Occupational exposure to endocrine-disrupting chemicals and the risk of uveal melanoma. *Scandinavian journal of work, environment & health*. 2012;38(5):476-483.
- [18] Dika E, Fanti PA, Vaccari S, Patrizi A, Maibach HI. Causal relationship between exposure to chemicals and malignant melanoma? A review and study proposal. *Reviews on environmental health*. 2010;25(3):255-259.
- [19] Song HZ, Kono M, Tomita Y. Establishment of a screening system for chemicals that upregulate a melanoma antigen, Melan-A/MART-1. *The Tohoku journal of experimental medicine*. 2009;217(3):231-237.
- [20] Siskind V, Hughes MC, Palmer JM, et al. Nevi, family history, and fair skin increase the risk of second primary melanoma. *The Journal of investigative dermatology*. 2011;131(2):461-467.
- [21] Mitra D, Luo X, Morgan A, et al. An ultraviolet-radiation-independent pathway to melanoma carcinogenesis in the red hair/fair skin background. *Nature*. 2012;491(7424):449-453.
- [22] Hansen CB, Wadge LM, Lowstuter K, Boucher K, Leachman SA. Clinical germline genetic testing for melanoma. *The Lancet. Oncology*. 2004;5(5):314-319.
- [23] Buecher B, Gauthier-Villars M, Desjardins L, et al. Contribution of CDKN2A/P16 ( INK4A ), P14 (ARF), CDK4 and BRCA1/2 germline mutations in individuals with suspected genetic predisposition to uveal melanoma. *Familial cancer*. 2010;9(4):663-667.
- [24] Soufir N, Avril MF, Chompret A, et al. Prevalence of p16 and CDK4 germline mutations in 48 melanoma-prone families in France. The French Familial Melanoma Study Group. *Human molecular genetics*. 1998;7(2):209-216.

- [25] Nelson AA, Tsao H. Melanoma and genetics. *Clinics in dermatology*. 2009;27(1):46-52.
- [26] Taylor A, Powell ME. Intensity-modulated radiotherapy--what is it? *Cancer imaging : the official publication of the International Cancer Imaging Society*. 2004;4(2):68-73.
- [27] Gaspar LE, Ding M. A review of intensity-modulated radiation therapy. *Current oncology reports*. 2008;10(4):294-299.
- [28] Michaloglou C, Vredeveld LC, Soengas MS, et al. BRAF600-associated senescence-like cell cycle arrest of human naevi. *Nature*. 2005;436(7051):720-724.
- [29] Carson CC, Moschos SJ, Edmiston SN, et al. IL2 Inducible T-cell Kinase, a Novel Therapeutic Target in Melanoma. *Clinical cancer research : an official journal of the American Association for Cancer Research*. 2015;21(9):2167-2176.
- [30] Vihinen P, Tervahartiala T, Sorsa T, et al. Benefit of adjuvant interferon alfa-2b (IFN-alpha) therapy in melanoma patients with high serum MMP-8 levels. *Cancer immunology, immunotherapy : CII*. 2015;64(2):173-180.
- [31] Galluzzi L, Eggermont A, Kroemer G. Doubling the blockade for melanoma immunotherapy. *Oncoimmunology*. 2016;5(1):e1106127.
- [32] Redman JM, Gibney GT, Atkins MB. Advances in immunotherapy for melanoma. *BMC medicine*. 2016;14(1):20.
- [33] Chmielowski B. Prognostic and predictive biomarkers for the benefit of immunotherapy in patients with metastatic melanoma. *The British journal of dermatology*. 2016;174(1):20.
- [34] Davies H, Bignell GR, Cox C, et al. Mutations of the BRAF gene in human cancer. *Nature*. 2002;417(6892):949-954.
- [35] Gray-Schopfer V, Wellbrock C, Marais R. Melanoma biology and new targeted therapy. *Nature*. 2007;445(7130):851-857.
- [36] Hauschild A, Grob JJ, Demidov LV, et al. Dabrafenib in BRAF-mutated metastatic melanoma: a multicentre, open-label, phase 3 randomised controlled trial. *Lancet*. 2012;380(9839):358-365.
- [37] Chapman PB, Hauschild A, Robert C, et al. Improved survival with vemurafenib in melanoma with BRAF V600E mutation. *The New England journal of medicine*. 2011;364(26):2507-2516.

- [38] Ribas A, Gonzalez R, Pavlick A, et al. Combination of vemurafenib and cobimetinib in patients with advanced BRAF(V600)-mutated melanoma: a phase 1b study. *The Lancet. Oncology*. 2014;15(9):954-965.
- [39] Lockshin RA, Williams CM. Programmed cell death. V. Cytolytic enzymes in relation to the breakdown of the intersegmental muscles of silkworms. *Journal of insect physiology*. 1965;11(7):831-844.
- [40] Stefanis L, Burke RE, Greene LA. Apoptosis in neurodegenerative disorders. *Current opinion in neurology*. 1997;10(4):299-305.
- [41] Gougeon ML, Montagnier L. Apoptosis in AIDS. *Science*. 1993;260(5112):1269-1270.
- [42] Eguchi K. Apoptosis in autoimmune diseases. *Internal medicine*. 2001;40(4):275-284.
- [43] Su Z, Yang Z, Xu Y, Chen Y, Yu Q. Apoptosis, autophagy, necroptosis, and cancer metastasis. *Molecular cancer*. 2015;14:48.
- [44] Ouyang L, Shi Z, Zhao S, et al. Programmed cell death pathways in cancer: a review of apoptosis, autophagy and programmed necrosis. *Cell proliferation*. 2012;45(6):487-498.
- [45] Elmore S. Apoptosis: a review of programmed cell death. *Toxicologic pathology*. 2007;35(4):495-516.
- [46] Thornberry NA, Rano TA, Peterson EP, et al. A combinatorial approach defines specificities of members of the caspase family and granzyme B. Functional relationships established for key mediators of apoptosis. *The Journal of biological chemistry*. 1997;272(29):17907-17911.
- [47] Fuentes-Prior P, Salvesen GS. The protein structures that shape caspase activity, specificity, activation and inhibition. *The Biochemical journal*. 2004;384(Pt 2):201-232.
- [48] Chereau D, Kodandapani L, Tomaselli KJ, Spada AP, Wu JC. Structural and functional analysis of caspase active sites. *Biochemistry*. 2003;42(14):4151-4160.
- [49] Blanchard H, Kodandapani L, Mittl PR, et al. The three-dimensional structure of caspase-8: an initiator enzyme in apoptosis. *Structure*. 1999;7(9):1125-1133.
- [50] Renatus M, Stennicke HR, Scott FL, Liddington RC, Salvesen GS. Dimer formation drives the activation of the cell death protease caspase 9.

- Proceedings of the National Academy of Sciences of the United States of America. 2001;98(25):14250-14255.
- [51] Ekert PG, Silke J, Vaux DL. Caspase inhibitors. Cell death and differentiation. 1999;6(11):1081-1086.
- [52] Walczak H, Krammer PH. The CD95 (APO-1/Fas) and the TRAIL (APO-2L) apoptosis systems. Experimental cell research. 2000;256(1):58-66.
- [53] Naismith JH, Sprang SR. Modularity in the TNF-receptor family. Trends in biochemical sciences. 1998;23(2):74-79.
- [54] Schneider P, Tschopp J. Apoptosis induced by death receptors. Pharmaceutica acta Helvetiae. 2000;74(2-3):281-286.
- [55] Kischkel FC, Hellbardt S, Behrmann I, et al. Cytotoxicity-dependent APO-1 (Fas/CD95)-associated proteins form a death-inducing signaling complex (DISC) with the receptor. The EMBO journal. 1995;14(22):5579-5588.
- [56] Logue SE, Martin SJ. Caspase activation cascades in apoptosis. Biochemical Society transactions. 2008;36(Pt 1):1-9.
- [57] Ferreira KS, Kreutz C, Macnelly S, et al. Caspase-3 feeds back on caspase-8, Bid and XIAP in type I Fas signaling in primary mouse hepatocytes. Apoptosis : an international journal on programmed cell death. 2012;17(5):503-515.
- [58] Jin Z, El-Deiry WS. Overview of cell death signaling pathways. Cancer biology & therapy. 2005;4(2):139-163.
- [59] Kroemer G. Mitochondrial control of apoptosis: an introduction. Biochemical and biophysical research communications. 2003;304(3):433-435.
- [60] Esposti MD, Cristea IM, Gaskell SJ, Nakao Y, Dive C. Proapoptotic Bid binds to monolysocardiolipin, a new molecular connection between mitochondrial membranes and cell death. Cell death and differentiation. 2003;10(12):1300-1309.
- [61] Green DR, Kroemer G. The pathophysiology of mitochondrial cell death. Science. 2004;305(5684):626-629.
- [62] Kuwana T, Mackey MR, Perkins G, et al. Bid, Bax, and lipids cooperate to form supramolecular openings in the outer mitochondrial membrane. Cell. 2002;111(3):331-342.
- [63] Zamzami N, Kroemer G. The mitochondrion in apoptosis: how Pandora's

- box opens. *Nature reviews. Molecular cell biology*. 2001;2(1):67-71.
- [64] Acehan D, Jiang X, Morgan DG, Heuser JE, Wang X, Akey CW. Three-dimensional structure of the apoptosome: implications for assembly, procaspase-9 binding, and activation. *Molecular cell*. 2002;9(2):423-432.
- [65] Adrain C, Slee EA, Harte MT, Martin SJ. Regulation of apoptotic protease activating factor-1 oligomerization and apoptosis by the WD-40 repeat region. *The Journal of biological chemistry*. 1999;274(30):20855-20860.
- [66] Srinivasula SM, Ahmad M, Guo Y, et al. Identification of an endogenous dominant-negative short isoform of caspase-9 that can regulate apoptosis. *Cancer research*. 1999;59(5):999-1002.
- [67] Ekert PG, Silke J, Hawkins CJ, Verhagen AM, Vaux DL. DIABLO promotes apoptosis by removing MIHA/XIAP from processed caspase 9. *The Journal of cell biology*. 2001;152(3):483-490.
- [68] Verhagen AM, Vaux DL. Cell death regulation by the mammalian IAP antagonist Diablo/Smac. *Apoptosis : an international journal on programmed cell death*. 2002;7(2):163-166.
- [69] Taylor RC, Cullen SP, Martin SJ. Apoptosis: controlled demolition at the cellular level. *Nature reviews. Molecular cell biology*. 2008;9(3):231-241.
- [70] Scaffidi C, Fulda S, Srinivasan A, et al. Two CD95 (APO-1/Fas) signaling pathways. *The EMBO journal*. 1998;17(6):1675-1687.
- [71] Strasser A, O'Connor L, Dixit VM. Apoptosis signaling. *Annual review of biochemistry*. 2000;69:217-245.
- [72] Laster SM, Wood JG, Gooding LR. Tumor necrosis factor can induce both apoptic and necrotic forms of cell lysis. *Journal of immunology*. 1988;141(8):2629-2634.
- [73] Holler N, Zaru R, Micheau O, et al. Fas triggers an alternative, caspase-8-independent cell death pathway using the kinase RIP as effector molecule. *Nature immunology*. 2000;1(6):489-495.
- [74] Cho YS, Challa S, Moquin D, et al. Phosphorylation-driven assembly of the RIP1-RIP3 complex regulates programmed necrosis and virus-induced inflammation. *Cell*. 2009;137(6):1112-1123.
- [75] He F, Dang W, Saito K, et al. Solution structure of the cysteine-rich domain in Fn14, a member of the tumor necrosis factor receptor superfamily. *Protein science : a publication of the Protein Society*. 2009;18(3):650-656.

- [76] Zhang DW, Shao J, Lin J, et al. RIP3, an energy metabolism regulator that switches TNF-induced cell death from apoptosis to necrosis. *Science*. 2009;325(5938):332-336.
- [77] Chan FK, Shisler J, Bixby JG, et al. A role for tumor necrosis factor receptor-2 and receptor-interacting protein in programmed necrosis and antiviral responses. *The Journal of biological chemistry*. 2003;278(51):51613-51621.
- [78] Vanden Berghe T, Linkermann A, Jouan-Lanhouet S, Walczak H, Vandenabeele P. Regulated necrosis: the expanding network of non-apoptotic cell death pathways. *Nature reviews. Molecular cell biology*. 2014;15(2):135-147.
- [79] Vandenabeele P, Galluzzi L, Vanden Berghe T, Kroemer G. Molecular mechanisms of necroptosis: an ordered cellular explosion. *Nature reviews. Molecular cell biology*. 2010;11(10):700-714.
- [80] Vanlangenakker N, Bertrand MJ, Bogaert P, Vandenabeele P, Vanden Berghe T. TNF-induced necroptosis in L929 cells is tightly regulated by multiple TNFR1 complex I and II members. *Cell death & disease*. 2011;2:e230.
- [81] Sawai H. Differential effects of caspase inhibitors on TNF-induced necroptosis. *Biochemical and biophysical research communications*. 2013;432(3):451-455.
- [82] Polykratis A, Hermance N, Zelic M, et al. Cutting edge: RIPK1 Kinase inactive mice are viable and protected from TNF-induced necroptosis in vivo. *Journal of immunology*. 2014;193(4):1539-1543.
- [83] Ch'en IL, Tsau JS, Molkenstin JD, Komatsu M, Hedrick SM. Mechanisms of necroptosis in T cells. *The Journal of experimental medicine*. 2011;208(4):633-641.
- [84] He S, Liang Y, Shao F, Wang X. Toll-like receptors activate programmed necrosis in macrophages through a receptor-interacting kinase-3-mediated pathway. *Proceedings of the National Academy of Sciences of the United States of America*. 2011;108(50):20054-20059.
- [85] Thapa RJ, Nogusa S, Chen P, et al. Interferon-induced RIP1/RIP3-mediated necrosis requires PKR and is licensed by FADD and caspases. *Proceedings of the National Academy of Sciences of the United States of America*. 2013;110(33):E3109-3118.
- [86] Robinson N, McComb S, Mulligan R, Dudani R, Krishnan L, Sad S. Type I interferon induces necroptosis in macrophages during infection with

- Salmonella enterica serovar Typhimurium. *Nature immunology*. 2012;13(10):954-962.
- [87] Huang H, Xiao T, He L, Ji H, Liu XY. Interferon-beta-armed oncolytic adenovirus induces both apoptosis and necroptosis in cancer cells. *Acta biochimica et biophysica Sinica*. 2012;44(9):737-745.
- [88] Fulda S. The mechanism of necroptosis in normal and cancer cells. *Cancer biology & therapy*. 2013;14(11):999-1004.
- [89] Vanlangenakker N, Vanden Berghe T, Vandenabeele P. Many stimuli pull the necrotic trigger, an overview. *Cell death and differentiation*. 2012;19(1):75-86.
- [90] Zhang D, Lin J, Han J. Receptor-interacting protein (RIP) kinase family. *Cellular & molecular immunology*. 2010;7(4):243-249.
- [91] Humphries F, Yang S, Wang B, Moynagh PN. RIP kinases: key decision makers in cell death and innate immunity. *Cell death and differentiation*. 2015;22(2):225-236.
- [92] Micheau O, Tschopp J. Induction of TNF receptor I-mediated apoptosis via two sequential signaling complexes. *Cell*. 2003;114(2):181-190.
- [93] Shu HB, Takeuchi M, Goeddel DV. The tumor necrosis factor receptor 2 signal transducers TRAF2 and c-IAP1 are components of the tumor necrosis factor receptor 1 signaling complex. *Proceedings of the National Academy of Sciences of the United States of America*. 1996;93(24):13973-13978.
- [94] Rothe M, Pan MG, Henzel WJ, Ayres TM, Goeddel DV. The TNFR2-TRAF signaling complex contains two novel proteins related to baculoviral inhibitor of apoptosis proteins. *Cell*. 1995;83(7):1243-1252.
- [95] Csomos RA, Brady GF, Duckett CS. Enhanced cytoprotective effects of the inhibitor of apoptosis protein cellular IAP1 through stabilization with TRAF2. *The Journal of biological chemistry*. 2009;284(31):20531-20539.
- [96] Ea CK, Deng L, Xia ZP, Pineda G, Chen ZJ. Activation of IKK by TNFalpha requires site-specific ubiquitination of RIP1 and polyubiquitin binding by NEMO. *Molecular cell*. 2006;22(2):245-257.
- [97] Bertrand MJ, Milutinovic S, Dickson KM, et al. cIAP1 and cIAP2 facilitate cancer cell survival by functioning as E3 ligases that promote RIP1 ubiquitination. *Molecular cell*. 2008;30(6):689-700.
- [98] Schneider-Brachert W, Tchikov V, Neumeyer J, et al. Compartmentalization

- of TNF receptor 1 signaling: internalized TNF receptors as death signaling vesicles. *Immunity*. 2004;21(3):415-428.
- [99] Feoktistova M, Geserick P, Kellert B, et al. cIAPs block Ripoptosome formation, a RIP1/caspase-8 containing intracellular cell death complex differentially regulated by cFLIP isoforms. *Molecular cell*. 2011;43(3):449-463.
- [100] Tenev T, Bianchi K, Darding M, et al. The Ripoptosome, a signaling platform that assembles in response to genotoxic stress and loss of IAPs. *Molecular cell*. 2011;43(3):432-448.
- [101] Feng S, Yang Y, Mei Y, et al. Cleavage of RIP3 inactivates its caspase-independent apoptosis pathway by removal of kinase domain. *Cellular signalling*. 2007;19(10):2056-2067.
- [102] Murphy JM, Czabotar PE, Hildebrand JM, et al. The pseudokinase MLKL mediates necroptosis via a molecular switch mechanism. *Immunity*. 2013;39(3):443-453.
- [103] Hildebrand JM, Tanzer MC, Lucet IS, et al. Activation of the pseudokinase MLKL unleashes the four-helix bundle domain to induce membrane localization and necroptotic cell death. *Proceedings of the National Academy of Sciences of the United States of America*. 2014;111(42):15072-15077.
- [104] Tanzer MC, Matti I, Hildebrand JM, et al. Evolutionary divergence of the necroptosis effector MLKL. *Cell death and differentiation*. 2016.
- [105] Cai Z, Jitkaew S, Zhao J, et al. Plasma membrane translocation of trimerized MLKL protein is required for TNF-induced necroptosis. *Nature cell biology*. 2014;16(1):55-65.
- [106] Chen X, Li W, Ren J, et al. Translocation of mixed lineage kinase domain-like protein to plasma membrane leads to necrotic cell death. *Cell research*. 2014;24(1):105-121.
- [107] Wang H, Sun L, Su L, et al. Mixed lineage kinase domain-like protein MLKL causes necrotic membrane disruption upon phosphorylation by RIP3. *Molecular cell*. 2014;54(1):133-146.
- [108] Dondelinger Y, Declercq W, Montessuit S, et al. MLKL compromises plasma membrane integrity by binding to phosphatidylinositol phosphates. *Cell reports*. 2014;7(4):971-981.
- [109] Quarato G, Guy CS, Grace CR, et al. Sequential Engagement of Distinct MLKL Phosphatidylinositol-Binding Sites Executes Necroptosis. *Molecular*

- cell. 2016;61(4):589-601.
- [110] Ofengeim D, Yuan J. Regulation of RIP1 kinase signalling at the crossroads of inflammation and cell death. *Nature reviews. Molecular cell biology*. 2013;14(11):727-736.
- [111] Degtarev A, Huang Z, Boyce M, et al. Chemical inhibitor of nonapoptotic cell death with therapeutic potential for ischemic brain injury. *Nature chemical biology*. 2005;1(2):112-119.
- [112] Duckett CS, Nava VE, Gedrich RW, et al. A conserved family of cellular genes related to the baculovirus iap gene and encoding apoptosis inhibitors. *The EMBO journal*. 1996;15(11):2685-2694.
- [113] Bertrand MJ, Lippens S, Staes A, et al. cIAP1/2 are direct E3 ligases conjugating diverse types of ubiquitin chains to receptor interacting proteins kinases 1 to 4 (RIP1-4). *PloS one*. 2011;6(9):e22356.
- [114] Crook NE, Clem RJ, Miller LK. An apoptosis-inhibiting baculovirus gene with a zinc finger-like motif. *Journal of virology*. 1993;67(4):2168-2174.
- [115] Deveraux QL, Takahashi R, Salvesen GS, Reed JC. X-linked IAP is a direct inhibitor of cell-death proteases. *Nature*. 1997;388(6639):300-304.
- [116] Silke J, Vucic D. IAP family of cell death and signaling regulators. *Methods in enzymology*. 2014;545:35-65.
- [117] Du C, Fang M, Li Y, Li L, Wang X. Smac, a mitochondrial protein that promotes cytochrome c-dependent caspase activation by eliminating IAP inhibition. *Cell*. 2000;102(1):33-42.
- [118] Verhagen AM, Ekert PG, Pakusch M, et al. Identification of DIABLO, a mammalian protein that promotes apoptosis by binding to and antagonizing IAP proteins. *Cell*. 2000;102(1):43-53.
- [119] Dueber EC, Schoeffler AJ, Lingel A, et al. Antagonists induce a conformational change in cIAP1 that promotes autoubiquitination. *Science*. 2011;334(6054):376-380.
- [120] Vince JE, Wong WW, Khan N, et al. IAP antagonists target cIAP1 to induce TNFalpha-dependent apoptosis. *Cell*. 2007;131(4):682-693.
- [121] Darding M, Feltham R, Tenev T, et al. Molecular determinants of Smac mimetic induced degradation of cIAP1 and cIAP2. *Cell death and differentiation*. 2011;18(8):1376-1386.
- [122] Feltham R, Bettjeman B, Budhidarmo R, et al. Smac mimetics activate the

- E3 ligase activity of cIAP1 protein by promoting RING domain dimerization. *The Journal of biological chemistry*. 2011;286(19):17015-17028.
- [123] Compere SJ, Palmiter RD. DNA methylation controls the inducibility of the mouse metallothionein-I gene lymphoid cells. *Cell*. 1981;25(1):233-240.
- [124] McGhee JD, Ginder GD. Specific DNA methylation sites in the vicinity of the chicken beta-globin genes. *Nature*. 1979;280(5721):419-420.
- [125] Lee JT, Bartolomei MS. X-inactivation, imprinting, and long noncoding RNAs in health and disease. *Cell*. 2013;152(6):1308-1323.
- [126] Portela A, Esteller M. Epigenetic modifications and human disease. *Nature biotechnology*. 2010;28(10):1057-1068.
- [127] Robertson KD. DNA methylation and human disease. *Nature reviews. Genetics*. 2005;6(8):597-610.
- [128] El-Osta A. DNMT cooperativity--the developing links between methylation, chromatin structure and cancer. *BioEssays : news and reviews in molecular, cellular and developmental biology*. 2003;25(11):1071-1084.
- [129] Weisenberger DJ. Characterizing DNA methylation alterations from The Cancer Genome Atlas. *The Journal of clinical investigation*. 2014;124(1):17-23.
- [130] Schinke C, Mo Y, Yu Y, et al. Aberrant DNA methylation in malignant melanoma. *Melanoma research*. 2010;20(4):253-265.
- [131] Mirmohammadsadegh A, Marini A, Nambiar S, et al. Epigenetic silencing of the PTEN gene in melanoma. *Cancer research*. 2006;66(13):6546-6552.
- [132] Marini A, Mirmohammadsadegh A, Nambiar S, Gustrau A, Ruzicka T, Hengge UR. Epigenetic inactivation of tumor suppressor genes in serum of patients with cutaneous melanoma. *The Journal of investigative dermatology*. 2006;126(2):422-431.
- [133] Roh MR, Gupta S, Park KH, et al. Promoter Methylation of PTEN Is a Significant Prognostic Factor in Melanoma Survival. *The Journal of investigative dermatology*. 2016.
- [134] Tanemura A, Terando AM, Sim MS, et al. CpG island methylator phenotype predicts progression of malignant melanoma. *Clinical cancer research : an official journal of the American Association for Cancer Research*. 2009;15(5):1801-1807.
- [135] Chuang JC, Warner SL, Vollmer D, et al. S110, a

- 5-Aza-2'-deoxycytidine-containing dinucleotide, is an effective DNA methylation inhibitor in vivo and can reduce tumor growth. *Molecular cancer therapeutics*. 2010;9(5):1443-1450.
- [136] Thakur S, Feng X, Qiao Shi Z, et al. ING1 and 5-azacytidine act synergistically to block breast cancer cell growth. *PloS one*. 2012;7(8):e43671.
- [137] Mikyskova R, Indrova M, Vlkova V, et al. DNA demethylating agent 5-azacytidine inhibits myeloid-derived suppressor cells induced by tumor growth and cyclophosphamide treatment. *Journal of leukocyte biology*. 2014.
- [138] Lindner DJ, Wu Y, Haney R, et al. Thrombospondin-1 expression in melanoma is blocked by methylation and targeted reversal by 5-Aza-deoxycytidine suppresses angiogenesis. *Matrix biology : journal of the International Society for Matrix Biology*. 2013;32(2):123-132.
- [139] Bonizzi G, Karin M. The two NF-kappaB activation pathways and their role in innate and adaptive immunity. *Trends in immunology*. 2004;25(6):280-288.
- [140] Gilmore TD. The Rel/NF-kappaB signal transduction pathway: introduction. *Oncogene*. 1999;18(49):6842-6844.
- [141] DiDonato J, Mercurio F, Rosette C, et al. Mapping of the inducible IkappaB phosphorylation sites that signal its ubiquitination and degradation. *Molecular and cellular biology*. 1996;16(4):1295-1304.
- [142] Kanarek N, Ben-Neriah Y. Regulation of NF-kappaB by ubiquitination and degradation of the IkappaBs. *Immunological reviews*. 2012;246(1):77-94.
- [143] Hayden MS, Ghosh S. Shared principles in NF-kappaB signaling. *Cell*. 2008;132(3):344-362.
- [144] Razani B, Zarnegar B, Ytterberg AJ, et al. Negative feedback in noncanonical NF-kappaB signaling modulates NIK stability through IKKalpha-mediated phosphorylation. *Science signaling*. 2010;3(123):ra41.
- [145] Wang RP, Zhang M, Li Y, et al. Differential regulation of IKK alpha-mediated activation of IRF3/7 by NIK. *Molecular immunology*. 2008;45(7):1926-1934.
- [146] Vallabhapurapu S, Matsuzawa A, Zhang W, et al. Nonredundant and complementary functions of TRAF2 and TRAF3 in a ubiquitination cascade that activates NIK-dependent alternative NF-kappaB signaling. *Nature immunology*. 2008;9(12):1364-1370.

- [147] May MJ, Madge LA. Caspase inhibition sensitizes inhibitor of NF-kappaB kinase beta-deficient fibroblasts to caspase-independent cell death via the generation of reactive oxygen species. *The Journal of biological chemistry*. 2007;282(22):16105-16116.
- [148] Dror R, Lederman M, Umezawa K, Barak V, Pe'er J, Chowers I. Characterizing the involvement of the nuclear factor-kappa B (NF kappa B) transcription factor in uveal melanoma. *Investigative ophthalmology & visual science*. 2010;51(4):1811-1816.
- [149] Huang S, DeGuzman A, Bucana CD, Fidler IJ. Nuclear factor-kappaB activity correlates with growth, angiogenesis, and metastasis of human melanoma cells in nude mice. *Clinical cancer research : an official journal of the American Association for Cancer Research*. 2000;6(6):2573-2581.
- [150] Franco AV, Zhang XD, Van Berkel E, et al. The role of NF-kappa B in TNF-related apoptosis-inducing ligand (TRAIL)-induced apoptosis of melanoma cells. *Journal of immunology*. 2001;166(9):5337-5345.
- [151] Aggarwal S, Takada Y, Mhashilkar AM, Sieger K, Chada S, Aggarwal BB. Melanoma differentiation-associated gene-7/IL-24 gene enhances NF-kappa B activation and suppresses apoptosis induced by TNF. *Journal of immunology*. 2004;173(7):4368-4376.
- [152] Oliver Metzigg M, Fuchs D, Tagscherer KE, Grone HJ, Schirmacher P, Roth W. Inhibition of caspases primes colon cancer cells for 5-fluorouracil-induced TNF-alpha-dependent necroptosis driven by RIP1 kinase and NF-kappaB. *Oncogene*. 2015.
- [153] Geserick P, Hupe M, Moulin M, et al. Cellular IAPs inhibit a cryptic CD95-induced cell death by limiting RIP1 kinase recruitment. *The Journal of cell biology*. 2009;187(7):1037-1054.
- [154] Koo GB, Morgan MJ, Lee DG, et al. Methylation-dependent loss of RIP3 expression in cancer represses programmed necrosis in response to chemotherapeutics. *Cell research*. 2015;25(6):707-725.
- [155] Hanahan D, Weinberg RA. Hallmarks of cancer: the next generation. *Cell*. 2011;144(5):646-674.
- [156] Moujalled DM, Cook WD, Murphy JM, Vaux DL. Necroptosis induced by RIPK3 requires MLKL but not Drp1. *Cell death & disease*. 2014;5:e1086.
- [157] Sun L, Wang H, Wang Z, et al. Mixed lineage kinase domain-like protein mediates necrosis signaling downstream of RIP3 kinase. *Cell*. 2012;148(1-2):213-227.

- [158] Wu X, Tian L, Li J, et al. Investigation of receptor interacting protein (RIP3)-dependent protein phosphorylation by quantitative phosphoproteomics. *Molecular & cellular proteomics* : MCP. 2012;11(12):1640-1651.
- [159] Li J, McQuade T, Siemer AB, et al. The RIP1/RIP3 necrosome forms a functional amyloid signaling complex required for programmed necrosis. *Cell*. 2012;150(2):339-350.
- [160] Harris PA, Bandyopadhyay D, Berger SB, et al. Discovery of Small Molecule RIP1 Kinase Inhibitors for the Treatment of Pathologies Associated with Necroptosis. *ACS medicinal chemistry letters*. 2013;4(12):1238-1243.
- [161] Mandal P, Berger SB, Pillay S, et al. RIP3 induces apoptosis independent of pronecrotic kinase activity. *Molecular cell*. 2014;56(4):481-495.
- [162] Ascierto PA, Kirkwood JM, Grob JJ, et al. The role of BRAF V600 mutation in melanoma. *Journal of translational medicine*. 2012;10:85.
- [163] Li JX, Feng JM, Wang Y, et al. The B-Raf(V600E) inhibitor dabrafenib selectively inhibits RIP3 and alleviates acetaminophen-induced liver injury. *Cell death & disease*. 2014;5:e1278.
- [164] Pahl HL. Activators and target genes of Rel/NF-kappaB transcription factors. *Oncogene*. 1999;18(49):6853-6866.
- [165] Mercurio F, Zhu H, Murray BW, et al. IKK-1 and IKK-2: cytokine-activated IkkappaB kinases essential for NF-kappaB activation. *Science*. 1997;278(5339):860-866.
- [166] Diessenbacher P, Hupe M, Sprick MR, et al. NF-kappaB inhibition reveals differential mechanisms of TNF versus TRAIL-induced apoptosis upstream or at the level of caspase-8 activation independent of cIAP2. *The Journal of investigative dermatology*. 2008;128(5):1134-1147.
- [167] Sun C, Wang L, Huang S, et al. Reversible and adaptive resistance to BRAF(V600E) inhibition in melanoma. *Nature*. 2014;508(7494):118-122.
- [168] Geserick P, Drewniok C, Hupe M, et al. Suppression of cFLIP is sufficient to sensitize human melanoma cells to TRAIL- and CD95L-mediated apoptosis. *Oncogene*. 2008;27(22):3211-3220.
- [169] Armstrong CW, Maxwell PJ, Ong CW, et al. PTEN deficiency promotes macrophage infiltration and hypersensitivity of prostate cancer to IAP antagonist/radiation combination therapy. *Oncotarget*. 2016;7(7):7885-7898.

- [170] Zakaria Z, Tivnan A, Flanagan L, et al. Patient-derived glioblastoma cells show significant heterogeneity in treatment responses to the inhibitor-of-apoptosis-protein antagonist birinapan. *British journal of cancer*. 2016;114(2):188-198.
- [171] Dannappel M, Vlantis K, Kumari S, et al. RIPK1 maintains epithelial homeostasis by inhibiting apoptosis and necroptosis. *Nature*. 2014;513(7516):90-94.
- [172] Meng L, Jin W, Wang X. RIP3-mediated necrotic cell death accelerates systematic inflammation and mortality. *Proceedings of the National Academy of Sciences of the United States of America*. 2015;112(35):11007-11012.
- [173] Rickard JA, O'Donnell JA, Evans JM, et al. RIPK1 regulates RIPK3-MLKL-driven systemic inflammation and emergency hematopoiesis. *Cell*. 2014;157(5):1175-1188.
- [174] Zhang H, Zhong C, Shi L, Guo Y, Fan Z. Granulysin induces cathepsin B release from lysosomes of target tumor cells to attack mitochondria through processing of bid leading to Necroptosis. *Journal of immunology*. 2009;182(11):6993-7000.
- [175] Cabon L, Galan-Malo P, Bouharrou A, et al. BID regulates AIF-mediated caspase-independent necroptosis by promoting BAX activation. *Cell death and differentiation*. 2012;19(2):245-256.
- [176] Tait SW, Oberst A, Quarato G, et al. Widespread mitochondrial depletion via mitophagy does not compromise necroptosis. *Cell reports*. 2013;5(4):878-885.
- [177] Moquin D, Chan FK. The molecular regulation of programmed necrotic cell injury. *Trends in biochemical sciences*. 2010;35(8):434-441.
- [178] Li D, Xu T, Cao Y, et al. A cytosolic heat shock protein 90 and cochaperone CDC37 complex is required for RIP3 activation during necroptosis. *Proceedings of the National Academy of Sciences of the United States of America*. 2015;112(16):5017-5022.
- [179] Jacobsen AV, Lowes KN, Tanzer MC, et al. HSP90 activity is required for MLKL oligomerisation and membrane translocation and the induction of necroptotic cell death. *Cell death & disease*. 2016;7:e2051.
- [180] Hamamoto R, Toyokawa G, Nakakido M, Ueda K, Nakamura Y. SMYD2-dependent HSP90 methylation promotes cancer cell proliferation by regulating the chaperone complex formation. *Cancer letters*.

- 2014;351(1):126-133.
- [181] Kaiser WJ, Upton JW, Long AB, et al. RIP3 mediates the embryonic lethality of caspase-8-deficient mice. *Nature*. 2011;471(7338):368-372.
- [182] Zhang H, Zhou X, McQuade T, Li J, Chan FK, Zhang J. Functional complementation between FADD and RIP1 in embryos and lymphocytes. *Nature*. 2011;471(7338):373-376.
- [183] Li Z, Scott MJ, Fan EK, et al. Tissue damage negatively regulates LPS-induced macrophage necroptosis. *Cell death and differentiation*. 2016.
- [184] Newton K, Manning G. Necroptosis and Inflammation. *Annual review of biochemistry*. 2016.
- [185] Weng D, Marty-Roix R, Ganesan S, et al. Caspase-8 and RIP kinases regulate bacteria-induced innate immune responses and cell death. *Proceedings of the National Academy of Sciences of the United States of America*. 2014;111(20):7391-7396.
- [186] Nikseresht S, Khodaghali F, Nategh M, Dargahi L. RIP1 Inhibition Rescues from LPS-Induced RIP3-Mediated Programmed Cell Death, Distributed Energy Metabolism and Spatial Memory Impairment. *Journal of molecular neuroscience : MN*. 2015;57(2):219-230.
- [187] Ling L, Cao Z, Goeddel DV. NF-kappaB-inducing kinase activates IKK-alpha by phosphorylation of Ser-176. *Proceedings of the National Academy of Sciences of the United States of America*. 1998;95(7):3792-3797.
- [188] Lombardi L, Ciana P, Cappellini C, et al. Structural and functional characterization of the promoter regions of the NFkB2 gene. *Nucleic acids research*. 1995;23(12):2328-2336.
- [189] Wertz IE, O'Rourke KM, Zhou H, et al. De-ubiquitination and ubiquitin ligase domains of A20 downregulate NF-kappaB signalling. *Nature*. 2004;430(7000):694-699.
- [190] Hutti JE, Turk BE, Asara JM, Ma A, Cantley LC, Abbott DW. IkappaB kinase beta phosphorylates the K63 deubiquitinase A20 to cause feedback inhibition of the NF-kappaB pathway. *Molecular and cellular biology*. 2007;27(21):7451-7461.
- [191] Varfolomeev E, Blankenship JW, Wayson SM, et al. IAP antagonists induce autoubiquitination of c-IAPs, NF-kappaB activation, and TNFalpha-dependent apoptosis. *Cell*. 2007;131(4):669-681.

- 
- [192] Imre G, Larisch S, Rajalingam K. Ripoptosome: a novel IAP-regulated cell death-signalling platform. *Journal of molecular cell biology*. 2011;3(6):324-326.
- [193] Bertrand MJ, Vandenabeele P. The Ripoptosome: death decision in the cytosol. *Molecular cell*. 2011;43(3):323-325.
- [194] Degterev A, Hitomi J, Germscheid M, et al. Identification of RIP1 kinase as a specific cellular target of necrostatins. *Nature chemical biology*. 2008;4(5):313-321.
- [195] Xie T, Peng W, Liu Y, et al. Structural basis of RIP1 inhibition by necrostatins. *Structure*. 2013;21(3):493-499.

## Publications during PhD study

Geserick, P., **Wang, J.**, Schilling, R., Horn, S., Harris, P.A., Bertin, J., Gough, P.J., Feoktistova, M., and Leverkus, M. (2015). Absence of RIPK3 predicts necroptosis resistance in malignant melanoma. *Cell death & disease* 6, e1884.

Geserick, P., **Wang, J.**, Feoktistova, M., and Leverkus, M. (2014). The ratio of Mcl-1 and Noxa determines ABT737 resistance in squamous cell carcinoma of the skin. *Cell death & disease* 5, e1412.

Geserick, P., Badawi, M., **Wang, J.**, Feoktistova, M., and Leverkus, M. (2014) Abstract: cFLIP isoforms differentially regulate CD95L-mediated cell death and Ripoptosome formation in melanoma. *Experimental Dermatology*, 41th Annual Meeting of the Arbeitsgemeinschaft Dermatologische Forschung (ADF): e44

**Wang J.**, Geserick P., Schilling R., Horn S., Feoktistova M., Leverkus M. Oral presentation "RIPK3 is indispensable for necroptosis in malignant melanoma" 2nd ADF Round Table, 30-31 October 2015, Bad Sassendorf, German

## Acknowledgements

During the three years of my PhD study, many thanks I would like to give the people who offered me suggestions and helped me get through the difficulties. All things I experienced during these three years have made me a better researcher and person.

Firstly, I would like to thank Professor Dr. Martin Leverkus for offering me the opportunity to carry out these interesting projects under his supervision. I still remembered the questions you asked me when you interviewed me first time. Even though I cannot give an accurate answer now, but it become more clear during the three year study. I really appreciate your supervision and patience whenever I was stuck in the problems of my projects. Even though you are not with us any longer, your enthusiastic and optimistic attitude will influence me in the rest of my research life. My deepest sympathies are with your beloved wife and daughters.

I want to thank Prof. Dr. Jochen Utikal and Prof. Dr. Victor Umansky for being the supervisor and examiner for my thesis and defence. I am also grateful for them offering me murine melanoma cell lines and valuable suggestion for my project. I also would like to acknowledge Prof. Dr. Thomas Holstein as well as Dr. Haikun Liu for being examiners of my PhD defence.

More specifically, I would like to express my gratitude to the Dr. Peter Geserick, as my mentor, for your guidance in experimental design, techniques-teaching and thesis revision. After every discussion with you, I acquired valuable suggestion and input to my project. In the meanwhile, I am grateful for Dr. Maria Feoktistova's help for improving the quality of my thesis with her incredible patience and critical comments.

I also would like to thank my colleagues Diana, Sebastian, Ramon, Anu and Biswajit. Thank you for making an active, friendly and comfortable research atmosphere. It is valuable experience to discuss with you not only scientific work and also the foods, cultures beside the bench. I really feel lucky to have you as my colleagues. I would like to give a special thanks to my friends Xue. Thank you for your support during the most difficult time!

In the last, but the most important, I would like to thank my parents and my boyfriend Xiao. I am sorry for being so far away from you in the last three years. Your love and support are the strength to make me overcome all the difficulties and complete my study in Germany. Thank you for accepting my shorts and encouraging me to pursue the direction I want to follow. I cannot finish my PhD study without your understanding and encouragement.

## Abbreviations

%	Percent
°C	Degree Celsius
μ	Micro
4-HT	4-hydroxytamoxifen
APAF1	Apoptotic protease-activating factor 1
Bak	Bcl-2 antagonist or killer
Bax	Bcl-2-associated X protein
Bcl-2	B-cell lymphoma 2
BH3	Bcl-2 homology 3
Bid	BH3 interacting-domain death agonist
BIR	baculovirus inhibitor repeat
BSA	Bovine serum albumin
C	Cysteine
C10	Caspase 10
C8	Caspase 8
CAD	Caspase-activated DNase
CD40L	Cluster of differentiation 40 ligand
CD95L	Cluster of differentiation 95 ligand
cFLIP	Cellular FLICE-like inhibitory protein
cIAPs	Cellular inhibitor of apoptosis proteins
CRD	Cysteine-rich domain
CTRL	Control
d	Days
DD	Death domain
DED	Death effector domain
DISC	Death-inducing signalling complex
DNA	Deoxyribonucleic acid
dNTP	Deoxynucleoside triphosphate
Doxy	Doxycycline
EDTA	Ethylenediaminetetraacetic acid
ERK	Extracellular-signal-regulated kinase
FADD	Fas-associated protein with death domain
FCS	Fetal Bovine serum
FLICE	FADD-like IL-1β-converting enzyme
g	Gramm
GAPDH	Glyceraldehyde 3-phosphosphate dehydrogenase

---

h	Hour
HEPES	2-[4-(2-hydroxyethyl)piperazin-1-yl] ethanesulfonic acid
IKK	I $\kappa$ B kinase
IL-8	Interleukin-8
HPCE	high-performance capillary electrophoresis
HPLC	high-precision liquid chromatography
JNK	c-Jun N-terminal kinase
kDa	Kilo Dalton
l	Liter
LB	Lysogeny broth
m	Milli
M	Molarity
MAPK	Mitogen-activated protein kinases
min	Minute
MLKL	Mixed lineage kinase domain-like
MOMP	Mitochondrial outer membrane permeabilization
n	Nano
n.s.	Not significant
Nec-1	Necrostatin-1
Necrosulfonamide	NSA
NEMO	NF- $\kappa$ B-essential modulator
NF- $\kappa$ B	Nuclear factor 'kappa-light-chain-enhancer' of activated B-cells
NIK	NF- $\kappa$ B-inducing kinase
PBS	Phosphate buffered saline
PCR	Polymerase chain reaction
PI	Propidium iodide
PVDF	Polyvinylidene difluoride
RIPK	Receptor-interacting protein kinase
RNA	Ribonucleic acid
RT	Room temperature
Ser	Serine
siRNA	Small interfering RNA
SMAC	Second mitochondria-derived activator of caspases
TAB1	TAK1 binding protein 1
TAK1	Transforming growth factor $\beta$ -activated kinase 1
tBid	Truncated Bid
TL	Total cell lysate
TLR	Toll-like receptor

---

T <sub>m</sub>	Melting temperature
TNF	Tumor necrosis factor
TNFAIP3/A20	TNF $\alpha$ -induced protein3
TNF-R2	TNF receptor 2
TRADD	TNF receptor type 1-associated death domain protein
TRAF2	TNF receptor-associated factor 2
TRAIL	TNF-related apoptosis inducing ligand
TRAIL-R	TRAIL receptor
TWEAK	TNF-related weak inducer of apoptosis
UV	Ultra violet
V	Volt
v/v	Volume per volume
w/v	Weight per volume
x	G Gravitational acceleration
XIAP	X-linked inhibitor of apoptosis protein
zVAD-fmk	z-Val-Ala-DL-Asp-fluoromethylketone